
Wayne State University Dissertations

January 2019

Optimal Assessment Of Weigh-In-Motion Data For Structural Reliability Based Rating Of Bridge Superstructures

Sasan Siavashi
Wayne State University, fi8234@wayne.edu

Follow this and additional works at: https://digitalcommons.wayne.edu/oa_dissertations



Part of the [Civil Engineering Commons](#)

Recommended Citation

Siavashi, Sasan, "Optimal Assessment Of Weigh-In-Motion Data For Structural Reliability Based Rating Of Bridge Superstructures" (2019). *Wayne State University Dissertations*. 2225.
https://digitalcommons.wayne.edu/oa_dissertations/2225

This Open Access Dissertation is brought to you for free and open access by DigitalCommons@WayneState. It has been accepted for inclusion in Wayne State University Dissertations by an authorized administrator of DigitalCommons@WayneState.

**OPTIMAL ASSESSMENT OF WEIGH-IN-MOTION DATA FOR STRUCTURAL
RELIABILITY BASED RATING OF BRIDGE SUPERSTRUCTURES**

by

SASAN SIAVASHI

DISSERTATION

Submitted to the Graduate School

of Wayne State University,

Detroit, Michigan

in partial fulfillment of the requirements

for the degree of

DOCTOR OF PHILOSOPHY

2019

MAJOR: CIVIL ENGINEERING (Structural)

Approved By

Advisor

Date

DEDICATION

I would like to dedicate my work to my parents, my sister, my brother and my beloved wife who provided me with love and support unconditionally. They have sacrificed a great deal for my education and this research. I certainly could not have completed this without them.

ACKNOWLEDGMENTS

I take immense pleasure in thanking my advisor, Dr. Christopher D. Eamon, for his continuous guidance, support and professional academic supervision, which assisted me in completing this Ph.D. dissertation. It was an honor for me to conduct this research under his supervision and guidance. I could not have imagined having a better advisor and I believe the lessons I learned from him would be the invaluable assets for my future career.

I am grateful to Dr. Hwai-Chung Wu, and Dr. Fatmir Menkulasi from the Department of Civil and Environmental Engineering at Wayne State University, and Dr. Kazuhiko Shinki from the Department of Mathematics at Wayne State University, for their time and effort serving as my Dissertation Committee Members.

Finally, and most importantly, nobody has been more important to me in the pursuit of this research than the members of my family. I would like to express gratitude to my parents, my sister, and my brother for their endless love, support, and sacrifices. I wish to thank my loving and supportive wife who provide unending inspiration. I am truly thankful for having you in my life.

PREFACE

OPTIMAL ASSESSMENT OF WEIGH-IN-MOTION DATA FOR STRUCTURAL RELIABILITY BASED RATING OF BRIDGE SUPERSTRUCTURES

The objectives of this research are to: propose a simplified procedure to reduce the vehicle dataset needed to be considered for load rating of bridge superstructures; examine the effectiveness of a Reliability-Based Design Optimization (RBDO) procedure to develop State-specific rating load models for a set of bridge superstructures; and to develop an alternative approach to develop rating models more efficiently than the ideal RBDO procedure. The proposed solutions can substantially reduce the computational effort while maintaining reasonable levels of accuracy.

Keywords: Reliability-Based Design Optimization; Load rating; Load model; Weigh-in-Motion; WIM data; Structural reliability

TABLE OF CONTENTS

DEDICATION.....	ii
ACKNOWLEDGMENTS.....	iii
PREFACE.....	iv
LIST OF TABLES.....	vii
LIST OF FIGURES.....	ix
CHAPTER 1: INTRODUCTION.....	1
1.1 Statement of The Problem.....	1
1.2 Objectives of The Study.....	2
CHAPTER 2: LITERATURE REVIEW.....	4
2.1 Models Developed for AASHTO Standards.....	4
2.2 MDOT Reports and Standards.....	6
2.3 NCHRP Reports and Related Research.....	7
2.4 Collecting and Analyzing WIM Data.....	12
2.5 Additional Load Model Development for Bridge Design and Rating.....	14
CHAPTER 3: WEIGH-IN-MOTION DATA ANALYSIS.....	20
3.1 WIM Data Analysis.....	20
3.2 Vehicle Load Effects.....	30
3.3 Determination of Required Load Effects.....	37
3.4 Bridge Structures Considered.....	45
3.5 Data Projection.....	46
3.5.1 Projection Results.....	48

CHAPTER 4: DEVELOPING A SIMPLIFIED PROCEDURE FOR BRIDGE LOAD RATING	58
4.1 Correlation of Vehicle Parameters and Load Effect	59
4.2 Reliability Analysis	67
4.3 Implementation of the Proposed Approach	71
4.4 Effect of Data Reduction on Live Load Factors	76
CHAPTER 5: RBDO AND MODIFIED BEST SELECTION APPROACH	83
5.1 RBDO Model	84
5.2 Reliability Analysis	86
5.3 Design Variables	91
5.4 Solution of RBDO Problem	94
5.5 Modified Best Selection Method	96
CHAPTER 6 SUMMARY, CONCLUSION AND RECOMMENDATIONS	114
REFERENCES	118
ABSTRACT	128
AUTOBIOGRAPHICAL STATEMENT	129

LIST OF TABLES

Table 3. 1 WIM Sites.	20
Table 3. 2 Small Vehicles Filtering Criteria.	22
Table 3. 3 Filtering Criteria.	23
Table 3. 4 Legal/Extended Permit Filtering Criteria.....	23
Table 3. 5 Vehicle Statistics for LEP Vehicles.....	28
Table 3. 6 Simplified CFR Filtering Criteria.....	28
Table 3. 7 Vehicle Statistics for Simplified CFR Vehicles.	29
Table 3. 8 Statistical Parameters for DF.....	43
Table 3. 9 Random Variable Statistics.	44
Table 3. 10 k Values for CS, PC, RC, BS Moments and BS Shears.	55
Table 3. 11 k Values for CS, PC, RC Shears and BT Moments and Shears.	56
Table 3. 12 k Values Used for Two Lane Load Effects, Moment.	56
Table 3. 13 k Values Used for Two Lane Load Effects, Shear.	57
Table 4. 1 Required Load Effect Ratios.	77
Table 4. 2 Reliability Results for Different Vehicle Database Sizes	78
Table 4. 3 AASHTO and Proposed Simplified Procedure Over Exact Method Ratio	82
Table 5. 1 Random Variables.	86
Table 5. 2 Demerit Points Classification.....	101
Table 5. 3 Modified Demerit Points Classification Used in this study.....	102
Table 5. 4 Coefficients for Sum of Sines Model.	104
Table 5. 5 Comparison of Moment Design Load Models, Simplified CFR Moment	106
Table 5. 6 Comparison of Moment Design Load Models, Simplified CFR Shear.....	107

Table 5. 7 Comparison of Moment Design Load Models, MI-LEP Moment	108
Table 5. 8 Comparison of Shear Design Load Models, MI-LEP Shear.....	109
Table 5. 9 Comparison of Total Penalty Points and average VLE*LF/RLE	110

LIST OF FIGURES

Figure 3.1 WIM Sites With ADTT ≥ 5000	21
Figure 3.2 WIM Sites With ADTT ~ 3500	21
Figure 3.3 WIM Sites With ADTT ~ 1500	22
Figure 3.4 WIM Sites With ADTT ~ 400	22
Figure 3.5 All MI-LEP GVW (kips) Frequency Histogram.....	25
Figure 3.6 All MI-LEP Vehicle Length Frequency Histogram.	25
Figure 3.7 All MI-LEP Number of Axles Frequency Histogram.	26
Figure 3.8 Top 20% MI-LEP GVW (kips) Frequency Histogram.	26
Figure 3.9 Top 20% MI-LEP Vehicle Length (ft) Frequency Histogram.....	27
Figure 3.10 Top 20% MI-LEP Vehicle Number of Axles Frequency Histogram.	27
Figure 3.11 All Simplified CFR GVW (kips) Frequency Histogram.	29
Figure 3.12 Top 20% Simplified CFR GVW (kips) Frequency Histogram.....	30
Figure 3.13 Simple Span Moments, Single LEP Vehicles.....	32
Figure 3.14 Simple Span Shears, Single LEP Vehicles.	32
Figure 3.15 Maximum Single, Following, and Side-by-side Simple Span Moments.	33
Figure 3.16 Maximum Single, Following, and Side-by-side Simple Span Shears.....	33
Figure 3.17 CDF of Top 5% of Simple 200 ft Span Moments, Single LEP Vehicles.....	34
Figure 3.18 CDF of Top 5% of Simple 200 ft Span Shears, Single LEP Vehicles	34
Figure 3.19 CDF of Simple 200 ft Span Moments, Two Lane LEP Vehicles.	35
Figure 3.20 CDF of Continuous 200 ft Span Shears, Two Lane LEP Vehicles.....	35
Figure 3.21 Simple Span Moments, Single Simplified CFR Vehicles.	36
Figure 3.22 Simple Span Shears, Single Simplified CFR Vehicles.	37

Figure 3.23 CDFs of Top 350 Simple Span, Single Lane Moments for Spans From 20 – 200 ft.	50
Figure 3.24 CDFs of Top 1% of Simple Span, Single Lane Moments for Spans From 20 – 200 ft.	50
Figure 3.25 CDFs of Top 5% of Simple Span, Single Lane Moments for Spans From 20 – 200 ft.	51
Figure 3.26 Projected Mean Maximum Simple Span, Single Lane Moment for Different n Values.....	51
Figure 3.27 Projected Mean Maximum Simple Span, Single Lane Shear for Different n Values.	52
Figure 3.28 Load Projections for One Lane Simple Shear, 20'-200' Spans.	52
Figure 3.29 Load Projections for Two Lane Simple Moment, 200' Span.	53
Figure 3.30 Load Projections for Two Lane Simple Shear, 200' Span.	53
Figure 4.1 Correlation Between Vehicle Parameter and Moment, MI-LEP	60
Figure 4.2 Correlation Between Vehicle Parameter and Shear, MI-LEP	60
Figure 4.3 Correlation Between Vehicle Parameter and Moment, Simplified CFR	61
Figure 4.4 Correlation Between Vehicle Parameter and Shear, Simplified CFR.....	61
Figure 4.5 Mean top 20% simplified CFR GVW, (kips)	65
Figure 4.6 Standard deviation top 20% simplified CFR GVW, (kips)	65
Figure 4.7 Mean top 20% MI-LEP GVW, (kips)	65
Figure 4.8 Standard deviation top 20% MI-LEP GVW, (kips)	66
Figure 4.9 Side by side event, %	66
Figure 4.10 Effect of Database Reduction on V_{maxL} for Moment, MI-LEP Vehicles.	72
Figure 4.11 Effect of Database Reduction on V_{maxL} for Shear, MI-LEP Vehicles.....	72
Figure 4.12 Effect of Database Reduction on V_{site} for Moment, MI-LEP Vehicles.	73

Figure 4.13 Effect of Database Reduction on <i>VProjection</i> for Moment, MI-LEP Vehicles. ...	73
Figure 4.14 Effect of Database Reduction on Mean Maximum Load Effect, MI-LEP Moment. .	74
Figure 4.15 Effect of Database Reduction on Mean Maximum Load Effect, MI-LEP Shear.	75
Figure 4.16 Effect of Database Reduction on Mean Maximum Load Effect, Simplified CFR Moment.	76
Figure 4.17 Effect of Database Reduction on Mean Maximum Load Effect, Simplified CFR Shear.....	76
Figure 4.18 Comparison between AASHTO and Proposed simplified procedure, MI-LEP data pool.....	80
Figure 4.19 Comparison between AASHTO and Proposed simplified procedure, Simplified CFR data pool	80
Figure 4. 20 AASHTO and proposed simplified procedure over all-data load factor ratio.....	81
Figure 5.1 AASHTO Rating Trucks (kips, ft.)	91
Figure 5.2 MDOT Rating Trucks (kips, ft.)	92
Figure 5.3 Best Selection Method Flowchart.	97
Figure 5.4 Example Comparison of Load Effect Ratios Using Best Selection Method.....	99
Figure 5.5 Example Comparison of Load Effect Ratios Using Modified Best Selection Method.	101
Figure 5.6 Example Comparison of Load Effect Ratios With The Same Penalty Points.	103
Figure 5.7 Best Selection Approach Trucks (kips, ft.).....	104
Figure 5.8 Vehicle to Required Load Effect Ratios for Simplified CFR Moment.....	105
Figure 5.9 Vehicle to Required Load Effect Ratios for Simplified CFR Shear	107
Figure 5.10 Vehicle to Required Load Effect Ratios for MI-LEP Moment.....	109

Figure 5.11 Vehicle to Required Load Effect Ratios for MI-LEP Shear.....	110
Figure 5.12 Comparing Best Selection and Modified Best Selection, MI-LEP Moment (ADTT 350)	111
Figure 5.13 Comparing Best Selection and Modified Best Selection, MI-LEP Shear (ADTT 350)	112
Figure 5.14 Best Selection Method Flowchart	113

CHAPTER 1: INTRODUCTION

1.1 Statement of The Problem

Over the last several decades, the configuration of trucks traveling over States bridges, as well as federally required bridge load rating procedures, have undergone significant changes. In 1974, the Federal Highway Act legally established Bridge Formula B, limiting gross vehicle weight (GVW) to 80 kips, depending on the number of axles and spacing. However, states with legal vehicles that exceeded the Bridge Formula limits were allowed to keep their legal vehicle configurations that were currently in use. For example, in Michigan, many of these grandfathered legal vehicles were established years earlier, where the maximum GVW can approach 164 kips, depending on configuration (MDOT 2013).

Bridges need to be rated based on the AASHTO Legal trucks as well as State Legal trucks. In Michigan, there are currently 28 idealized legal vehicle configurations that the Michigan Department of Transportation (MDOT) considers for load rating. However, recent weigh-in-motion (WIM) data analysis has shown that few of these vehicle configurations still exist on the roads today (Eamon et al. 2014), resulting in a significant mismatch between the vehicles used for rating and those that actually load Michigan bridges. This is a common problem across various states, requiring revision of the models used for bridge rating to maintain an accurate assessment of reliability-based structural performance.

Additionally, various changes in rating requirements developed in the last two decades. Prior to 2003, bridges were rated based on the Manual for Condition Evaluation of Bridges (based on Load Factor Rating, LFR), modeled after the AASHTO Load Factor Design (LFD)-based Standard Specifications. However, following the release of the 1994 AASHTO Load and Resistance Factor Design (LRFD) Bridge Design Specifications, the LFR Condition Evaluation

(rating) manual was replaced with the Manual for Condition Evaluation and Load and Resistance Factor Rating (LRFR) of Highway Bridges in 2003. Significant revisions to the rating process occurred again in 2008, when the earlier manual was replaced with the Manual for Bridge Evaluation (MBE), and then again in 2011 another revision that incorporated additional significant changes was released (Sivakumar and Ghosn 2011). Moreover, in 2010, FHWA required that structures designed by LRFD were to be rated with the LRFR procedure in the MBE rather than the LFR manual.

Considering the changes in vehicle configurations as well as rating procedures, recent research (Eamon et al. 2014 and Eamon and Siavashi 2018) determined that significant inconsistencies in bridge reliability exist under the current rating process. These inconsistencies lead to an undesirable situation where some structures are under or over-rated with regard to actual traffic loads. This results in some structures not meeting target safety levels, while traffic is unnecessarily restricted on others. This problem can be solved with the development of new, regional load rating models based on state-specific traffic data. Unfortunately, the development of accurate, reliability-based load rating models requires large computational effort and in some cases, substantial computational complexity. These drawbacks represent significant hurdles to state-specific load model development. The development of new simplified but accurate approaches to reduce the computational time in the reliability-based load rating analysis while not compromising bridge structure safety is the main focus of this study.

1.2 Objectives of The Study

The first objective of this research is to propose a simplified procedure to reduce the vehicle dataset need to be considered for load rating of bridge superstructures. The second objective is to explore the effectiveness of Reliability-Based Design Optimization (RBDO) to develop a State-

specific rating load model for a set of bridge superstructures. Finally, an alternative novel approach to develop rating models as reasonably accurate as compare to RBDO solution is proposed. The proposed solutions can substantially reduce the computational effort resulting in a minimal loss of accuracy while not compromising safety level. To meet the mentioned research objectives, the following tasks are defined:

1. Collect and analyze weigh-in-motion (WIM) data to characterize and quantify truck traffic and corresponding load effects, particularly for vehicles used in the rating.
2. Quantify the level of inconsistency in bridge reliability that exists under the current rating process based on the LRFR method.
3. Develop and assess an optimal simplified approach to reduce the computational time of reliability-based bridge rating and determine the shortcomings of existing methods.
4. Develop novel approaches for live load models for bridge rating which significantly reduce the computational effort resulting in a minimal loss of accuracy.

CHAPTER 2: LITERATURE REVIEW

The literature review represents a summary of standards, research, and best practices related to the development of vehicle configurations for bridge load rating. The review included a broad search of technical engineering journals, conference proceedings, standards, and handbooks. In addition, technical reports relevant to the topic such as those published by The Michigan Department of Transportation (MDOT), The Federal Highway Administration (FHWA), The National Cooperative Highway Research Program (NCHRP), and other state Departments of Transportation (DOTs) were reviewed. The review focused on identifying methods for WIM data filtering, checking, sorting, and analysis; procedures that are used in practice to identify legal and permit vehicles; results of existing data analysis of Michigan loads; and methods for developing idealized truck load models.

2.1 Models Developed for AASHTO Standards

Due to the limited amount of traffic data available at the time, the AASHTO LRFD Bridge Design Specifications (2010) load model was developed from a 2-week sample of truck weights measured in Ontario in 1975. Moreover, several assumptions were made to allow extrapolation of the data to the 75-year expected mean maximum load used to calibrate the design load. Many of these assumptions concerned multiple presence, or more than one vehicle on the span at once. For multiple presence of side-by-side trucks in adjacent lanes, it was assumed that every 1 in 15 trucks was side-by-side with any other truck. It was also assumed that 1 in 30 side-by-side truck events occur with fully correlated (i.e. identical) truck weights. These assumptions resulted in a model which stipulates that for every 1 in 450 heavy truck crossings, it is side-by-side with an equally heavy truck. Simulations from this model determined that the case of two side-by-side, fully-correlated trucks governed maximum load effect. The governing trucks were each 85% of the maximum 75-year single lane truck, which was equivalent to 1.0-1.2 times the equivalent HL-93 load, depending on bridge span. This maximum governing load was assumed normally distributed

with a coefficient of variation from 0.14 to 0.18, depending on span length. In addition to vehicular live load, the statistics for other random variables (RVs) necessary for reliability assessment were established for the AASHTO LRFD Code development. These include bridge component dead loads and girder moment and shear resistances. These RVs, as well as the corresponding reliability models and associated limit states, have been identified and quantified for steel, concrete, and prestressed concrete bridge girders in NCHRP 368 (Nowak 1999), and were used for the calibration of the LRFD code. Using these statistics for reliability assessment led to the development of the HL-93 load, with a live load factor of 1.75 (without impact) and associated multi-lane and ADTT adjustment factors, to meet the minimum target reliability level for LRFD design of $\beta=3.5$. Bridges with spans greater than 200 ft were not considered.

The Manual for Bridge Evaluation (MBE) was published by AASHTO in 2008, replacing the 1998 Manual for Condition Evaluation of Bridges (based on Load Factor Rating, LFR) and the 2003 Manual for Condition Evaluation and Load and Resistance Factor Rating (LRFR) of Highway Bridges. In the original publication of the MBE, for $AADT \geq 5000$, the LRFD truck traffic model with side-by-side probability of 1 in 15 for heavy trucks was maintained for consistency, although this was known to be an extremely conservative value (Ghosn 2008; Sivakumar et al. 2007). It was also taken as 1 in 100 for an ADTT of 1000, and as 1 in 1000 for an ADTT of 100. The LRFD traffic load assumptions resulted in a mean maximum load event of two side-by-side 120 kip trucks for a 2-year return period or two side-by-side 130 kip trucks for a 5-year return period, assuming AASHTO Type 3S2 equivalent truck configurations. This governing live load was assumed to be lognormally distributed with a coefficient of variation of 0.18. To maintain the target evaluation reliability levels of $\beta=3.5$ for inventory ratings and $\beta=2.5$ for operating ratings using LRFR with this model, the resulting legal load factor was 1.8 for truck

weights up to 100 kips (for ADTT \geq 5000). To maintain the target reliability for permit trucks, the live load factor was linearly interpolated between 1.8 and 1.3 for truck gross vehicle weights (GVWs) between 100 and 150 kips.

The MBE was revised in 2011 (Sivakumar and Ghosn 2011) using WIM data from six states (New York, Mississippi, Indiana, Florida, California, and Texas). Four vehicle scenarios on a bridge were considered: a permit vehicle alone; two routine permit vehicles side-by-side; a routine permit vehicle alongside a random vehicle; and a special permit vehicle alongside a random vehicle. Based on a 5-year return period, the revisions recalibrated the LRFR live load factors to result in a target reliability level of $\beta=2.5$ for permit loads, with a minimum level of $\beta=1.5$. Using the LRFR rating procedures, permit live load factors varied from 1.4 to 1.15 using two-lane load distribution factors, depending on ADTT and the load effect (gross vehicle weight divided by truck axle length).

2.2 MDOT Reports and Standards

The current load rating procedure used by MDOT is summarized in the Bridge Analysis Guide (MDOT 2005, with 2009 Interim Update), as are the current legal vehicles used for rating. Currently, MDOT uses 28 vehicles for legal load rating and 20 vehicles for overload rating. Bridges that cannot carry all legal loads are accordingly posted, while if the load effect of a permit vehicle exceeds that associated with the corresponding bridge classification, it is prohibited from travelling over that structure without additional adjustment.

MDOT released several research reports that involve load model development from weigh-in-motion (WIM) data. WIM data is collected from sites where sensor systems are embedded in the roadway surface. When a vehicle crosses the sensors, high-fidelity systems can determine the number of vehicle axles, axle weight, and vehicle speed. Once the data are filtered to remove

spurious readings, a detailed record of the actual vehicle configurations passing over specific roadway locations can be developed. These configurations can then be used in place of a hypothetical design or rating vehicle to determine the expected load effects caused by actual traffic. Reports that made use of WIM data include RC-1413, *Investigation of the Adequacy of Current Bridge Design Loads in the State of Michigan* (Van de Lindt and Fu 2002), which estimates the reliability of MDOT bridges using Michigan WIM data; RC-1466, *LRFD Load Calibration for State of Michigan Trunkline Bridges* (Fu and Van de Lindt 2006), which calibrated the live load factor for design using LRFD based on WIM data; and R-1511, *Recommendations for Michigan Specific Load and Resistance Factor Design Loads and Load and Resistance Factor Rating Procedures* (Curtis and Till 2008), which developed modified load and rating models for LRFD/LRFR based on NCHRP 454 (Moses 2001) and RC-1601, *Side-By-Side Probability for Bridge Design and Analysis* (Eamon et al. 2014); to name few.

2.3 NCHRP Reports and Related Research

At a national level, various NCHRP reports have investigated development of rating vehicle configurations. This work includes NCHRP 108, *Bridge Weight-Limit Posting Practice* (Imbsen 1984); NCHRP 143, *Uniformity Efforts in Oversize/Overweight Permits* (Humphrey 1988); and NCHRP 359, *Bridge Rating Practices and Policies for Overweight Vehicles* (Fu and Fu 2006), which summarize bridge evaluation and rating practices. These studies found that a large variability exists in procedures throughout the US. NCHRP Report 368, *Calibration of LRFD Bridge Design Code* (Nowak 1999) describes the development of the LRFD load model discussed above, while NCHRP Reports 454, *Calibration of Load Factors for LRFR Bridge Evaluation* (Moses 2001) and 20-07(285), *Recalibration of LRFR Live Load Factors in the AASHTO Manual for Bridge Evaluation* (Sivakumar and Ghosn 2011) describe the development of the LRFR load

models. In NCHRP 454, it was found that characterizing the multiple presence (multiple trucks crossing the bridge simultaneously) probability for load modeling is difficult, as multiple presence is affected by traffic volume, speed, road grade, weather, traffic obstacles, truck grouping, as well as other parameters. Moreover, load effects from multiple presence are strongly interlinked with truck headway distance, defined as the distance between trucks, which is also a function of various road and traffic conditions. The LRFR live load factor is given in NCHRP Report 454 as a function of gross vehicle weight and expected maximum total weight of the rating vehicles and alongside vehicles.

In an effort to refine load models for special hauling vehicles, NCHRP 575, *Legal Truck Loads and AASHTO Legal Loads For Posting* (Sivakumar et al. 2007) developed a multiple presence model with additional complexity. Different multiple presence statistics were calculated for variations in bridge span as well as adjacent lane truck headway distances, where headway distance separations up to a maximum of 60 ft were considered to indicate multiple presence, depending on bridge span (headway distances greater than 60 ft were no longer considered to be a side-by-side event). Moreover, side-by-side presence was taken as a function of truck headway distance in adjacent lanes within the same direction of travel and bridge span. It was found that, depending on span and vehicle configuration, significant load effect from multiple presence could occur within headway distances of 10 to 60 ft. More precisely, it was found that for spans less than 100 ft, headway distance under 40 ft produced significant side-by-side multiple presence moments, while for longer spans, headway distances up to 60 ft should be considered. Using this model, multiple presence was calculated from WIM data from 18 states, including Michigan (on US-23) and Ohio (on I-75). It was found that multiple presence probabilities ranged from 1.4- 3.35%. These are much lower multiple presence probabilities than assumed in LRFD and LRFR, with the

maximum side-by-side probabilities of 3.35% occurring at a three-lane site with ADTT > 5,000 and 1.37% for a two-lane site with ADTT > 2,500.

NCHRP 683, *Protocols for Collecting and Using Traffic Data in Bridge Design* (Sivakumar et al. 2011) further developed the multiple presence model, considering various traffic configuration possibilities, including multiple side-by-side trucks in adjacent lanes, and developed multiple presence statistics from WIM data for different ADTT and bridge spans. It was suggested that multiple presence loads could be generated by developing single-lane truck weight probability densities, then combining the multi-lane effects by convolution, as suggested by Croce and Salvatore (Croce and Salvatore 2001), as well as Monte Carlo Simulation (MCS), while maximum load effects for longer time periods were estimated by statistical extrapolation. Note that MCS is a traditional technique often used for probabilistic simulation when actual field test or experimental results are unavailable. It involves generating random values for uncertain parameters in the model (random variables), based on their available statistical parameters, such as the mean, standard deviation, and assumed probability density function. These simulated values are then inserted within the model and the model is evaluated. Many such simulations are conducted to generate a large set of artificial model results. Limitations of the Croce and Salvatore model include an assumption that the GVW distribution is identical in adjacent lanes and that there is no correlation between truck weights. For the development of statistical load models used for reliability analysis, the upper tail of the distribution, where the heaviest vehicles are described, is most critical. However, it was noted that WIM data is particularly subject to various collection errors in this region, due to vehicle dynamics, tire configurations, and other factors.

NCHRP 683 further developed a general framework for data filtering, much of which is based on the FHWA Traffic Monitoring Guide (2001). Four main subtasks are described: data

filtering; review of eliminated data for verification; implementation of QC checks; and assessing the statistical adequacy of the data.

The purpose of the data filtering step is to flag collected results that appear to be unreliable or that may indicate an unrealistic vehicle. For example, axle weights and spacings that are unreasonably small or large; unreasonably high or low speeds (low-speed trucks are difficult to separate); and discrepancies in GVW and sum of axle weights. NCHRP 683, as well as other research efforts (O'Brien and Enright 2011; Pelphrey and Higgins 2006; Tabatabai et al. 2009), provide similar recommendations for a filtering process. The data recommended for flagging generally include: speeds below 10 or above 100 mph; truck length above 120 ft (or as appropriate for the expected local truck configurations); total number of axles less than 3 or greater than 13 (or as appropriate); first axle spacing less than 5 ft; any axle spacing less than 3.4 ft; sum of axle spacing greater than total truck length; individual axle greater than 70 kips (or as appropriate); steer axle greater than 25 kips or less than 6 kips; any axle less than 2 kips; GVW less than 12 kips or greater than 280 kips; sum of the axle weights is different from GVW beyond 5-10%.

Assessing the statistical adequacy of the data involves inspection of the confidence interval of the upper tail of WIM data. Because only a small sample of the entire truck population is collected from WIM data, using this limited data to model the entire population is associated with uncertainty. The uncertainty associated with the upper tail (heaviest) of the truck weights is of particular concern. This uncertainty is statistically quantifiable with confidence interval evaluation (Ang and Tang 2007). NCHRP 683 recommends that the 95% confidence interval of the upper 5% of truck weights from the WIM data is considered. That is, what range of uncertainty is associated with critical distribution parameters such as mean value and standard deviation, to a 95% level of confidence. Here, the distribution type that best-fits the upper 5% of the WIM data, per standard

goodness-of-fit tests, such as Kolmogorov-Smirnov, Chi-square, or Anderson Darling (Ang and Tang 2007), is determined. Then, the appropriate confidence interval is constructed for mean value and standard deviation. Thus, the range of values representing uncertainty in the mean and standard deviation can be quantified to a 95% confidence level. An unacceptably wide confidence interval indicates that an inadequate number of data were collected. In this case, additional data collection from these sites is recommended, or to remove the affected sites from the project database.

In NCHRP 683, several different truck placement possibilities that may cause variations in load effect were considered. Here, multiple presence statistics were generated for two “side-by-side” trucks, defined as two trucks in adjacent lanes overlapping by one-half of a truck length or more; two “staggered” trucks, defined as two trucks with an overlap less than one-half of a truck length but a gap between them of less than the bridge span; and for “multiple” trucks, where more than one truck side-by-side appears in both lanes.

The definition of multiple presence itself is not straightforward, as even holding various other factors such as ADTT and site location constant, the load effect caused by multiple presence varies greatly depending on truck headway distance in adjacent lanes, in the same lane, bridge span length, and truck weight correlations as well. Some approaches ignore these complexities and model multiple presence by placing two trucks exactly side-by-side on the analysis bridge. This provides an associated occurrence probability, such as in every 15 or 30 heavy truck passages, potentially based on WIM data (Moses 2001; AASHTO 2003). These multiple presence probabilities are directly calculated from the WIM data for various scenarios such as a ‘side-by-side’, ‘staggered’, or ‘multiple’ truck, for various span lengths. In this model, the precise definitions (truck headway distances and overlaps considered) used to characterize multiple presence statistics are determined based on those required to produce a significant increase in load

effect over that of a single lane truck load, such as suggested by NCHRP 575 (Sivakumar et al. 2007) and others (Fu and You 2009; O'Brien and Enright 2011). Fu and You (2009) used this approach and considered multiple presence to occur if an adjacent truck increased the single-lane truck moment by 20% or more. Based on an analysis of WIM data from New York, they found multiple presence probabilities from 0.4 - 3.5%, as a function of ADTT and bridge span. However, this approach generally will not produce the most accurate multiple presence load effects, as typically, all relevant load information simply cannot be captured using this method, as significant variations in load effect are neglected (Sivakumar et al. 2011; O'Brien and Enright 2011).

2.4 Collecting and Analyzing WIM Data

Various agencies have focused on the use of local WIM data to refine bridge rating models. These include the Texas, Missouri, Oregon, New York, and Wisconsin DOTs (Lee and Souny-Slitine 1998; Kwon et. al. 2010; Pelphery et al. 2006; Ghosn et al. 2011; Taatabai et al. 2009). The Texas Department of Transportation (TxDOT) developed a procedure to determine equivalent single axle loads (ESALs) from WIM-collected traffic volume and classification data (Lee, C.E. and Souny-Slitine 1998). The system was also used to monitor weekly and monthly data trends, such as the proportion of various vehicle classes and lane use. The system analyzed traffic data on-site by the WIM system computer and used an Excel spreadsheet for vehicle classification and calculation of ESALs. The method used traffic volume and vehicle class data rather than axle load data directly, but found that the cumulative ESALs at a site depend on the traffic volume and axle loads.

A significant complication that arises when using WIM data is that it generally contains a substantial number of erroneous records, requiring data filtering for accuracy. Various researchers have proposed WIM data management approaches, including Raz et al. (2004) and Monsere et al.

(2008), and Sivakumar et al. 2011, as discussed above. Raz et al. (2004) proposed a data mining approach for automatically detecting anomalies in WIM data. The procedure was useful for automatically detecting unlikely and erroneously classified vehicles, and could identify hardware or software problems in WIM systems. Monsere et al. (2008) studied methods for collecting, sorting, filtering, and archiving WIM data to permit development of long-term continuous records of high quality. The study used the WIM data archive to monitor WIM sensor health, develop loads for asphalt design and models for bridge rating and deck design. In addition, freight movement was monitored to develop volume, weight, safety, and time demands on highways. Data were analyzed and filtered to handle anomalous results. Axle load spectra and time of occurrence models were developed, and Monte Carlo techniques were used to generate load histories for pavement damage estimates. Moreover, side-by-side vehicular events were quantified using the precise time stamps available in the WIM data. The long term record was used to extrapolate the best possible statistical tail for single lane loading cases on bridges.

Pelphery et al. (2008) described a series of suggestions for collecting and analyzing WIM data that includes filtering, sorting, quality control, as well as how to use the data in a load factor calibration process. The data were cleaned and filtered to remove records with formatting mistakes, spurious data, and other errors identified by the following criteria: a record does not follow the general format pattern; GVW less than 2 kips or greater than 280 kips; GVW differs from the sum of axle weights by more than 7%; an individual axle is greater than 50 kips; the speed is less than 10 mph or greater than 99 mph; truck length is greater than 200 ft; the sum of the axle spacing lengths are less than 7 ft or greater than the truck length; the first axle spacing is less than 5 ft or any axle spacing is less than 3.4 ft; and the number of axles is greater than 13. Note the similarities to these recommendations and those made by NCHRP 683. A conventional and modified sorting

method for the WIM data were then developed and compared. The conventional method sorts vehicles based on their GVW, axle group weights, and truck length. This method accounts for the axle weights and spacing in assigning each vehicle to an appropriate weight table. The method tends to assign more vehicles to higher weight tables than the modified sort. The modified methods sort vehicles based only on their GVW and rear-to-steer axle length, and it does not account for axle groupings. This method assigns more vehicles to lower weight tables than the conventional sort. However, it produces higher coefficients of variation and hence higher live load factors, resulting in a more conservative method overall than the conventional method. In the study, the conventional sort method was used to calculate live load factors, because this was believed to better represent the traffic regulatory and enforcement procedures used. Additionally, only the top 20% of the truck weight data from each category was considered, as projected from the upper tail of the weight histogram.

As different load rating processes are used for legal and permit loads, the associated vehicle pools are best considered separately for accuracy. Unfortunately, this separation is often difficult, as recognized by various sources (Enright et al. 2015; Eamon et al. 2014; Sivakumar et al. 2011). Due to this difficulty, many researchers (Nowak 1993; Bailey & Bez 1999; Enright & O'Brien 2013; etc.) make no distinction between permit and standard trucks. Some more recent research efforts attempted to develop methods to separate the vehicle pools, such as by GVW (Enright and Obrien 2010), number of axles (Sivakumar et al. 2011), and axle spacing configuration (Enright et al. 2015).

2.5 Additional Load Model Development for Bridge Design and Rating

Early work includes that by Ghosn and Moses (1986), who, as a precursor to Nowak (1999) used reliability analysis with data from large scale field measurements of actual truck loadings and

bridge responses. The data were used to project maximum expected live loads in the lifetime of the structure and to calculate a safety index. A target safety index was extracted from these values and a new design procedure was proposed to achieve this target index to provide uniform reliability for the spans considered. The target safety index was derived from average AASHTO performance, and it was suggested that the approach could be extended to allow rating of existing bridges where load conditions were monitored by WIM systems.

Ghosn (2000) considered a reliability-based procedure to determine the optimal allowable loads on highway bridges considering static and dynamic effects and the effect of increasing the legal load limit on bridge safety. The procedure used to select the most appropriate allowable truck weight was developed as follows: choose suitable safety criteria; select an acceptable reliability level; choose a range of typical bridges (designed with different code criteria, span lengths, configurations, material types, and capacity levels); statistically describe the safety margins of these typical bridges (including the likelihood of overloads and simultaneous truck occurrence); calibrate a new allowable truck load; check the effect of the proposed truck loads on the existing network of bridges, and verify that the number of bridge deficiencies under the new regulation will be acceptable in terms of the additional costs required to maintain the existing bridge network. In this process, the maximum permissible live load moment would be determined by trial and error to satisfy the target safety index for all of the bridge types considered. The allowable truck loads that would produce the permissible live load envelope is then to be determined.

Rather than relying upon WIM, Fu and Hag-Elsafi (2000) suggested that live load model development could be based on records of granted overload permits. They presented a method to develop live load models based on the permit data, developed associated models for assessing reliability, and proposed permit-load factors for overload checking.

Miao and Chan (2002) developed a new approach for load model for short span bridges to obtain extreme daily moments and shears in simply supported bridges and compared the results to the traditional normal probability paper approach used to form the AASHTO LRFD load model. The method involved the following steps: calculate extreme daily bending moments and shear forces based on the WIM data; analyze the data statistically for load model parameters (axle weights, gross vehicle weights and axle spacing); divide the traffic into two types: loose and dense traffic status; use the Equivalent Base Length for modeling bridge live load models. In the procedure, MCS was used to simulate the complex interactions of random parameters governing truck loads. Axle spacings were divided into internal and tandem spacings. It was found that axle spacing was best modeled with a lognormal distribution, while axle weights as well as GVW best followed an inverse normal distribution. For lower traffic densities, where a single vehicle model can be used to represent load effects, the maximum value of axle weight and GVW for bridge design was found to follow an Extreme Type I distribution, while a Weibull distribution was found to better model more dense traffic, when multiple vehicles are on the span.

Ghosn et al. (2008) describes how site-specific truck weight and traffic data collected using WIM data can be used to obtain estimates of the maximum live load for a 75-year design life for new bridges as well as the two year return period for capacity evaluation of an existing bridge. It was determined that data from the upper tails of WIM data histograms from several sites match normal probability distributions, a finding allowing the application of extreme value theory to obtain the statistics of maximum load effect. Extreme value theory is a technique that can be used to extrapolate statistics of a small data pool to those describing a larger pool containing more extreme events; for example, the use of a year of traffic data to estimate maximum load effects over 75 years. It was also found that average bridge reliability varies considerably from state to

state, and that the reliability levels associated with two-lane load effects, as designed/rated, are significantly higher than the one-lane load effects. This occurs because of the lower number of side-by-side events, as well as the lower load effect produced by two-lane events when compared to the conservative multiple presence model used to calibrate the AASHTO LRFD Code. The conservativeness of the LRFD multiple presence assumptions are demonstrated by Ghosn (2008), who considered load data found in California, and determined that the LRFD load factor would require a reduction from 1.75 to 1.2 for the two-lanes loaded case to maintain a consistent reliability level with the one-lane loaded case.

O'Brien et al. (2010) predicted lifetime maximum truck load by using MCS to simulate traffic representative of measured vehicle data for a given bridge. Such parameters as GVW, number of axles, axle spacing, distribution of GVW between axles, and inter-vehicle spacing were included as parameters in the model. The study used WIM systems at two European sites and considered three different methods of modeling GVW, based on histograms of the weight data: parametric fitting, which produced a moderately good fit for most of the GVW range, but significantly underestimated the probabilities in the critical upper tail; nonparametric fitting, which produced a reasonable fit for the range of commonly observed GVWs, but presented problems in the upper region of the histogram where observations are few and there are gaps with no measured data, and GVWs heavier than the maximum measured value cannot be simulated; and semi-parametric fitting, which had the best accuracy in the critical tail region, and was the ultimately recommended approach.

For development of the Eurocode traffic live load model, load effects were estimated by extrapolating from WIM data as well as MCS. However, each lane was simulated independently

(Bruls et al. 1996; O'Connor et al. 2001), limiting the multiple presence model accuracy, similar to the NCHRP 683 model.

In addition to his work on the LRFD Code calibration, Nowak (Nowak et al. 2010) recently considered load models for long-span bridges, and developed a corresponding traffic simulation model for this case. It was found that the maximum load scenario is a traffic jam in which trucks tend to line up in one lane. He noted, however, that trucks are usually separated by lighter vehicles, and in this typical situation, a single overloaded truck did not have a significant effect on total load effect.

Ghosn et al. (2011), used the simplified adjustment procedure suggested in the MBE to develop a load and resistance factor rating method for permit and legal loading for New York State DOT from WIM data. Oregon DOT calibrated live load factors used for design from WIM data (Pelphery et al. 2006), and Wisconsin DOT statistically modeled maximum load effects from WIM data by fitting multi-modal distributions to axle loads and spacings, then using MCS with empirical copulas to model the axle load and spacing relationships (Taatabai et al. 2009).

Missouri DOT recently completed a recalibration of load factors for bridge design and rating, based on local WIM data (Kwon et al. 2010). Assumptions in the traffic model were that: minimum headway distance is 0.5 s; the time between trucks could be modeled with a shifted exponential distribution; and that 70% of trucks were in the right lane. Maximum load effects were then assumed to follow a Gumbel distribution, and extreme value theory was used for projection to the design maximum load. Similar to previous methods used to characterize multiple presence, the loads in adjacent traffic lanes were treated as independent.

Zhao and Tabatabai (2012) evaluated the effectiveness of the standard permit vehicle (Wis-SPV) used for bridge design and rating in Wisconsin, and proposed a 5-axle single-unit rating truck to supplement the existing evaluation vehicle.

These latest research efforts noted above relied heavily upon WIM data for model development. However, some work has been done to refine bridge evaluation procedures based on permit data alone (Fu and Hag-Elsafi 2000; Fu and Moses 1991; Fu and Hag-Elsafi 1996). Similarly, Chang et al (2015) recently verified the applicability of bridge rating vehicles to evaluate a superload using finite element modeling.

CHAPTER 3: WEIGH-IN-MOTION DATA ANALYSIS

3.1 WIM Data Analysis

DOTs collect weigh-in-motion (WIM) data for various reasons. FHWA requires that states provide monthly traffic reports and WIM data facilitates these counts. These data can be used to determine the truck over passenger vehicle ratio in traffic planning (Kamyab et al. 2019), and transportation (i.e., interchange) design (Molan et al. 2017; Mehrara Molan 2017; Molan et al. 2019). From the 41 Michigan Weigh-in-Motion (WIM) sites available with high-speed data (at least 100 Hz) collection necessary to accurately record vehicle configurations and positioning, a selection of 20 representative sites throughout the Michigan were chosen in four general average daily truck traffic (ADTT) categories, as shown in Table 3.1 and figure 3.1-3.4. Sixteen of these sites are on major interstate routes (i.e., I-94, I-69, I-75, and I-96) while four are on lower-volume state highways (i.e., US-127, US-2, and M-95). The data were collected for 34 months from February 2014 to January 2017 (excluding April and May 2014, which were unavailable).

Table 3. 1 WIM Sites.

Site	Location	ADTT	Site	Location	ADTT
High ADTT (≥ 5000)			Mid ADTT (~ 3500)		
9209	I-275	8529	5059	I-196	3376
7029	I-94	9479	6369	I-69	3870
8869	I-69	5983	6469	I-94	3966
9189	I-275	7313	5289	US-31	2903
7269	I-69	7050	5099	I-96	3245
8839	I-94	10041	Low ADTT (~ 1500)		
7169	I-94	8091	4049	I-75	907
7219	I-94	9265	6429	I-75	1732
7159	I-94	14161	8029	US-127	1995
9699	I-75	16516	Very Low ADTT (~ 400)		
			1199	M-95 (UP)	361
			2029	US-2 (UP)	491

The WIM data used were collected for 34 months from February 2014 to January 2017 (excluding April and May 2014, which were unavailable). Out of the 159,513,070 total vehicles represented by all high-speed WIM sites in this period of time, the 20 sites selected contained 101,417,034 vehicles (63.6% of the total available).

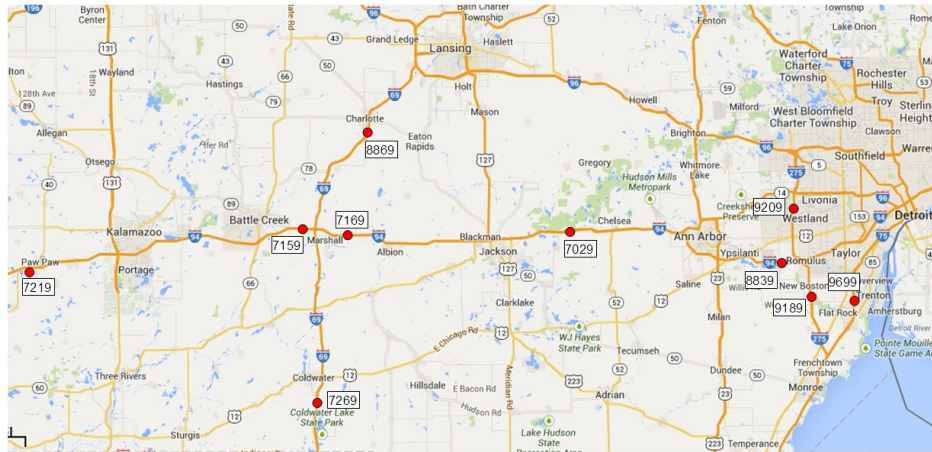


Figure 3.1 WIM Sites With ADTT ≥ 5000 .



Figure 3.2 WIM Sites With ADTT ~ 3500 .

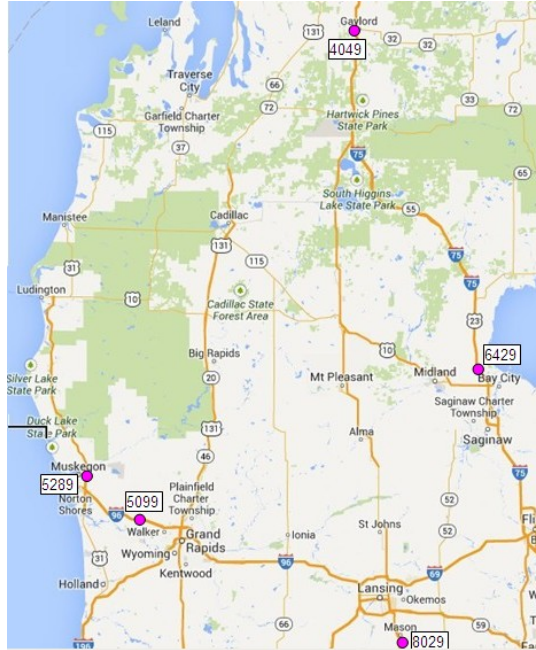


Figure 3.3 WIM Sites With ADTT ~1500.

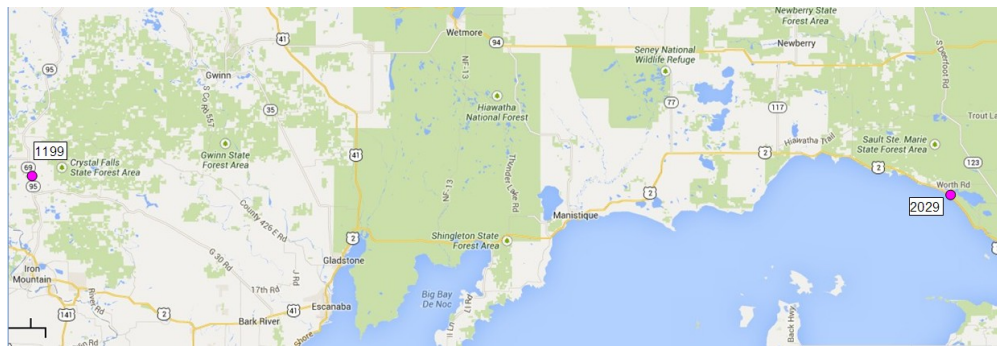


Figure 3.4 WIM Sites With ADTT ~400.

Each WIM station employs an automatic filtering system that removes the majority of non-critical traffic from the database. These lightweight vehicles include motorcycles, cars, and light trucks (vehicle classes 1-3). These vehicles are summarized in Table 3.2.

Table 3. 2 Small Vehicles Filtering Criteria.

Class	Vehicle	Axles	Axle Spacing (ft)				Weight (k)
			1st	2nd	3rd	4th	
1	Motorcycle	2	0.1-6				0.1-3
2	Car	2	6-10.1				1-8
3	Truck	2	10.1-16				1-9
2	Car, 1-Axle Trailer	3	6-10.1	6-30			1-12
3	Truck, 1-Axle Trailer	3	10.1-16	6-30			1-15
2	Car, 2-Axle Trailer	4	6-10.1	6-30	1-12		1-12
3	Truck, 2-Axle Trailer	4	10.1-16	6-30	1-12		1-15
3	Truck, 3-Axle Trailer	5	10.1-16	6-30	1-12	1-12	1-15

Additional data filtering criteria were employed to eliminate unrealistic vehicles from the database. These criteria are given in Table 3.3. Additional criteria used to categorize a vehicle as legal or extended permit (LEP) are given in Table 3.4.

Overall, 11,849,377 (11.7%) of the results from the 20 selected sites were removed due to data filtering. From the remaining 89,567,657 vehicle records, 88,943,172 (99.3%) fall into legal and extended permit categories. Note that a 5% tolerance is given to classify these vehicles, in terms of axle weight, axle spacing, and gross vehicle weight (GVW).

Table 3. 3 Filtering Criteria.

Criteria Type	Criteria for Elimination
Vehicle Class	Class 1-3 (automatic elimination)
Gross Vehicle Weight	GVW < 12 kips (no upper limit)
Axle Weight	GVW differs from axle weight sum by more than 10%
Vehicle Length	First Axle > 25 kips or < 6 kips Any axle > 40 kips or < 2 kips
Axle Spacing	Length < 5 ft Length > 200 ft
Speed	First axle spacing < 5 ft Any axle spacing < 3 ft
Number of Axles	Speed < 20 or > 100 MPH for GVW vehicles < 200 kips Speed < 20 or > 85 MPH for GVW vehicles > 200 kips
	Number of axles < 2 or > 13*

* The WIM equipment does not store axle weight and configuration data beyond 13 axles.

Table 3. 4 Legal/Extended Permit Filtering Criteria.

Vehicle Type	Criteria
Legal, GVW > 80 kips	For axles spaced ≥ 9 ft, axles ≤ 18 kips
	For axles spaced from 3.5 – 9 ft, axles ≤ 13 kips
	For axles spaced < 3.5 ft, axles ≤ 9 kips
Legal, GVW < 80 kips	Any individual axle ≤ 20 kips
	Sum of tandem axles ≤ 34 kips
Extended Permit (Construction)	Length ≤ 85 ft
	Any axle ≤ 24 kips
	GVW ≤ 150 kips

To confirm the reasonableness of the WIM data, several checks were implemented as recommended in NCHRP 683 (2011). Among these, the following numerical comparisons for 5-axle (Class 9 or 3S2) semi-trailer truck data were considered.

Drive tandem axle spacing. The mean distance between the drive axles is compared to a standard value of 4.3 ft (Fu et al. 2003). The computed mean value among all sites is 5.1 ft, while the median and mode are both 4.3 ft. Although the mean value found is about 1 ft longer than the NCHRP value, since most vehicles have the expected value of 4.3 ft, the results appear reasonable. The mean value from 2011-2012 WIM data was found from 4.5-4.9 ft. (Eamon et al. 2014). This appears to indicate a trend of more modern vehicles having greater axle spacing.

Drive axle weight. The mean drive (2nd) axle weight is compared to the mean values found in NCHRP Report 505 (2003), which was taken as a maximum of 13 kips. The mean drive axle found from all sites was 11 kips with a median of 10.6 kips. The mean drive axle weight found from the analysis of 2011-2012 WIM data was found to be 11.4 kips (Eamon et al. 2014).

Steering axle weight. The typical range for steering axle weight was reported to be 9 - 11 kips (NCHRP 683). The mean steering axle found was 10.8 kips, with a median of 10.6 kips and mode of 11.0 kips. These values match those found in the 2011-2012 WIM data analysis (Eamon et al. 2014).

GVW histogram. The histogram is expected to have a bimodal shape with peaks near 30 and 72-

80 kips, representing unloaded and loaded trucks (NCHRP 683). The site histograms were found to have a similar bimodal shape with nearly identical expected peaks of 32 and 73 kips.

The all vehicles and top 20% (heaviest) MI-LEP GVW, length, and number of axles frequency histogram are presented in Figures 3.5-3.10.

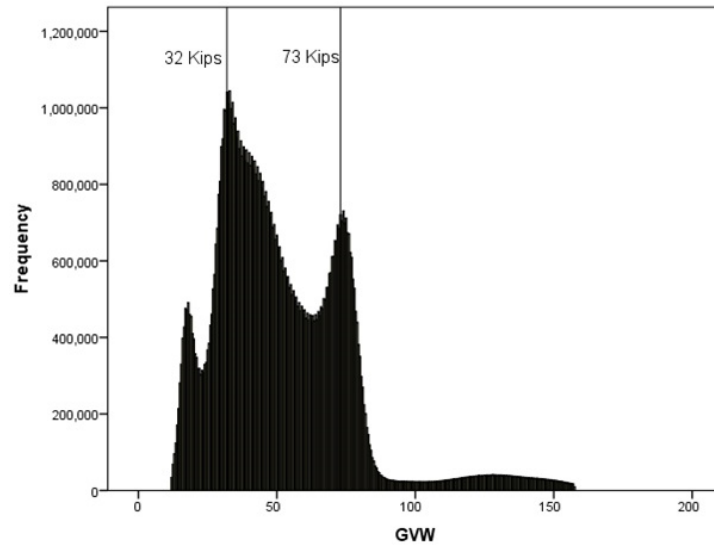


Figure 3.5 All MI-LEP GVW (kips) Frequency Histogram.

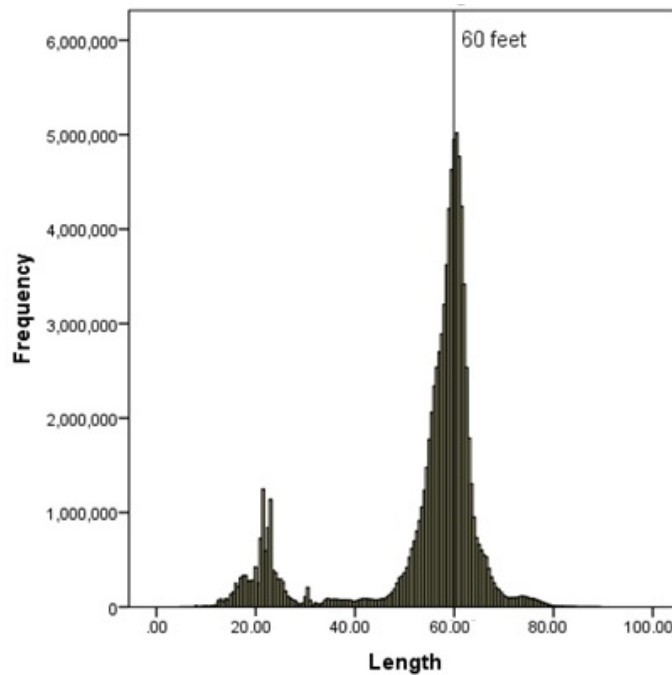


Figure 3.6 All MI-LEP Vehicle Length Frequency Histogram.

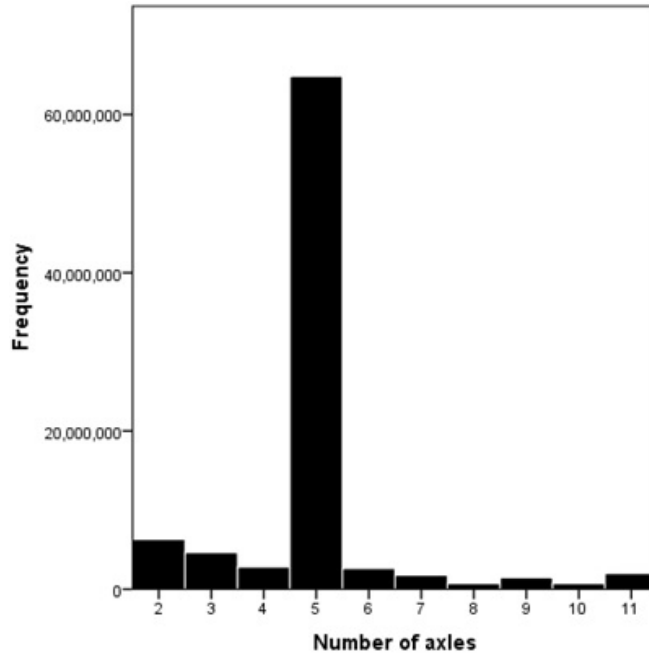


Figure 3.7 All MI-LEP Number of Axles Frequency Histogram.

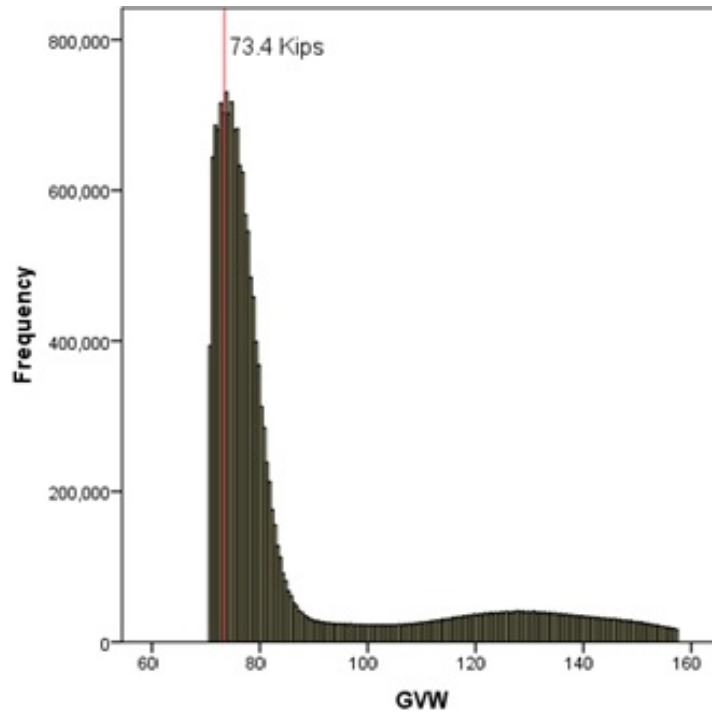


Figure 3.8 Top 20% MI-LEP GVW (kips) Frequency Histogram.

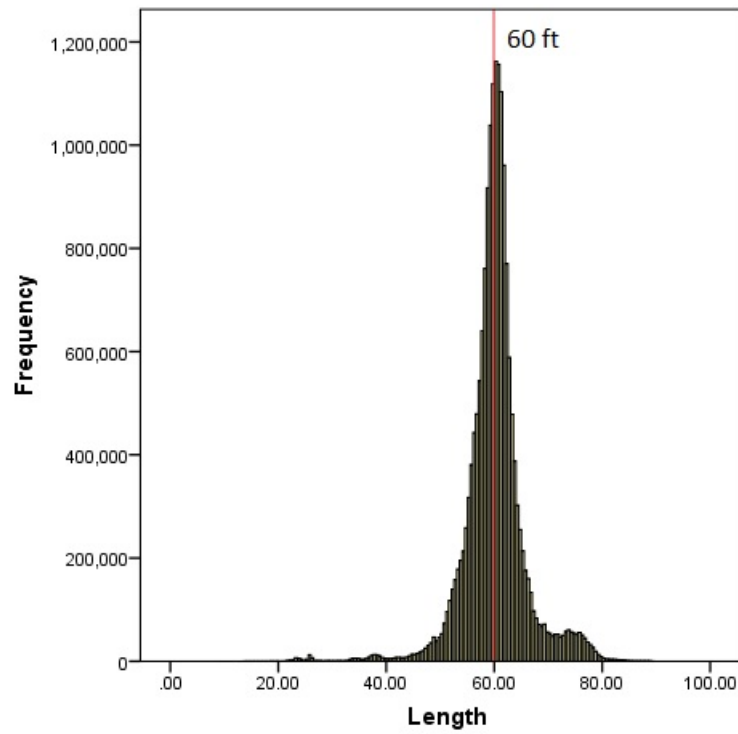


Figure 3.9 Top 20% MI-LEP Vehicle Length (ft) Frequency Histogram.

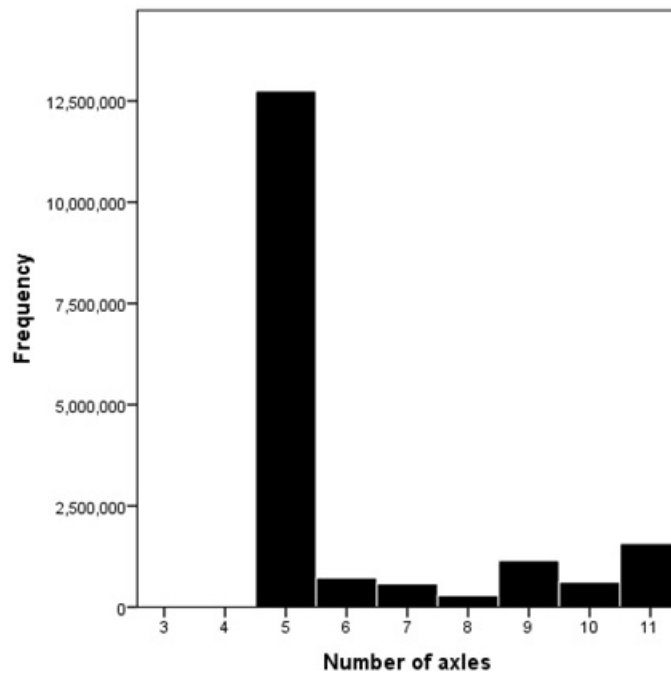


Figure 3.10 Top 20% MI-LEP Vehicle Number of Axles Frequency Histogram.

MI-LEP vehicle statistics (after filtering) are given in Table 3.5. In the table, percentiles are given independently for each parameter considered and do not necessarily represent the same vehicle. Note that a 5% tolerance is given to classify these vehicles (MI-LEP), in terms of axle weight, axle spacing, and gross vehicle weight (GVW).

Table 3. 5 Vehicle Statistics for LEP Vehicles.

	No. Axles	Vehicle Length (ft)	GVW (kips)
Mean	5	54.0	51.8
Median	5	58.7	46.9
Mode	5	60.4	32.4
Minimum	2	5.0	12.0
Maximum	11	89.2	157.5
80%	5	61.6	71.2
85%	5	62.2	74.3
90%	6	63.2	77.6
95%	9	65.7	88.3
98%	11	69.8	130.6
99%	11	74.0	141.8
99.9%	11	80.3	155.3

As Michigan has unusually high legal vehicle weights, up to approximately twice the Federal limit for some configurations, a vehicle pool representative of most other states that follow the Federal limit was also developed. This alternative database was created by imposing more restrictive limits based on the Code of Federal Regulations Part 658.17, which represents a simplified version of the axle weight and spacing rule commonly known as the “Bridge Formula”. The filtering criteria are presented in Table 3.6. Approximately 78.4 million vehicles fell into this group. Simplified CFR vehicle statistics (after filtering) are given in Table 3.7.

Table 3. 6 Simplified CFR Filtering Criteria.

Vehicle Type	Criteria
--------------	----------

Simplified CFR	$GVW \leq 80$ kips Any axle ≤ 20 kips For axles spaced from 3.33 – 8 ft, Sum of tandem axles ≤ 34 kips
----------------	------------------------------------------------------------------------------------------------------------------------

Table 3. 7 Vehicle Statistics for Simplified CFR Vehicles.

	No. Axles	Vehicle Length (ft)	GVW (kips)
Mean	5	54	46
Median	5	59	44
Mode	5	60	33
Minimum	2	5	12
Maximum	11	89	80
80%	5	61	64
90%	5	63	72
95%	6	65	75
98%	7	68	77
99%	9	71	78
99.9%	11	79	80

All vehicles and top 20% (heaviest) Simplified CFR GVW frequency histogram are presented in Figures 3.11-3.12.

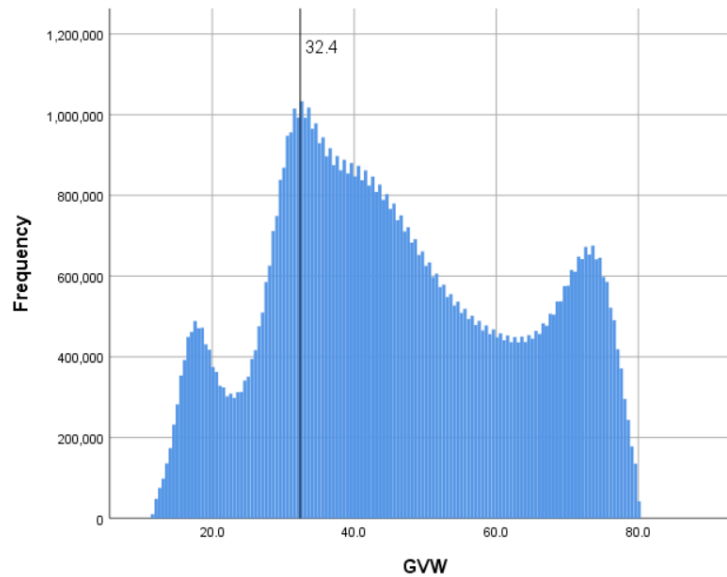


Figure 3.11 All Simplified CFR GVW (kips) Frequency Histogram.

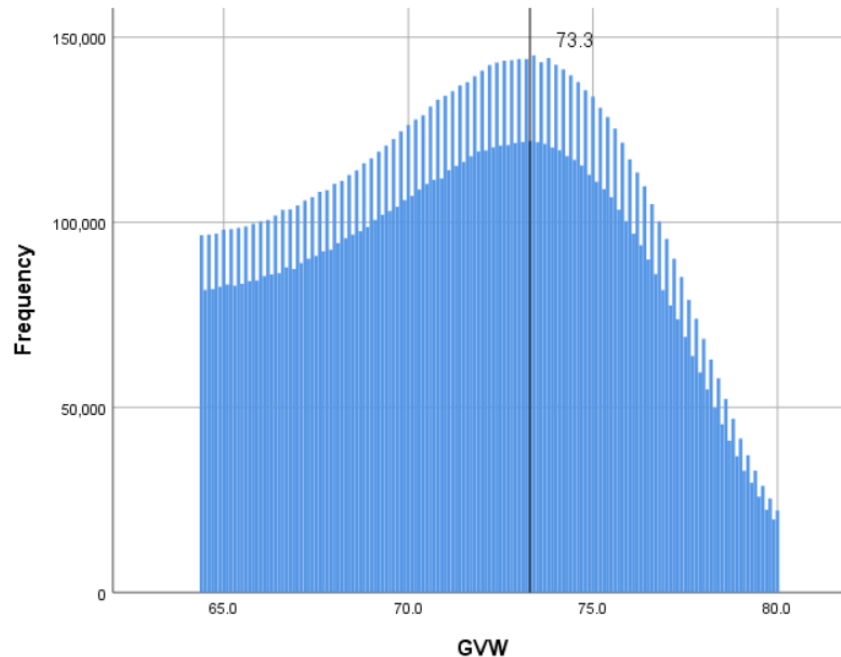


Figure 3.12 Top 20% Simplified CFR GVW (kips) Frequency Histogram.

3.2 Vehicle Load Effects

Vehicle load effects were calculated for span lengths of 20-200 ft in increments of 20 ft. Considered effects were maximum simple span moments and shears. Load effects were calculated by incrementing vehicle configurations recorded from the WIM data across the considered span lengths and recording maximum load effect values. Due to the large volume of data considered, to maintain computational feasibility, the speeds of multiple presence vehicles were taken to be identical, such that their positions relative to one another do not change over the span length. Overall results of MI-LEP single vehicles load effects are given in Figures 3.13-3.14 below, where figures present load effect values per span and corresponding vehicle percentiles in increments between 80 and 99.9% for the load effect in question. Figures 3.15-3.16 compare MI-LEP single vehicle load effects to following and two lane load effects. In the Figures 3.15-3.16, *Max Single* means maximum load effect caused by a single vehicle, *Max Single+Following* means greatest of maximum load effect caused by a single vehicle or multiple (“following”) vehicles in a single lane,

and *Max Two-Lane* means maximum load effect caused by vehicles in adjacent lanes. The value reported represents the entire two lane load effect on the bridge. In most cases of simple span load effects, the maximum two lane load effect exceeded the maximum following load effect, which in turn exceeded the single vehicle load effect (note that the two lane load effect represents the total load effect in both lanes). In the figures 3.13-3.14, “MDOT” refers to the governing (maximum) load effects of MDOT 28 legal trucks (more described later). As shown in Figures 3.13-3.14, although the maximum load effects for two lane and following vehicles may be significantly higher than for single vehicles, for moments and shears, no significant difference among single and following occurs throughout the vast majority of the vehicle sample, even up to the 99.9 percentile. Two lane moments and shears are significantly greater than single vehicle effects throughout the majority of the vehicle sample considered, and, as following effects, generally increase as span length increases. Cumulative distribution functions (CDFs) of single vehicle load effects as well as two-lane vehicle load effects are presented in Figures 3.17-3.20. Note that here only a CDF of single vehicle load effects for 200 ft. span length is presented. More results can be found in Eamon and Siavashi (2018).

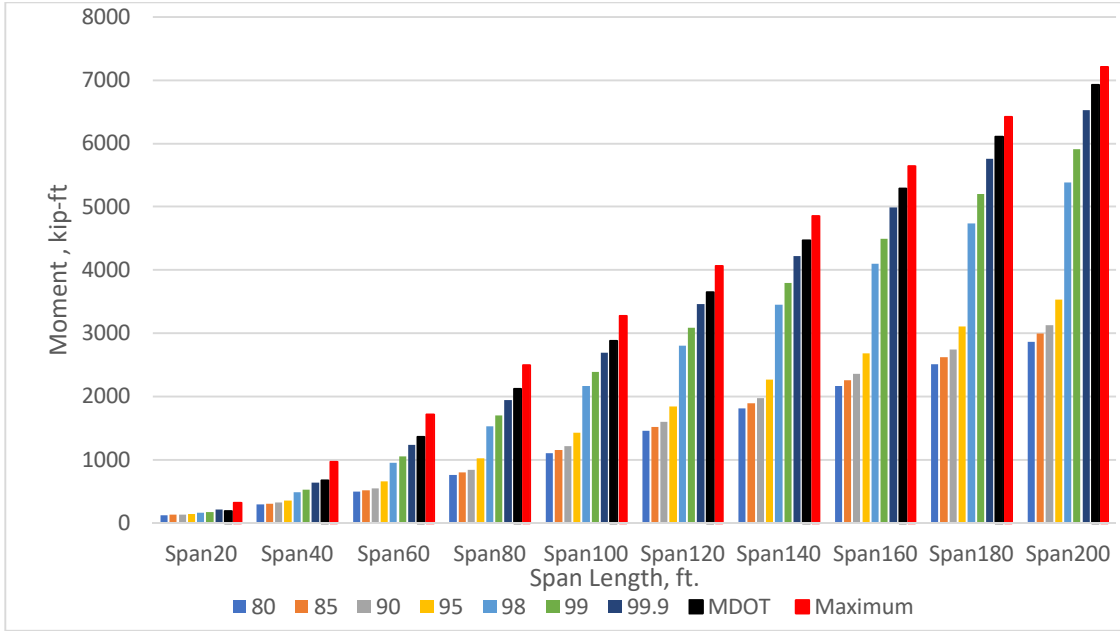


Figure 3.13 Simple Span Moments, Single LEP Vehicles.

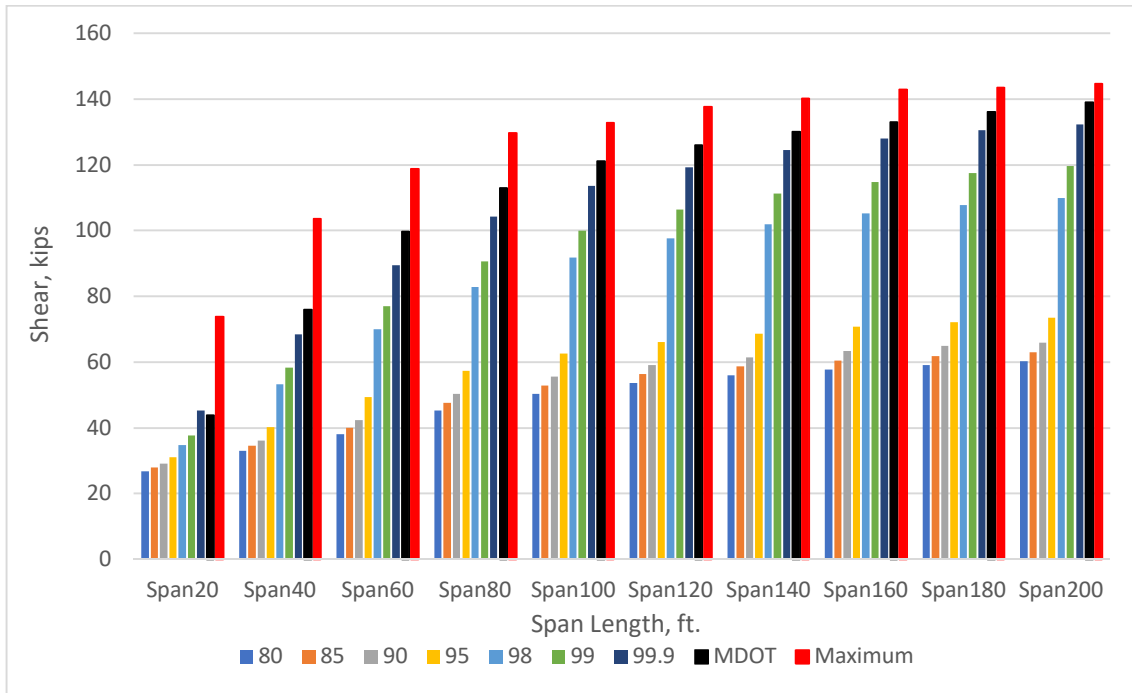


Figure 3.14 Simple Span Shears, Single LEP Vehicles.

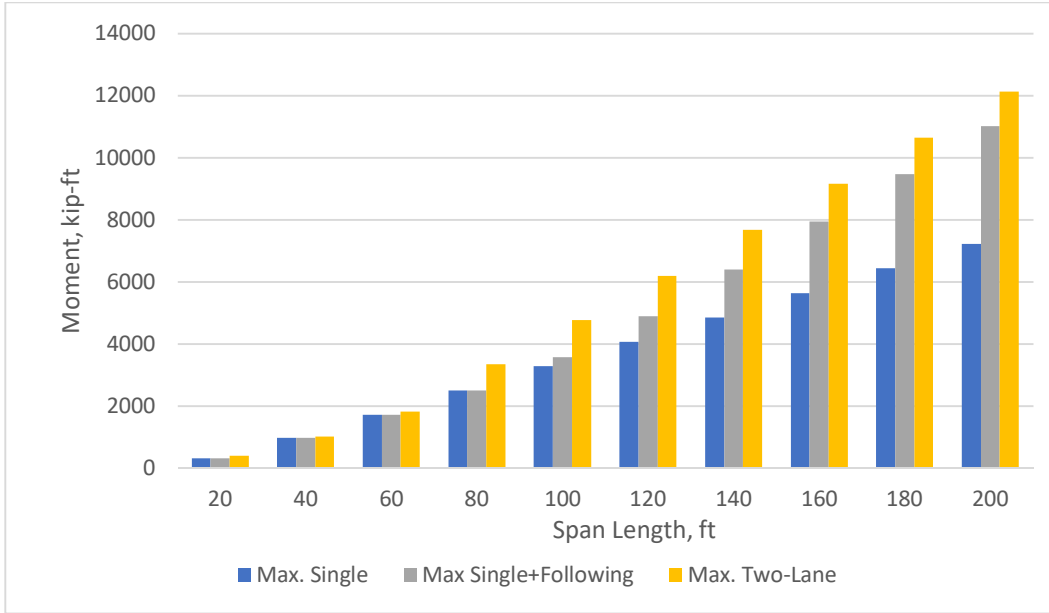


Figure 3.15 Maximum Single, Following, and Side-by-side Simple Span Moments.

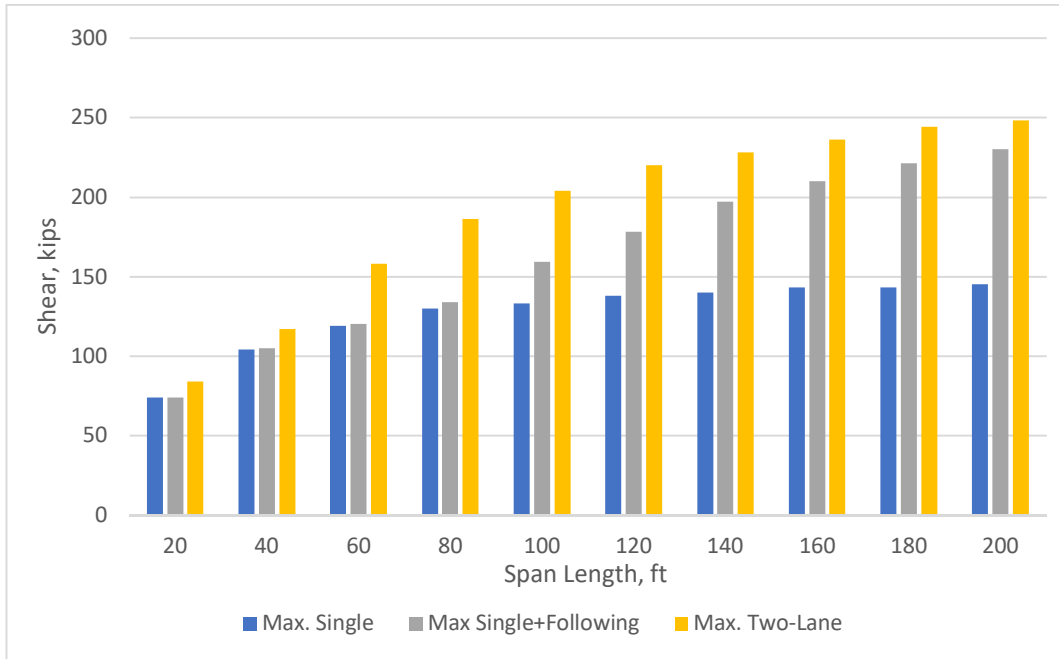


Figure 3.16 Maximum Single, Following, and Side-by-side Simple Span Shears.

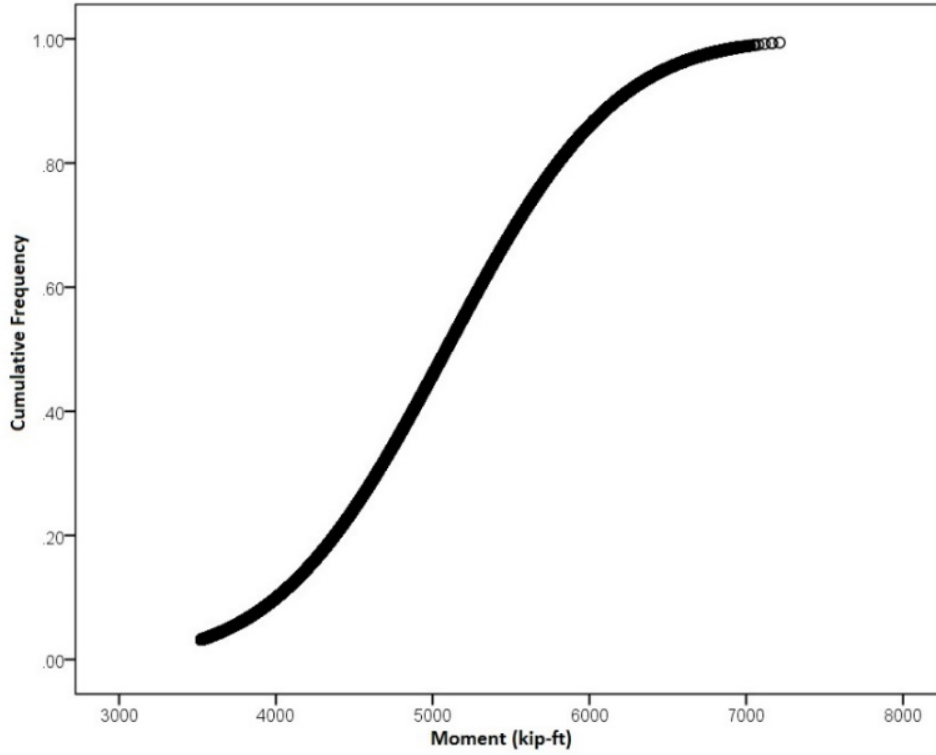


Figure 3.17 CDF of Top 5% of Simple 200 ft Span Moments, Single LEP Vehicles.

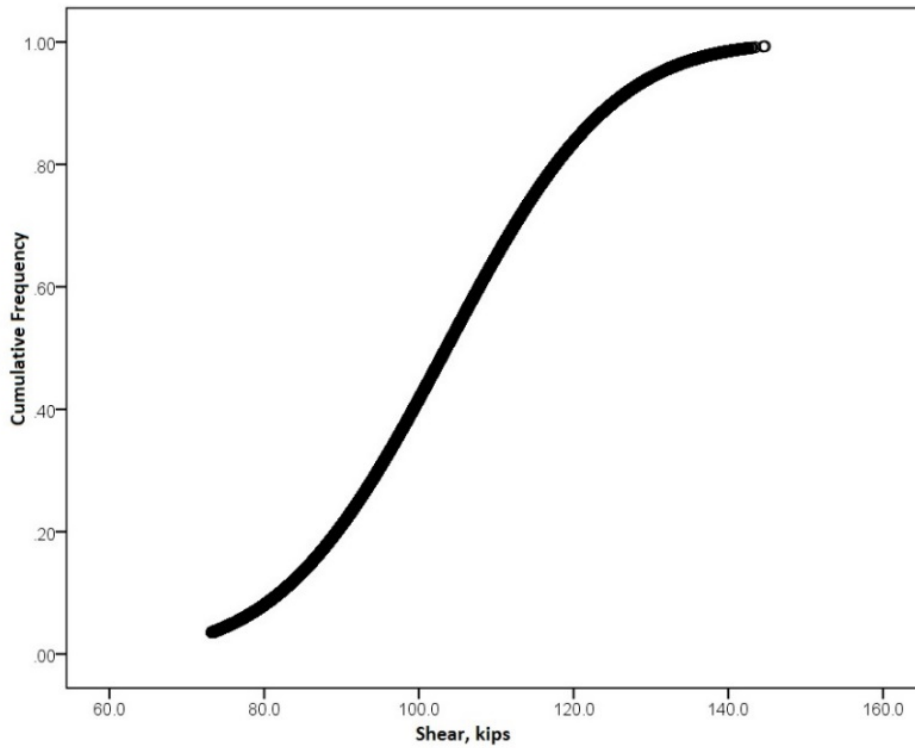


Figure 3.18 CDF of Top 5% of Simple 200 ft Span Shears, Single LEP Vehicles

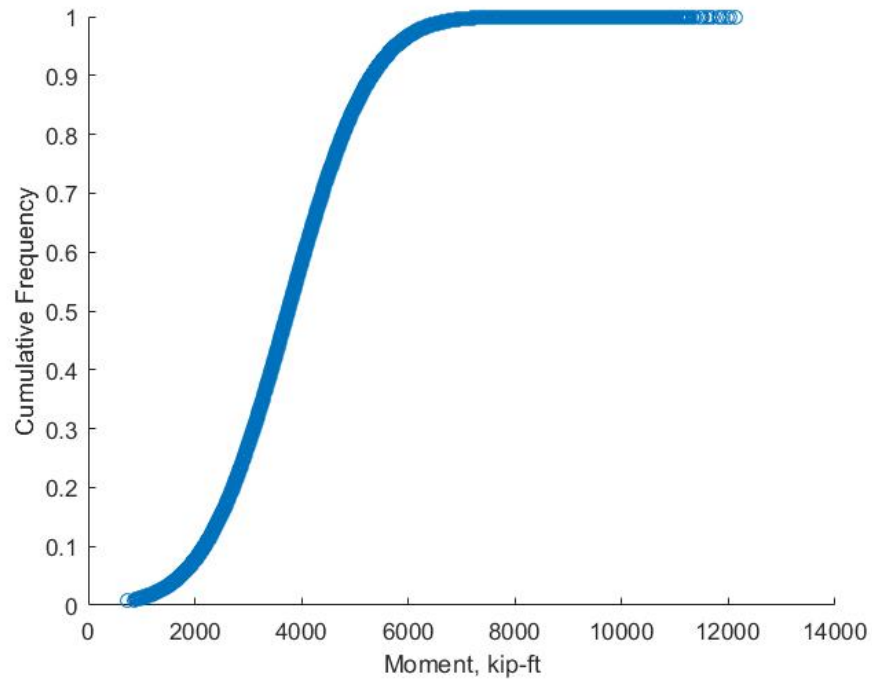


Figure 3.19 CDF of Simple 200 ft Span Moments, Two Lane LEP Vehicles.

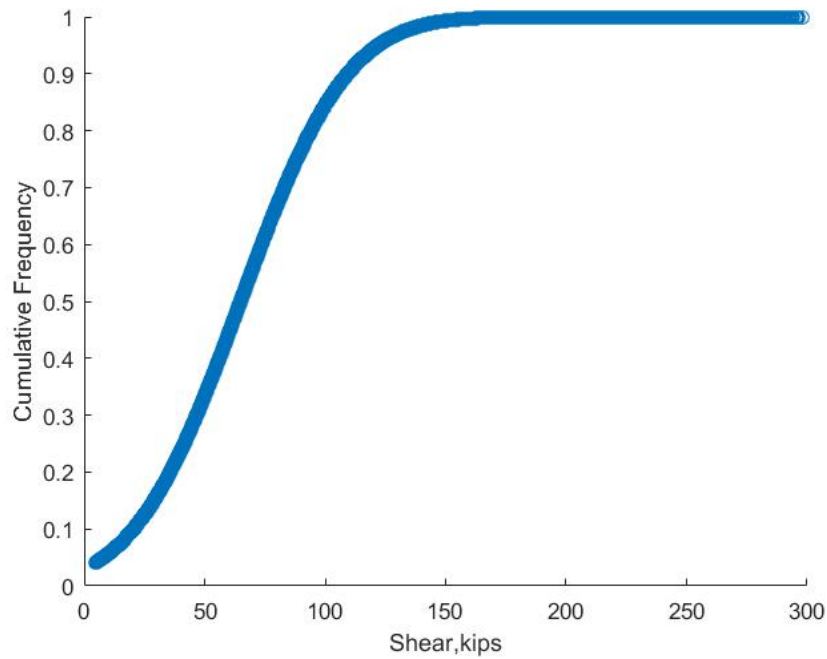


Figure 3.20 CDF of Continuous 200 ft Span Shears, Two Lane LEP Vehicles.

Overall results of Simplified CFR single vehicles load effects are given in Figures 3.21-3.22 below, where figures present load effect values per span and corresponding vehicle percentiles in increments between 80 and 99.9% for the load effect in question. In the Figures 3.21-3.22, “AASHTO Trucks” refer to the governing (max) load effects of AASHTO 3 legal trucks (more described later).

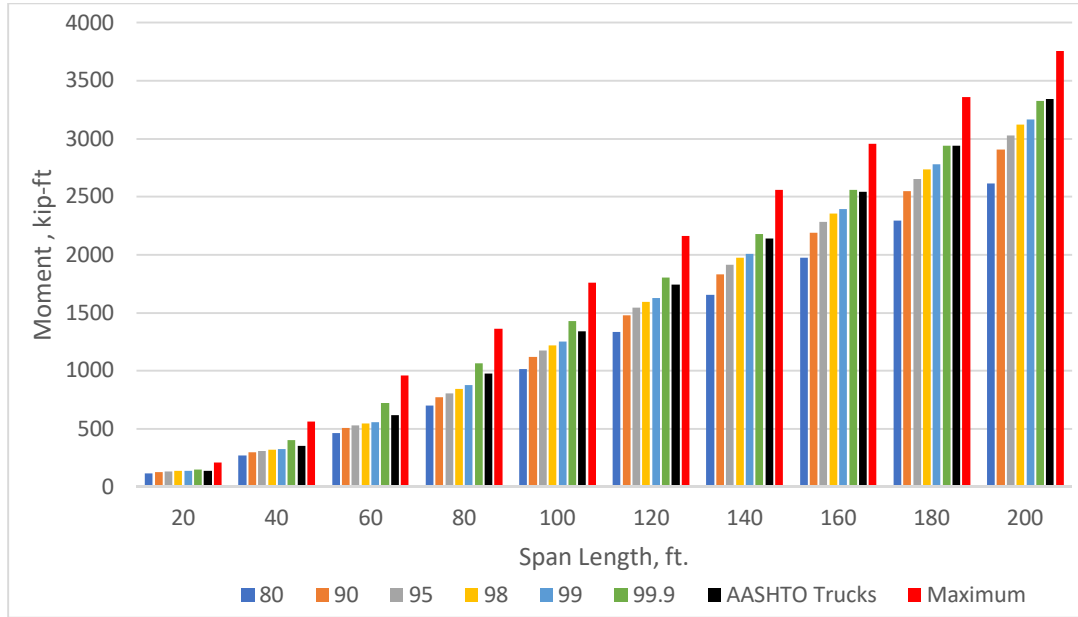


Figure 3.21 Simple Span Moments, Single Simplified CFR Vehicles.

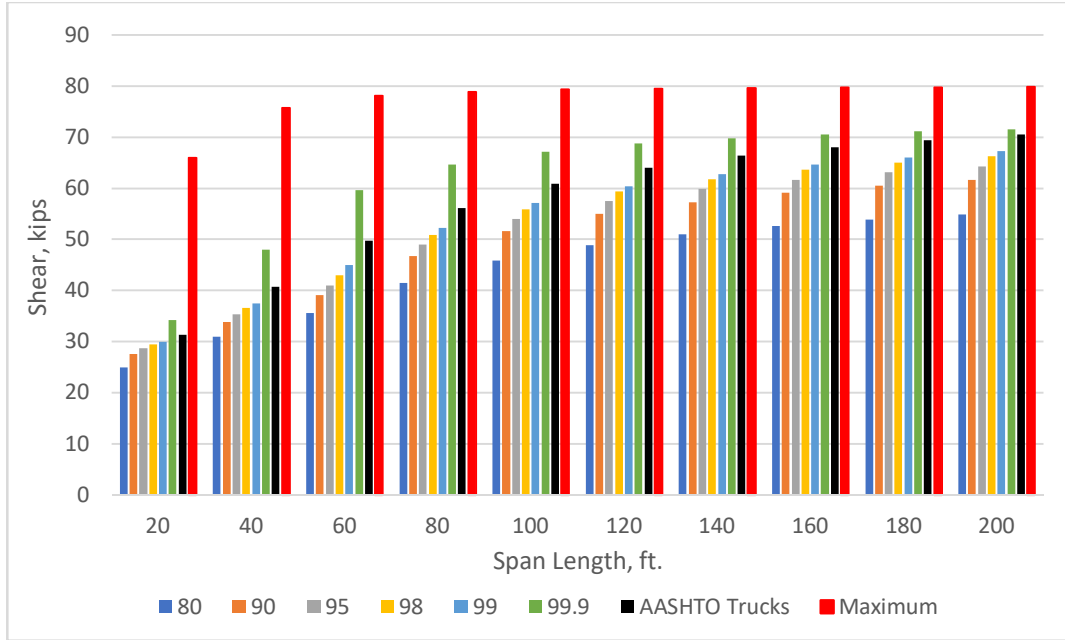


Figure 3.22 Simple Span Shears, Single Simplified CFR Vehicles.

3.3 Determination of Required Load Effects

Required load effects to rate bridges for LEP vehicles are determined such that bridge girders meet the minimum and target reliability levels specified in the MBE calibration. To be consistent with the current LRFR procedure, this study follows the general framework established in NCHRP Reports 683 (use of WIM data in design calibration) and 20-07(285) (LRFR Calibration). This research only concerns the Strength I limit state, where it is assumed that extended permit vehicles are included along with legal vehicles within the legal load rating framework. Strength I refers to strength-based limit states that involve the normal use of the bridge. Maximum load effects are based on a 5-year return period. The Strength I rating calibration will use the data pool of WIM MI-LEP vehicles, as described earlier. Here it is assumed that illegal vehicles are not accounted for in the Strength I framework, but will be considered in a future Strength II rating calibration effort. Note that the same procedure can be applied for simplified CFR data pool. For the Strength I rating calibration, a target reliability index for rating is specified

as 2.5, with a minimum limit of 1.5 for any specific bridge girder case. A rating factor of 1.0 implies that if a bridge is designed to the legal load (rather than the design load), the reliability index for the structure will match the target (rating) level. Practically, the analysis is done by determining the hypothetical nominal capacity of the bridge as a function of a required live load effect in place of the design load, along with the corresponding AASHTO (LRFR or LFR, as appropriate) rating procedure. Once nominal capacity is determined (as a function of the unknown required live load), the rating factor is set at 1.0 and the load effect is adjusted such that the required reliability level is met. The procedure is as follows:

1-Lane Load Effects

1. A selection of representative WIM sites is used to develop load effects. Individual site data must be kept separate, such that site-to-site variation in the results can be computed. However, mean results from the pool of sites are used to generate load effect statistics. This process is described in the *Data Projection* section below. The ten highest ADTT sites given in Table 3.1 were used for this procedure.

2. For each site, the vehicle load effects (moments and shears) are determined, as described earlier, above, where actual following vehicle (i.e. vehicle trains) load effects are included.

3. A data projection technique based on an Extreme Type I distribution fit, as described below, is used to estimate the mean and the coefficient of variation (COV, or V) of the maximum load effect, \bar{L}_{\max} and V_{\max} , respectively, at 5 years.

4. \bar{L}_{\max} is determined as a load effect on a selection of hypothetical bridge girders. First, a selection of typical bridges is compiled such that dead load effects and girder distribution factors (DF)s can be calculated. The selection of bridges used for rating in this study is given near the end of this Chapter.

\bar{L}_{\max} for 1-lane moment on a girder ($\bar{L}_{\max 1M}$) is given by:

$$\bar{L}_{\max 1M} = \bar{L}_{\max} * IM * DF_1/1.2 \quad (3.1)$$

where DF_1 = the 1-lane DF, as given in AASHTO LRFD. Note that it is divided by 1.2 to remove the multiple presence factor, which is directly accounted for in \bar{L}_{\max} .

For most steel, prestressed concrete, and reinforced concrete girder bridges supporting a concrete deck, the AASHTO LRFD 1-lane DF for moment is taken as:

$$DF_1 = 0.06 + \left(\frac{S}{14}\right)^{0.4} \left(\frac{S}{L}\right)^{0.3} \left(\frac{K_g}{12Lt_s^3}\right)^{0.1} \quad (3.2)$$

where $K_g = n(I + Ae_g^2)$; A is the beam cross-sectional area; e is the distance between the centroids of the beam and deck; I is for the beam; and n is the modular ratio of the beam and deck.

For most girder bridges, the AASHTO LRFD 1-lane DF for shear is taken as:

$$DF_1 = 0.36 + \left(\frac{S}{25}\right) \quad (3.3)$$

Expressions in AASHTO LRFD for the other types of structures considered (for example, spread and side-by-side box beam bridges), or those with geometric parameters outside of the range of that specified for the above equations are similarly used when appropriate.

IM = the impact factor, taken as a mean value of 1.13 for one lane loaded with heavy vehicles, as used in the MBE calibration (Sivakumar et al. 2011).

5. Continue to step 6 below.

2-Lane Load Effects

1. A selection of representative WIM sites is used to develop load effects. Individual site data must be kept separate, such that site-to-site variation in the results can be computed. However,

mean results from the pool of sites are used to generate load effect statistics. The same sites considered for the 1-lane effects are considered for 2-lane load effects.

2. For each site, the 2-lane vehicle load effects (moments and shears) are determined, as described earlier, above, where actual following vehicle (i.e. vehicle trains) load effects are included in each lane. Here, a complication arises in that there is no DF equation in AASHTO that allows for side-by-side vehicles of different weights and configurations. An analysis technique such as FEA or grillage modeling would be ideal in this case. However, the time involved to construct detailed numerical models for each of the many different bridge configurations considered is not feasible. Therefore, an approximate method is used, as suggested by Moses (2001) and implemented by Sivakumar et al. (2011a,b). Here, the total 2-lane moment effect (M_{12}) is given by:

$$M_{12} = M_1 * DF_1 + M_2(DF_2 - DF_1) \quad (3.4)$$

where

M_1 = the moment due to the vehicle(s) in lane 1.

DF_1 = the AASHTO LRFD single lane DF (after dividing out the 1.2 multiple presence factor).

M_2 = the moment due to the vehicle(s) in lane 2 (while in the recorded spatial position on the span relative to the lane 1 vehicle(s)).

DF_2 = the AASHTO LRFD 2-lane DF, which for most steel, prestressed concrete, and reinforced concrete girder bridges supporting a concrete deck, is given as:

$$DF_2 = 0.075 + \left(\frac{S}{9.5}\right)^{0.6} \left(\frac{S}{L}\right)^{0.2} \left(\frac{K_g}{12Lt_s^3}\right)^{0.1} \quad (3.5)$$

For shear, the same process is followed above using equation 6.4, but 1 and 2-lane moment DFs are replaced with shear DFs. For example, for most steel, prestressed concrete, and reinforced concrete girder bridges supporting a concrete deck, the 2-lane shear DF is given as:

$$DF_2 = 0.2 + \left(\frac{S}{12}\right) - \left(\frac{S}{35}\right)^{2.0} \quad (3.6)$$

This is done for each of the 2-lane load effects from the site considered.

3. The same data projection technique used for 1-lane load effects is also used for 2-lane effects.

The projection is used to estimate the mean and COV of the maximum load effect, \bar{L}_{\max} and V_{\max} , respectively, at 5 years, from the data set of the 2-lane load effects found in step 2, above.

4. \bar{L}_{\max} is determined as a load effect on the selection of hypothetical bridge girders. The same structures used for the 1-lane load effects are used here as well. \bar{L}_{\max} for 2-lane moments on a girder ($\bar{L}_{\max 2M}$) is given by:

$$\bar{L}_{\max 2M} = \bar{L}_{\max} * IM \quad (3.7)$$

Here, the DF is already embedded in the data, in Steps 2 and 3. IM is taken as a mean value of 1.10 for two lanes loaded with heavy traffic, as used in the MBE calibration (Sivakumar et al. 2011).

5. Continue to step 6 below.

For Both 1 and 2-Lane Load Effects (separately):

There are various uncertainties that must be accounted for in the live load model. These are as follows:

a) Uncertainty in the future data projection (V_{proj}). This is V_{\max} , as found from the projection technique, as in Step 3 above (determined as $V_{proj} = V_{\max} = \sigma_{L_{\max}} / \bar{L}_{\max}$, where $\sigma_{L_{\max}}$ and \bar{L}_{\max} are found from the projection; see below).

b) Uncertainty in mean maximum load effects among different sites (V_{site}). Here, V_{site} can be computed directly as the COV of \bar{L}_{\max} values found from the different sites, for 1- and 2 lane load

effects, for the particular load effect case considered. Note that different values in V_{site} will occur depending on bridge span and configuration.

c) Uncertainty in \bar{L}_{max} based on the WIM data at a particular site (V_{data}). There is no direct way to assess this uncertainty. However, Sivakumar et al. (2011) suggests that it be estimated based on a standard deviation taken equal to the value of data at the 95% upper and lower confidence intervals (assessed by using a proportion confidence interval based on an estimated 50-interval CDF), where it is assumed that these values fall within 1.96 standard deviations of the mean. Thus, the standard deviation to use for V_{data} , $\sigma_{V_{\text{data}}}$, is given by:

$$\sigma_{V_{\text{data}}} = |(d_{95}) - \bar{x}| / 1.96 \quad (3.8)$$

where

(d_{95}) = the upper 95% upper or lower confidence interval value for \bar{L}_{max} . \bar{x} = the mean; i.e. \bar{L}_{max} .

COV (V_{data}) can then be computed as usual (i.e. = $\sigma_{V_{\text{data}}} / \bar{x}$). V_{data} is reported to be approximately 2% for 1-lane effects and 3% for 2-lane effects, for 1 year of WIM data (Sivakumar 2011). Based on the analysis of WIM data conducted by Eamon et al. (2014), it was found that V_{data} was below 2% for all cases investigated. Therefore, the 2% and 3% values above are conservatively used. As reported by Eamon et al. (2014), total COV of live load is dominated by other sources of variation, and it was found that altering V_{data} from 0-3% has no significant effect on the total live load COV.

d) Uncertainty in impact factor (V_{IM}). V_{IM} is taken as 9% for 1-lane effects and 5.5% for 2-lane effects (Sivakumar et al. 2011).

e) Uncertainty in load distribution (V_{DF}). Based on a series of field tests comparing measured load distribution effects to the AASHTO LRFD DF formula, V_{DF} is given in Table 3.8 below (Sivakumar et al. 2011). Bias factor λ refers to the mean value divided by the AASHTO LRFD value.

Table 3. 8 Statistical Parameters for DF.

Bridge Type		Moment		Shear	
		1 Lane	2 Lane	1 Lane	2 Lane
Composite	λ	0.78	0.90	0.72	0.82
Steel	COV	0.11	0.14	0.14	0.18
Reinforced	λ	0.79	0.93	0.76	0.88
Concrete	COV	0.16	0.15	0.12	0.18
Prestressed	λ	0.78	0.90	0.77	0.88
Concrete	COV	0.12	0.13	0.11	0.16

For each of the case combinations above (i.e, for a particular WIM data site, bridge configuration, and 1 or 2-lane load effect), the final COV of mean maximum load effect, $V_{\max L}$, is then determined. For a product function of random variables such as equation 3.1 or 3.7 (and assuming the uncertainties from the data projection, site, and data are similarly represented in product form), it can be shown that if RVs are uncorrelated and COV is not too large, the COV of the function can be reasonably determined by ignoring the second order relationships as:

$$V_{\max L} = (V_{\text{proj}}^2 + V_{\text{site}}^2 + V_{\text{data}}^2 + V_{IM}^2 + V_{DF}^2)^{1/2} \quad (3.9)$$

7. Reliability for the selection of bridges is then calculated. The general limit state function is:

$$g = R - (D_p + D_s + D_w) - LL \quad (3.10)$$

Random variables considered are girder resistance (R), dead load from prefabricated (D_p), site-cast (D_s), and wearing surface (D_w) components, and vehicular live load (LL). Statistics are taken from Nowak (1999) to be consistent with the AASHTO LRFD and MBE calibrations, and are given in Table 3.9. Although it is not precisely correct, in previous AASHTO design and rating calibrations, for reliability analysis, girder resistance is taken as a lognormal random variable while the sum of load effects is assumed normal.

Mean R is calculated from $\bar{R} = R_n \lambda_r$. R_n is written as a function of the unknown nominal live load effect and live load factor needed such that reliability requirements are met with the appropriate AASHTO code rating procedure when the rating factor is set to 1.0.

Table 3. 9 Random Variable Statistics.

Random Variable		Bias Factor	COV
Resistance RVs		R	
Prestressed Concrete, Moment		1.05	0.075
Prestressed Concrete, Shear		1.15	0.14
Reinforced Concrete, Moment		1.14	0.13
Reinforced Concrete, Shear*		1.20	0.155
Steel, Moment		1.12	0.10
Steel, Shear		1.14	0.105
Load RVs			
Vehicle Live Load	LL	from L_{max} ; see above	
DL, Prefabricated	D_p	1.03	0.08
DL, Site-Cast	D_s	1.05	0.10
DL, Wearing Surface	D_w	mean 3.5"	0.25

*Assumes shear stirrups present

For LRFR calibration, R_n is determined by:

$$R_n = (1/\phi)(1.25DC + 1.5DW + \gamma_L (DF_2)(nominal\ live\ load\ effect + IM)) \quad (3.11)$$

where

γ_L = live load factor, to be determined in conjunction with the nominal live load effect

DC = component dead load.

DW = wearing surface dead load.

IM = impact factor, taken as 1.33 times the nominal vehicle design load (design truck or axle, but not lane load).

DF_2 = AASHTO 2-lane girder distribution factor, as given in Section 4 of the AASHTO LRFD Code.

ϕ = resistance factor, specific to the material and failure mode, as specified in AASHTO LRFD.

For steel members, $\phi=1.0$ for moment and shear effects; for prestressed concrete members (assuming tension controlled), $\phi=1.0$ for moment and 0.9 for shear effects; for reinforced concrete structures (not considered in design, but only for rating), assuming tension controlled, $\phi = 0.9$ for moment and shear effects).

For LRFR legal load rating, for simple spans (less than 200'), only the truck is considered for load effects. In some short span cases (spans 20' considering moment and 20' and 40' for shear), it was found that a single vehicle produced a larger load effect than two vehicles with the lane load. In these cases, the maximum load effect of either was case used.

Due to the large number of reliability calculations required, the reliability analysis is conducted with the closed form, simplified First Order, Second Moment (FOSM) procedure, such that the required LF can be solved for directly. This method assumes all RVs are normal, which is conservative when resistance is lognormal, as assumed for bridge member resistance. To account for this, an adjustment factor representing the ratio of (exact β / FOSM β) was applied such that the reliability index computed by FOSM better approximates the exact value, as determined by direct Monte Carlo Simulation (MCS). These adjustment factors are given in Eamon et al. (2014) and are: 1.04 when the desired $\beta=2.5$, and 1.0 when the desired $\beta=1.5$.

8. The nominal load effect and live load factor γ_L are adjusted to achieve reliability results closest to the target β for rating of 2.5, with a minimum β of 1.5. In the MBE, the load factor was chosen such that the average of all cases considered met the target index of 2.5, and all cases met the minimum value of 1.5. This is the process used here.

3.4 Bridge Structures Considered

The following bridge characteristics were used for analysis:

1. Girder Type:

- a. Prestressed concrete I-girders (PC).
- b. Steel girders (CS).
- c. Reinforced concrete girders (RC).
- d. Prestressed concrete box beams, spaced (BS).

e. Prestressed concrete box beams, side-by-side (BT).

2. Span Type:

a. Simple Span.

3. Span Lengths (ft):

a. 20-200 at increments of 20 for all girders except RC, which is limited to 100.

4. Girder Spacing (as applicable, ft):

a. 4-12 at increments of 2.

b. For side-by-side box beams, two widths (36", 48") are used.

5. Load Effects:

a. Simple moments (Ms)

b. Simple shears (Vs).

Bridges are assumed to support a 9 in. reinforced concrete deck and have a 2.5 in. wearing surface and additional typical non-structural items relevant for dead load calculation. The dead load of these components is based on values used in the AASHTO LRFD calibration as well as NCHRP reports 683 and 285. Note reinforced concrete bridges have no significant prefabricated dead load component.

For girder distribution for moment, the term $\left(\frac{K_g}{12L_t^3}\right)^{0.1}$ in equation 3.5 was found to have a minor effect on results for typical ranges of girder stiffness, and is taken as 1.0 as per the AASHTO LRFD and MBE calibrations.

3.5 Data Projection

The load effects calculated from the WIM data were based on truck traffic collected over a 34 month period. For rating, however, load effects are to be based on a 5 year period, respectively.

Thus, a data projection method is used to estimate load effect statistics for longer periods of time.

This projection does not account for any possible changes in vehicle weights nor uncertainties in potential future vehicles. Rather, the projection only estimates what maximum load effect statistics would be found for the desired return period by probabilistically extrapolating from the existing number of load effects calculated from the available WIM data pool.

If the tail end of the data is reasonably normally distributed, it can be shown that an Extreme Type I distribution can be used to extrapolate to future extreme load events with the following procedure (Ang and Tang 2007):

1. The cumulative distribution function (CDF; $F_x(x)$) of the load effects i : $F_x(x) = (i/1+n)$, is developed, where n is the number of data used to fit the trend line and x is the load effect. Here, the data are a set of the highest moments or shears calculated from the WIM data.
2. The inverse standard normal CDF of each computed CDF value is taken: $(F_x(x))$: $\Phi^{-1}(F_x(x))$.
3. The upper tail of the CDF values, representing the greatest load effects, are plotted as a function of load effect x . As the data are plotted on a normal probability axis, a generally linear trend indicates that the data approach a normal distribution. If the trend is reasonably linear, then a linear regression line is constructed that best fits this data. The slope (m) and intercept (n_o) of the line are determined.
5. It can be shown that the mean value of the best-fit normal distribution is given as: $\bar{x} = -n_o/m$ with standard deviation $\sigma = ((1 - n_o)/m) - \bar{x}$.
6. Load effect statistics are extrapolated to longer periods of time by first computing N , the number of expected events in the extrapolated return period. It can be calculated as $N = nw*(Y/tw)$, where Y is the length of the new return period (5 years); nw is the number of events in the WIM data (in step 1) that were collected, and tw is the number of years of WIM data considered for which the nw data were collected.

7. The load effect statistics (mean maximum and standard deviation) for the new return period can be computed as follows:

$$\bar{L}_{\max} = \mu_N + \frac{0.5772157}{\alpha_N} \quad (3.13)$$

$$\sigma_{L_{\max}} = \frac{\pi}{\sqrt{6}\alpha_N} \quad (3.14)$$

where

$$\mu_N = \bar{x} + \sigma \left(\sqrt{2 \ln(N)} - \frac{\ln(\ln(N)) + \ln(4\pi)}{2\sqrt{2 \ln(N)}} \right) \quad (3.15)$$

$$\alpha_N = \frac{\sqrt{2 \ln(N)}}{\sigma} \quad (3.16)$$

3.5.1 Projection Results

Per step 3 above, the upper tail of the load effect data is used to determine maximum load statistics. For the projection, the load effects from the ten WIM sites with the largest ADTT values were used; these sites were associated with the largest load effects. However, little guidance is available in the technical literature as to how much of the data (n) is to be considered within the upper tail used for projection. Although NCHRP 683 used the upper 5% of the data, it was found that for the data considered in this study, this amount of data often results in a significant nonlinear trend and would thus be poorly represented by the projection technique. It was determined that a much smaller proportion of the tail is needed to for a strong linear fit. For single-lane load effects, this was taken as the greatest 350 load effects for each case. For two-lane load effects, this was typically taken as 250, but in some cases 50, depending on the span and load effect, to generate the best fits. The number of vehicles used in the projection is similar to the number of vehicles used in the AASHTO LRFD Bridge Design Specification. The live load model in the AASHTO

LRFD Bridge Design Specification was developed based on the 10,000 trucks survey data collected in 1975 in Ontario, Canada assumed to represent about two-week traffic data. These vehicles were assumed to represent heaviest 20% of all vehicles. To develop AASHTO LRFD Bridge Design, in the NCHRP report 368 (1999), the CDF of 10,000 load effects were plotted on the normal probability paper and the “tail” of data was extrapolated by scatching to determine the projected live load effect in the bridge lifetime (75 years). Considering the 10,000 total number of vehicles (assumed to represent heaviest 20%) and projecting only the tail of data, the number of vehicles used in this study seems reasonable.

An example illustrating how n affects the goodness of fit is given in Figures 3.23-3.25 below, where it can be seen that the best fits are achieved with a low value for n (350). As shown in Figures 3.26-3.27, results are relatively insensitive to changes in n . An example of single lane shear load effect projection is presented in figure 3.28.

Note that the number of data used to fit the projection line (n) is not the number of data used (N) in Equations 3.15 and 3.16 to determine maximum load effect statistics, which is not an arbitrary value but a function of the number of WIM data collected. The value of N is estimated by taking a weighted average of ADTT among the 10 sites considered in the projection, based on

the number of load effects (ne_i) recorded for each site i : $ADTT_{ave} = \frac{\sum_{i=1}^{i=10} ADTT_i \times ne_i}{N_{34}}$, where N_{34}

is the total number of data for a given load effect collected at all 10 sites over the time period (34 months) available. $ADTT_{ave}$ values were 8009 for single and following events and 149 for side-by-side events. Values of N are then determined by: $N = ADTT_{ave} \times 365 \text{ days} \times 5 \text{ years}$. Final N values were approximately 1.46×10^7 for single and following events and 272,000 for side-by-side events.

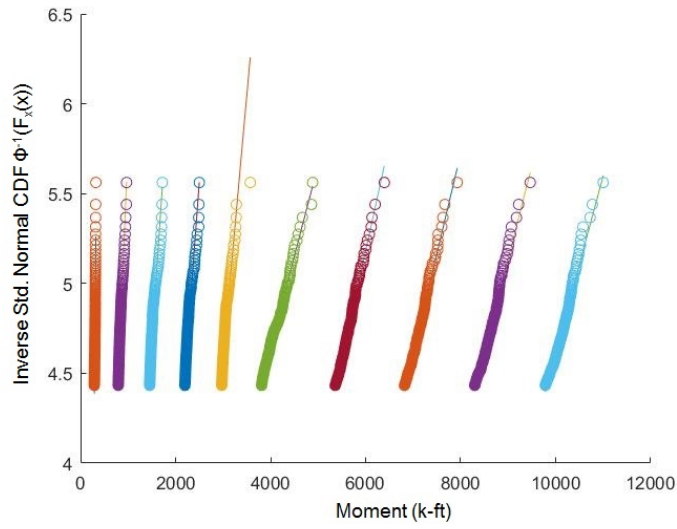


Figure 3.23 CDFs of Top 350 Simple Span, Single Lane Moments for Spans From 20 – 200 ft.

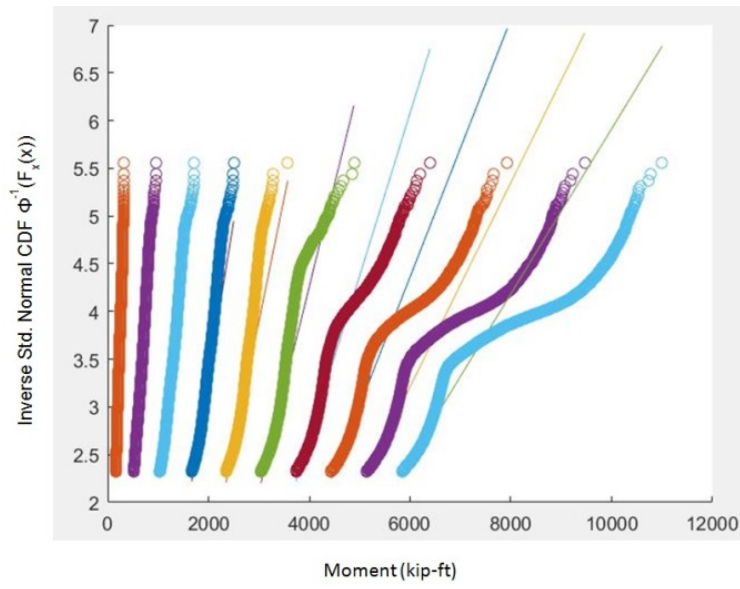


Figure 3.24 CDFs of Top 1% of Simple Span, Single Lane Moments for Spans From 20 – 200 ft.

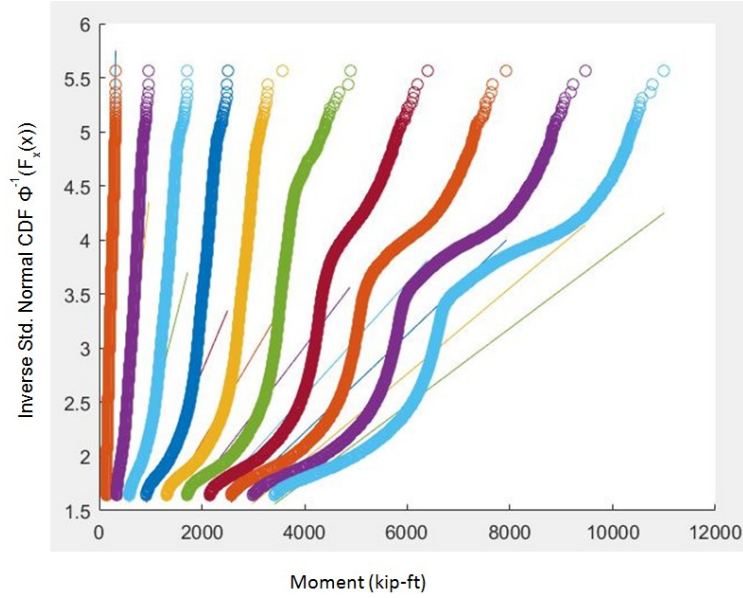


Figure 3.25 CDFs of Top 5% of Simple Span, Single Lane Moments for Spans From 20 – 200 ft.

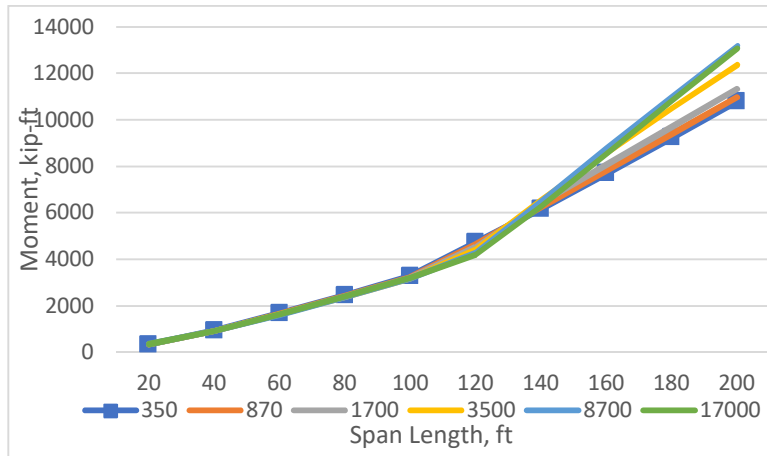


Figure 3.26 Projected Mean Maximum Simple Span, Single Lane Moment for Different n Values.

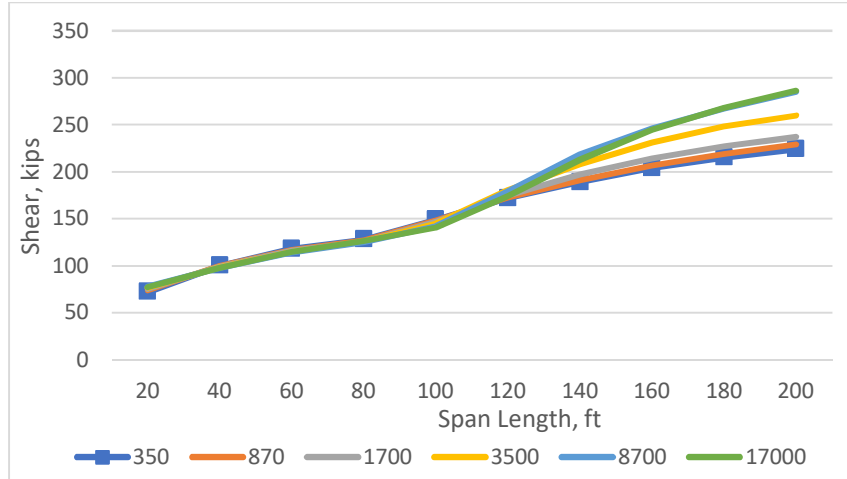


Figure 3.27 Projected Mean Maximum Simple Span, Single Lane Shear for Different n Values.

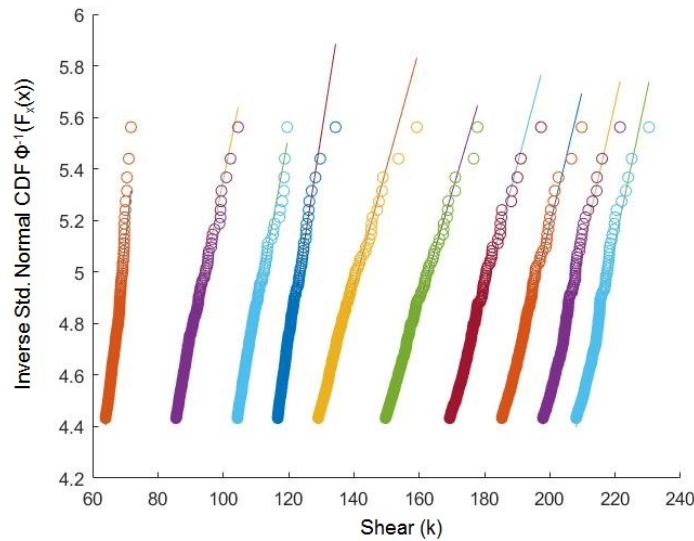


Figure 3.28 Load Projections for One Lane Simple Shear, 20'-200' Spans.

Note that to record possible two lane load effects, a side-by-side event was conservatively defined as occurring when two adjacent lane vehicles have closest axles separated no more than half of the longest bridge span length considered (or, within 100 ft); vehicles. Vehicles separated by up to 200 ft were considered for possible following load effects.

Figure 3.29 and 3.30 illustrate the two-lane load effects projection. For the two-lane results, multiple projection lines are given for each span and load effect.

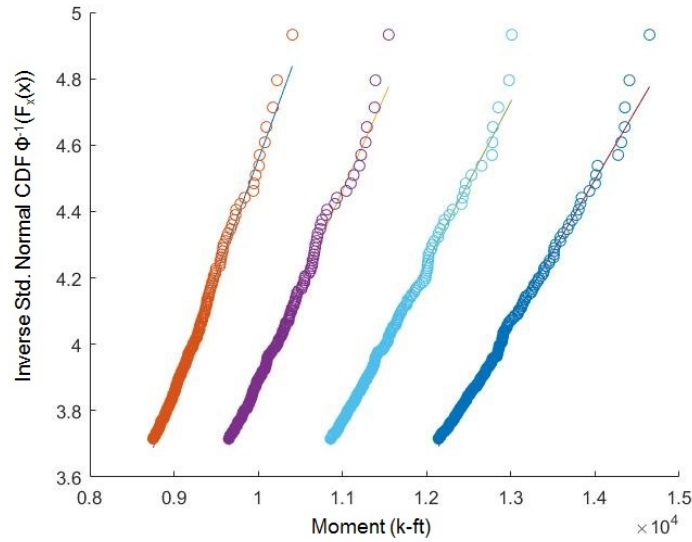


Figure 3.29 Load Projections for Two Lane Simple Moment, 200' Span.

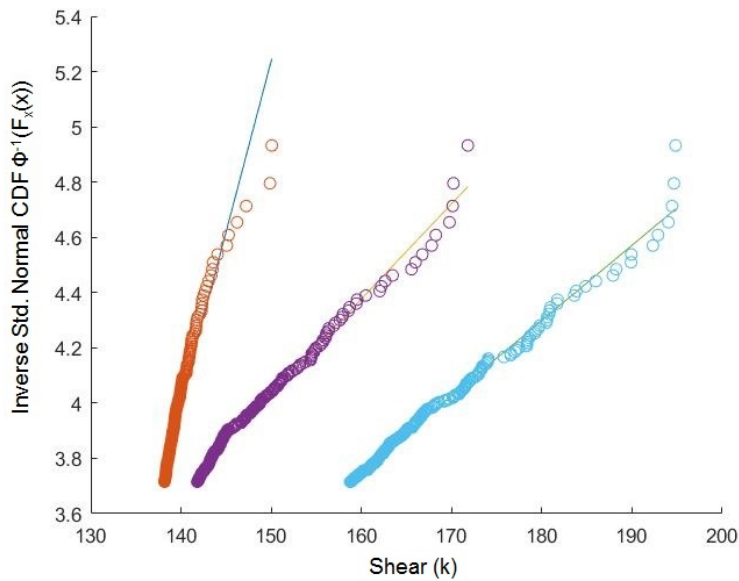


Figure 3.30 Load Projections for Two Lane Simple Shear, 200' Span.

These 3-4 multiple lines represent different fractional weights of the second lane vehicle used in conjunction with the full weight of the first lane vehicle. This is to generate load effects

for bridges with different load distribution factors. Consider Equation 3.4 used to distribute the total live load effect to a girder:

$$M_{12} = M_1 * DF_1 + M_2(DF_2 - DF_1) \quad (3.4)$$

In this format, load effects for the two lanes must be separated. However, because two-lane effects are determined considering the position of each vehicle in adjacent lanes relative to one-another, the total load effect must be combined together before projected to develop maximum load effect statistics. That is, simply taking the maximum load effect in each lane separately and adding these effects, without accounting for vehicle relative position, would significantly increase the two-lane load effect beyond what is actually present. Therefore, the load effects in adjacent lanes cannot be treated independently. Before these load effects are combined prior to projection, the fraction of load effect that a vehicle in each lane contributes to a single girder must be accounted for. This fraction is bridge-dependent, as it is governed by DF_1 and DF_2 . To account for this in the projection, Equation 3.17 can be rewritten as:

$$M_{12} = M_1 * DF_1 + M_2 * (kDF_1) = DF_1(M_1 + kM_2) \quad (3.17)$$

$$\text{where } k = (DF_2 - DF_1) / DF_1$$

Representative k factors for all bridges considered in this study have been computed using values for DF_1 and DF_2 as described with Equation 3.4, above. These values are given in Tables 3.10. and 3.11. A range of 3-4 k factors for each span length was then selected that would envelop these values. These k factors were used to adjust the second-lane vehicle load effect prior to combining the two-lane load effects for projection. The k factors used in the projections are given in Tables 3.12 and 3.13. For bridges with k values between the range of k values chosen, linear interpolation was used to determine load effects. More information about final results of the project, goodness of fit of equation, and more can be found in Eamon and Siavashi (2018).

Table 3. 10 k Values for CS, PC, RC, BS Moments and BS Shears.

Span (ft)	Spacing (ft)	k, Moment	k, Moment	k, Shear
		CS, PC, RC	BS	BS
20	4	0.40	0.37	0.27
20	6	0.45	0.44	0.38
20	8	0.49	0.49	0.46
20	10	0.52	0.54	0.53
20	12	0.54	0.57	0.58
40	4	0.49	0.63	0.27
40	6	0.54	0.71	0.38
40	8	0.58	0.78	0.46
40	10	0.61	0.83	0.53
40	12	0.64	0.87	0.58
60	4	0.54	0.75	0.27
60	6	0.59	0.84	0.38
60	8	0.64	0.91	0.46
60	10	0.67	0.96	0.53
60	12	0.70	1.00	0.58
80	4	0.57	0.81	0.27
80	6	0.63	0.91	0.38
80	8	0.68	0.98	0.46
80	10	0.72	1.03	0.53
80	12	0.75	1.08	0.58
100	4	0.60	0.90	0.27
100	6	0.66	0.99	0.38
100	8	0.71	1.07	0.46
100	10	0.75	1.13	0.53
100	12	0.78	1.18	0.58
120	4	0.62	0.93	0.27
120	6	0.69	1.03	0.38
120	8	0.74	1.11	0.46
120	10	0.78	1.17	0.53
120	12	0.81	1.22	0.58
140	4	0.64	1.01	0.27
140	6	0.71	1.11	0.38
140	8	0.76	1.19	0.46
140	10	0.80	1.25	0.53
140	12	0.83	1.31	0.58
160	4	0.66	1.08	0.27
160	6	0.72	1.19	0.38
160	8	0.78	1.27	0.46
160	10	0.82	1.33	0.53
160	12	0.85	1.38	0.58
180	4	0.67	1.08	0.27
180	6	0.74	1.19	0.38
180	8	0.79	1.27	0.46
180	10	0.84	1.33	0.53
180	12	0.87	1.39	0.58

200	4	0.68	1.14	0.27
200	6	0.75	1.25	0.38
200	8	0.81	1.33	0.46
200	10	0.85	1.40	0.53
200	12	0.89	1.45	0.58

Table 3. 11 k Values for CS, PC, RC Shears and BT Moments and Shears.

		k, Shear	
		Spacing (ft)	CS, PC, RC
		4	0.20
FOR		6	0.34
ALL		8	0.44
SPANS		10	0.50
		12	0.55

Span (ft)	Width (in)	k, Moment		k, Shear	
		BT	BT	BT	BT
20	36	0.15	0.05		
40	36	0.41	0.09		
60	36	0.60	0.11		
80	36	0.74	0.12		
100	36	0.86	0.14		
120	36	0.96	0.15		
140	36	1.06	0.16		
160	36	1.14	0.16		
180	36	1.22	0.17		
200	36	1.07	0.18		
20	48	0.16	0.16		
40	48	0.43	0.20		
60	48	0.62	0.23		
80	48	0.77	0.24		
100	48	0.89	0.26		
120	48	0.99	0.27		
140	48	1.09	0.28		
160	48	1.17	0.29		
180	48	1.25	0.30		
200	48	1.17	0.30		

Table 3. 12 k Values Used for Two Lane Load Effects, Moment.

Span	k1	k2	k3	k4
20	0.15	0.40	0.55	-
40	0.55	0.65	0.75	-
60	0.55	0.70	1.00	-
80	0.55	0.75	1.00	-
100	0.60	0.80	1.20	-
120	0.60	0.80	1.20	-

140	0.65	0.85	1.00	1.30
160	0.65	0.85	1.00	1.30
180	0.65	0.90	1.15	1.40
200	0.70	0.90	1.15	1.40

Table 3. 13 k Values Used for Two Lane Load Effects, Shear.

Span	k1	k2	k3	k4
20	0.10	0.20	0.40	0.60
40	0.10	0.20	0.40	0.60
60	0.10	0.20	0.40	0.60
80	0.10	0.20	0.40	0.60
100	0.10	0.20	0.40	0.60
120	0.20	0.40	0.60	-
140	0.20	0.40	0.60	-
160	0.20	0.40	0.60	-
180	0.20	0.40	0.60	-
200	0.20	0.40	0.60	-

CHAPTER 4: DEVELOPING A SIMPLIFIED PROCEDURE FOR BRIDGE LOAD RATING

As mentioned earlier, WIM stations can accurately capture vehicle configurations and relative vehicle positioning. The WIM data from six states were used by Sivakumar and Ghosn (2011) to revise the load factors used in MBE. Although the WIM data collected to develop the live load factors in the MBE represented a significant improvement in load modeling over previous versions, understandably, it does not necessarily well-represent the traffic loads in various other states that were not included in the MBE calibration effort. A number of states initiated efforts to develop unique live load models to better represent local traffic data. Some of these include Missouri (Kwon et al. 2010), Oregon (Pelphery and Higgins 2006), New York (Ghosn et al. 2011; Anitori et al. 2017), and Michigan (Eamon et al. 2014; Eamon and Siavashi 2018), where state-specific WIM data were used to develop new live load factors for bridge design and rating. In this procedure, the load effects from millions of vehicles should be calculated; load effects need to be projected to 2 or 5 years; From the projected load effects and by conducting a reliability analysis, load factors can be determined. This procedure desires a high computational cost and this drawback may render WIM-based solutions undesirable, if not practically inaccessible, depending on the time and resources available. Therefore, the purpose of this chapter is to propose a procedure that can reduce the computational cost while not compromising the level of accuracy. The main purpose of this approach is to identify the vehicles in the WIM database that does not involve in the load effects projection and as a result in the reliability analysis. The majority of the load effects calculation should be spent on the single vehicles. Usually, a ratio of multiple presence (i.e., following or side-by-side) to the single vehicles are below 2% (Eamon and Siavashi 2018; Eamon et al. 2014). As shown in chapter 3, for the majority of the spans, the multiple vehicles

(i.e., “following” or “side-by-side”) are the governing load effects. As such, the large majority of vehicle load effects that are calculated are not needed. This represents a considerable waste of computational effort.

4.1 Correlation of Vehicle Parameters and Load Effect

To reduce computational effort, the relationship between single vehicle load effects and the vehicle parameters available from the WIM data needs to be examined. This step can identify the parameter(s) can be used to include only the vehicles which will have a significant impact on the load effect statistics. The most obvious parameter is GVW. However, it is important to note that due to the truck axle weight and axle spacing limits, the heavier trucks are often longer, and may produce lower load effects compare to lighter, shorter trucks. Another factor is vehicle length which is especially important for shorter span lengths. Therefore, the following parameters are studied: GVW; length; number of axles; GVW/length; and GVW x length. The first three parameters are directly available from the WIM data and the latter two parameters can be calculated from the available parameters with minimal computational effort. The correlation coefficient (ρ) of each of these parameters to load effect was computed across various span lengths for the MI-LEP and Simplified CFR vehicle databases described above. Coefficient of correlation can be expressed as equation 4.1:

$$\rho_{xy} = \frac{COV(x,y)}{\sigma_x \sigma_y} \quad (4.1)$$

where x and y are the truck parameter (i.e. weight, length, etc.) and load effect (i.e. moment or shear), respectively.

ρ_{xy} can vary from -1 to 1 where $\rho_{xy} = 1$ means that two variables are perfectly linearly correlated,

$\rho_{xy} = 0$ means two variables are not correlated and $\rho_{xy} = -1$ indicates that two variables are

negatively linearly correlated. Results for moment and shear effects are shown in Figures 4.1 to 4.4.

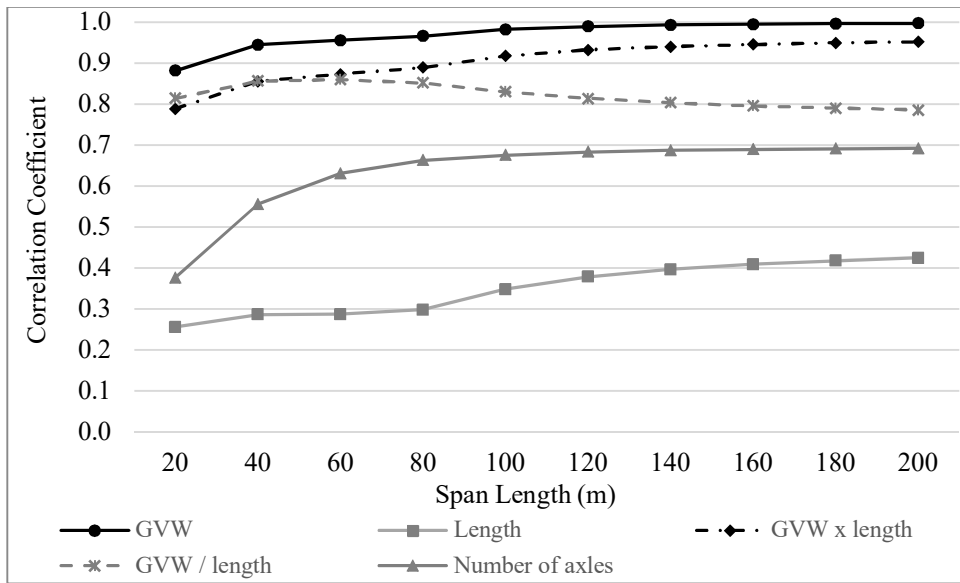


Figure 4. 1 Correlation Between Vehicle Parameter and Moment, MI-LEP

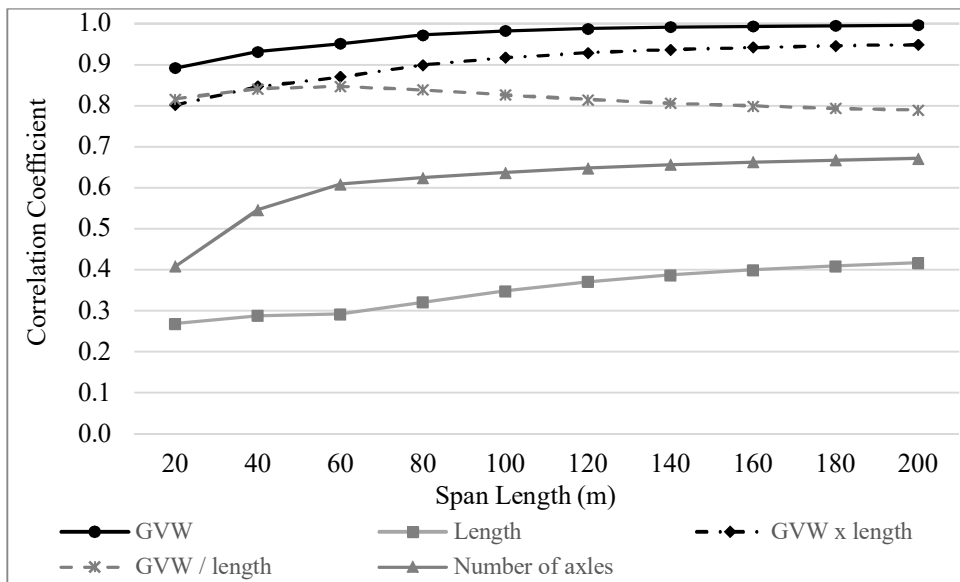


Figure 4. 2 Correlation Between Vehicle Parameter and Shear, MI-LEP

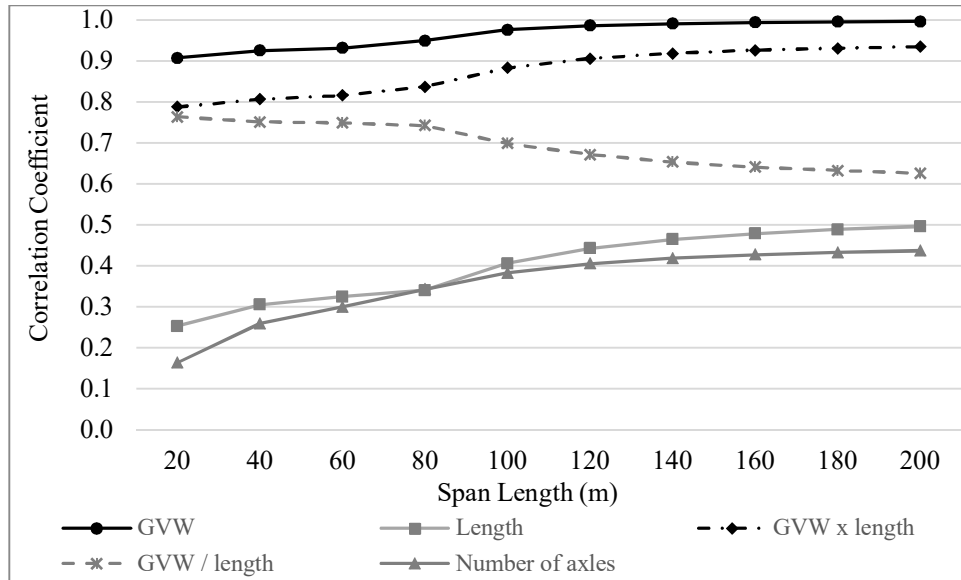


Figure 4. 3 Correlation Between Vehicle Parameter and Moment, Simplified CFR

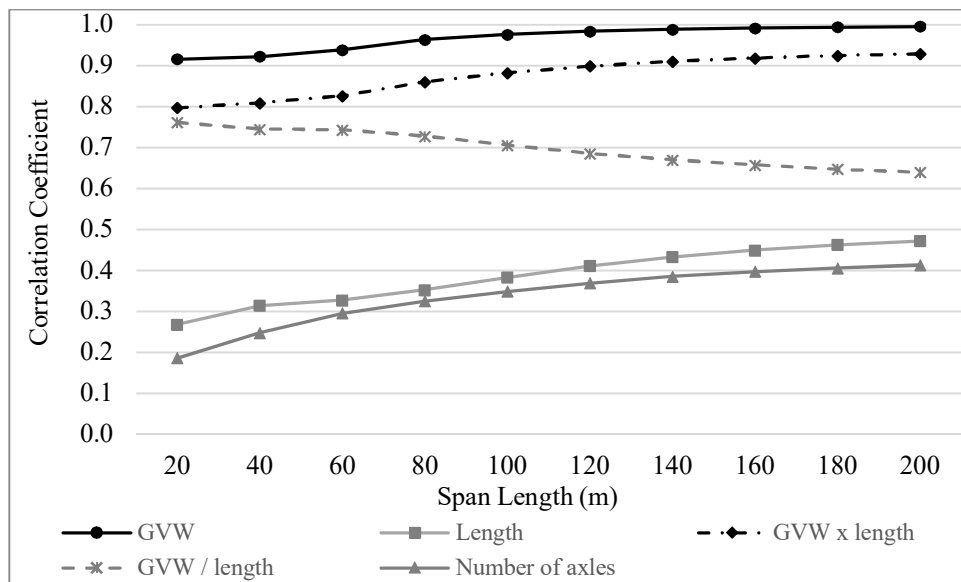


Figure 4. 4 Correlation Between Vehicle Parameter and Shear, Simplified CFR

In general, as span length increases, it is observed that coefficient of correlation between all considered parameters (i.e. GVW , length, weight \times length, number of axles) except weight over length and load effects increases as the span length increases. This is found to be the opposite for the weight over length. GVW is shown to have the highest correlation, with values varying

from about 0.9 to nearly 1. Due to the high coefficient of correlation, it appears that the GVW can be used to eliminate a large portion of vehicles.

In fact, a simplified method to estimate live load factors for rating based on GVW is already given in the MBE, based on NCHRP 454 (2001), and is taken as (for single lane loading):

$$\gamma_L = 1.8 \left[\frac{W^* + t_{(ADTT)}\sigma^*}{120} \right] \geq 1.80 \quad (4.2)$$

where W^* and σ^* are the mean truck weight and standard deviation of the top 20 percent of the vehicle sample (kips), and $t_{(ADTT)}$ is a fractile value appropriate for the maximum expected loading event, taken as 4.9, 4.5, and 3.9 for ADTT values of 5000, 1000, and 100, respectively. The accuracy of the existing MBE method, however, is not clearly documented. The effectiveness of the MBE approach, as well as an alternative approach proposed in this chapter, will be quantified.

First, it is important to study the background of equation 4.2 used by MBE. Initially, the live load model in the AASHTO LRFD Bridge Design Specification was developed based on the 10,000 trucks survey data collected in 1975 in Ontario, Canada assumed to represent about two week traffic data. It was assumed that 10,000 trucks survey data represent the heaviest top 20% of vehicles (NCHRP 454 2001). As stated in the NCHRP 368 (1999), at the time of calibration of the live load model, the weigh-in-motion (WIM) data technology was not reliable resulting with errors up to 40% . It was assumed that the truck population in Ontario at the time of collecting the surveys was representative on the U.S. trucks. Furthermore, it was assumed that the legal load limits will not change and the truck population remains constant (NCHRP 368 1999). When the code was calibrated, due to the limited available data for the multiple presence of trucks (i.e., following in one-lane and side-by-side in two or more lane), it was assumed that for the one-lane (i.e., following), every 50th truck is followed by another truck, about every 150th truck is followed by a partially correlated truck, and about every 500th truck is followed by a fully correlated (i.e.,

identical) truck weights (NCHRP 368 1999). These assumptions for the side-by-side trucks are every 1 in 15 trucks was side-by-side with any other truck. It was also assumed that 1 in 30 side-by-side truck events occur with fully correlated (i.e. identical) truck weights. These assumptions resulted in a model which stipulates that for every 1 in 450 heavy truck crossings, it is side-by-side with an equally heavy truck. In the MBE (AASHTO 2018), based on the research conducted in NCHRP 454 (2001), a simplified procedure to calculate the live load factors using the GVW data (i.e., mean and standard deviation) was used. To develop the model (NCHRP 454 (2001)), first, it was tried to retrieve the data used in AASHTO LRFD design calibration. However, gross vehicle weight (GVW) and standard deviation of 10,000 vehicles used in the AASHTO LRFD design calibration were not reported and only the cumulative frequency distribution of load effects (i.e. moment and shear) were reported. Therefore, in NCHRP 454 (2001), by trial and error, the weight parameters for the equivalent AASHTO Legal 3S2 vehicle fitting 10,000 vehicle database used in NCHRP 368 (1999) were estimated. The mean and standard deviation of the top 20% trucks GVW were estimated to be 68 kips and 18 kips, respectively. The GVW was calculated as the ratio of mean maximum moment of 10,000 truck over HS20 as reported by NCHRP 368 (1999) multiplied by the ratio of moment of HS20 over AASHTO 3S2 legal truck multiplied by the weight of AASHTO 3S2 truck (72 kips).

To calculate $t_{(ADTT)}$, a 5-year time interval for bridge evaluation was used. Therefore, the total number of top 20% of vehicles (N) by GVW can be determined by $\frac{ADTT}{5} \times 5 \text{ years} \times 365$. $t_{(ADTT)}$ were determined from the standard normal distribution table reading the value of $1 - \frac{1}{N}$. The limit of 1.80 in equation 4.2 is the load factor used for 3S2 AASHTO legal truck.

According to NCHRP 454 (2001), the expected maximum loading in 2 years is 240 kips in two lanes or 120 kips per lane. The 240 kips GVW is based on the assumption of the probability

of every 15th vehicle is side-by-side and the 10,000 vehicles used in the AASHTO LRFD calibration (NCHRP 368 1999) has a mean and standard deviation of 68 kips and 18 kips, respectively. However, from the analysis of 14 sites with various ADTT from 360 to 16500 as well as considering all data, it is found that the mentioned assumptions are substantially different from the actual truck traffic. The mean and standard deviation of GVW of heaviest 20% of simplified CFR dataset are presented in Figures 4.5 and 4.6. The mean and standard deviation of GVW of heaviest 20% of MI-LEP dataset are presented in Figures 4.7 and 4.8. In the Figures, “All” means considering all the 20 sites (see chapter 3). It is found that the mean of top 20% GVW of all sites in both data pools is higher than the NCHRP assumption. The standard deviation of heaviest 20% for simplified CFR is lower than the NCHRP assumption for the majority of sites. Considering all data in the simplified CFR dataset, the range of heaviest 20% of vehicles (approximately 16 millions) varies from approximately 64 kips to 80 kips. This results in a mean of 72 kips and a standard deviation of approximately 4 kips. The standard deviation is much lower than the assumptions when the method was developed. On the other hand, considering all data for MI-LEP dataset, the GVW heaviest 20% of vehicles (approximately 18 millions) varies from 71 to 157 kips with the mean and standard deviation of approximately 88 and 23 kips, respectively.

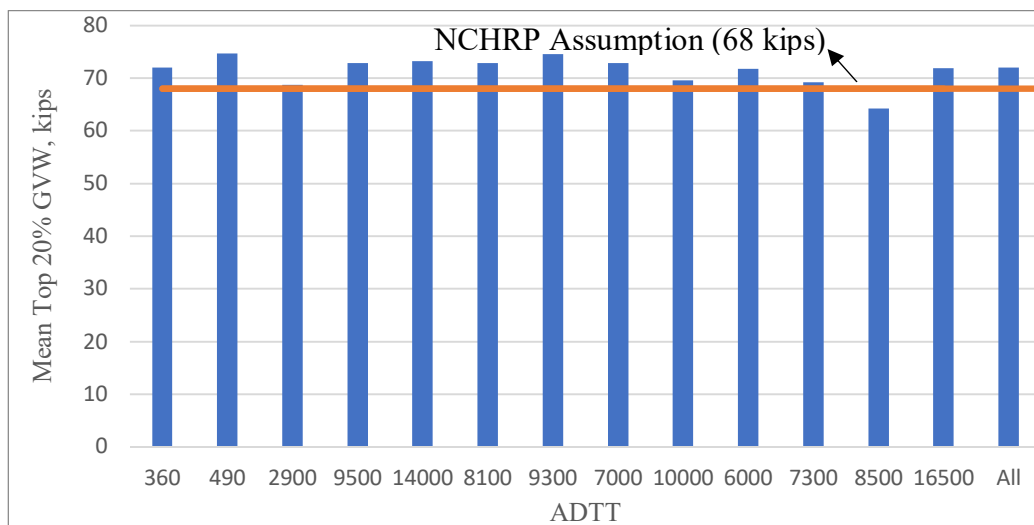


Figure 4. 5 Mean top 20% simplified CFR GVW, (kips)

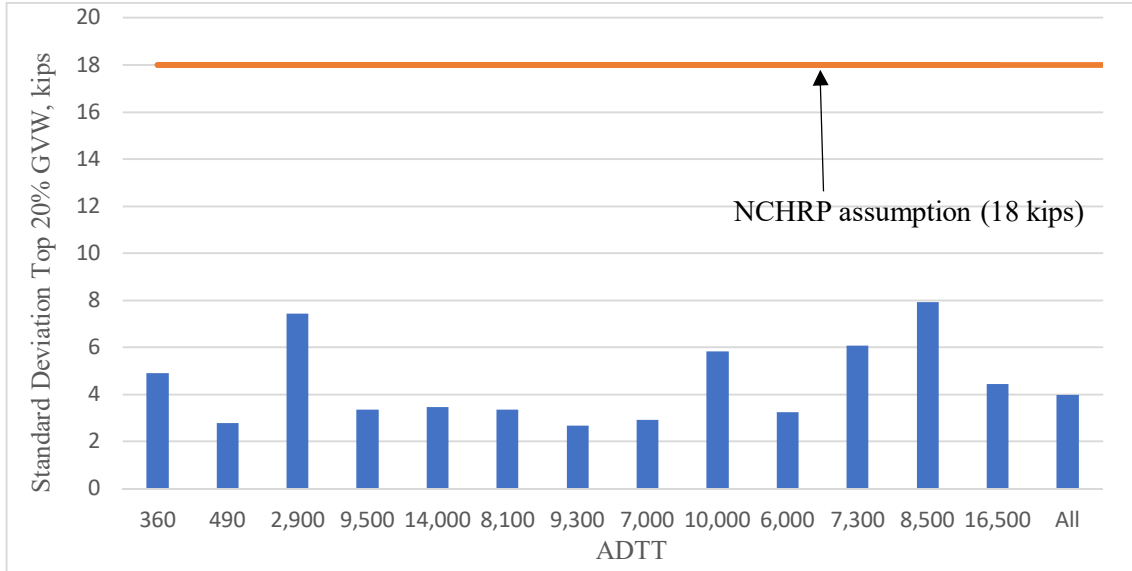


Figure 4. 6 Standard deviation top 20% simplified CFR GVW, (kips)

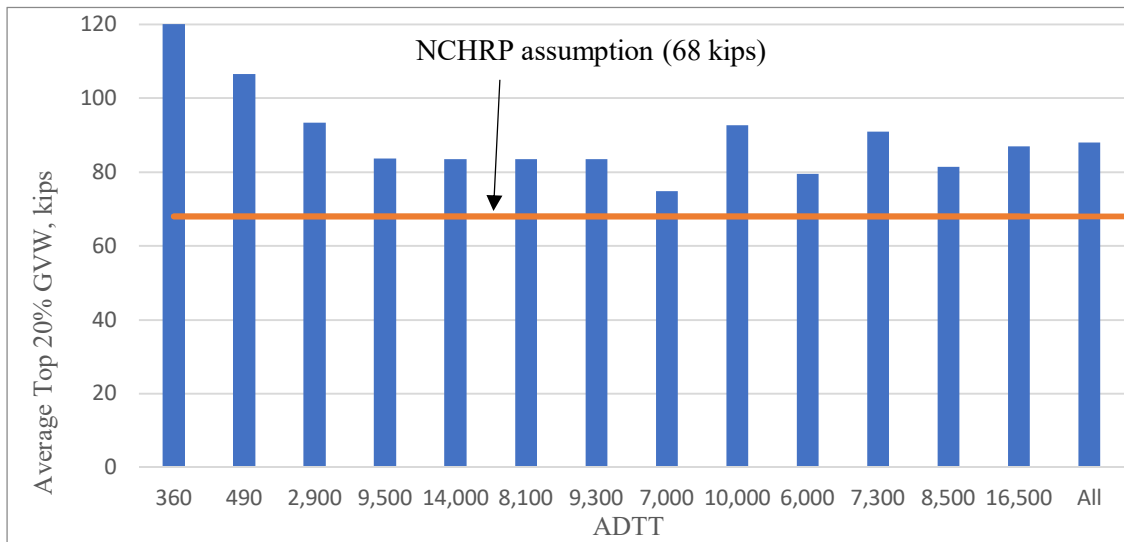


Figure 4. 7 Mean top 20% MI-LEP GVW, (kips)

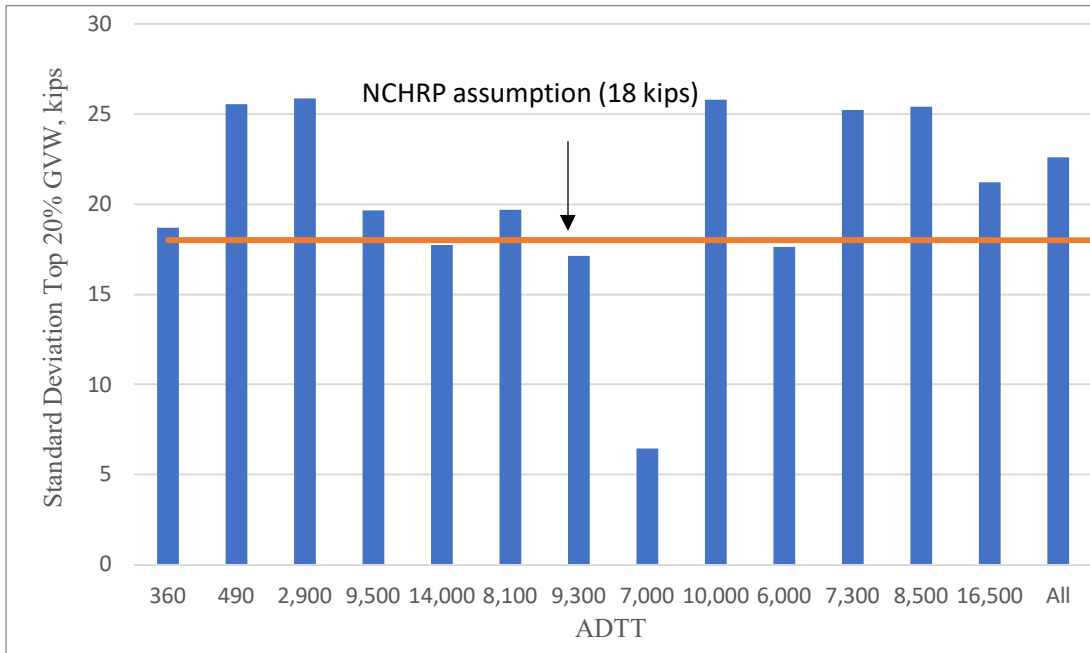


Figure 4. 8 Standard deviation top 20% MI-LEP GVW, (kips)

In Figure 4.9, the side-by-side probability of MI-LEP dataset is compared with the AASHTO assumption (which is further used in NCHRP 454 to develop equation 4.2).

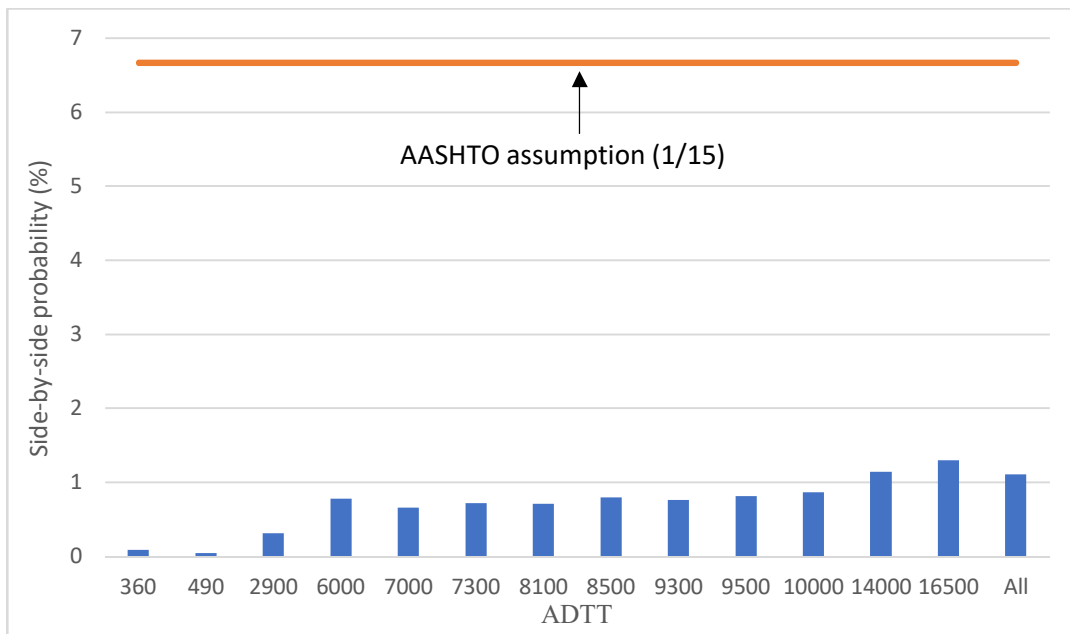


Figure 4. 9 Side by side event, %

To clarify the difference between the “exact”, MBE, and proposed approaches for live load factor development, first consider the exact procedure. In the exact method, as described in chapter 3, the load effects from all vehicles are first computed. From the computed load effects, the CDF of load effects is formed. From the CDF, the mean maximum load statistics for a five-year return period are developed. These statistics are then used along with other load effect uncertainties, as discussed further below, to form a random variable for live load which can be used in reliability analysis to determine appropriate live load factors for rating.

The alternative approach proposed in this study follows the same procedure of the exact approach. The only difference is the number of vehicles used to calculate load effects that are used to form CDF. Rather than use the entire vehicle database, load effects are computed and the CDF is formed only from the heaviest vehicles. Based on the discussion above regarding the strongest correlation between truck parameters and load effects, the number of vehicles is reduced to smaller portions based on the GVW.

4.2 Reliability Analysis

For the exact and proposed procedures, a reliability analysis is required to determine rating load factors. These factors, the ultimate product of interest, will be used to compare the accuracy of the alternative methods considered. For comparison, the analysis was conducted for bridges described in chapter 3 section 4. All considered bridges were assumed to support a 9 in. thick reinforced concrete deck, 2.5 in. wearing surface, and additional typical nonstructural items (primarily barriers and diaphragms) relevant to dead-load calculation. In summary, considering all combinations of length (10 spans from 20 to 200 ft. at increments of 20 ft.) and girder spacing (5 spacing from 4 to 12 ft. at increments of 2 ft.) increments results in 50 geometries each for prestressed concrete, steel, and spread box beam bridge types; 25 for reinforced concrete (span

length is limited to 100 ft.); and 20 side-by-side box beams (10 span lengths, two width (36",48")), for 195 cases. The range of these geometries and types covers nearly all girder bridges in state of Michigan as well as other state inventories.

Random variables used for reliability assessment are described in chapter 3. Random variables used for reliability assessment are girder resistance (R), dead load, and live load. Dead load includes prefabricated (D_p) site-cast (D_s) and deck wearing surface (D_w) components, while the live load consists of vehicle live load (L_{max}) and dynamic load (IM). In addition, uncertainty in the distribution of vehicular live load to an individual girder is considered (DF). Bias factor (ratio of mean to nominal value) and coefficient of variation (COV) of these random variables are presented in Table 3.9. With the exception of live load (LL), all random variable statistical parameters used in the AASHTO LRFD (Nowak 1999) and MBE calibrations (NCHRP 683) are used in this study. To be consistent with previous calibration efforts, it is also assumed that girder resistance is lognormal whereas the sum of load effects is taken as normally distributed.

The live load random variable statistical parameters are not only a function of the uncertainty in projected maximum vehicle load effect, characterized here by a coefficient of variation $V_{projection}$, with parameters determined by Equations 3.13 and 3.14 (where $V_{projection} = \frac{\sigma_{L_{max}}}{L_{max}}$), but other uncertainties as well.

As implemented in the MBE calibration, these uncertainties also include those of site location (V_{site}), characterizing the variation in mean maximum load effect from one site to another; the dynamic load effect, (V_{IM}), taken as 9% for one lane effects (NCHRP 20-07 2011); the uncertainty in WIM data collection at a particular site (V_{data}), taken as 2% for the database considered (Eamon and Siavashi 2018); and uncertainty in vehicular live load distribution to the

girder (V_{DF}), which varies as a function of girder type as shown in Table 3.9 (NCHRP 20-07 2011).

The resulting COV of total vehicular live load effect can be thus approximated as:

$$V_{\max L} = \sqrt{V_{\text{projection}}^2 + V_{\text{site}}^2 + V_{\text{data}}^2 + V_{IM}^2 + V_{DF}^2} \quad (4.3)$$

This final value was found to vary from 0.16-0.30, depending on the bridge type and vehicle database considered. Once random variables are defined, the general limit state function g_i for each bridge girder i can be written as:

$$g_i = R - (D_p + D_s + D_w) - DF(L_{\max} + IM) \quad (4.4)$$

with random variables D_p , D_s , D_w , DF , IM , and L_{\max} defined above. Limit states are formed for simple span load effects for moment and shear.

To establish nominal values for girder resistance R for use in the reliability analysis and to avoid biasing reliability results upward by analyzing conservatively-designed components, the minimum requirements of acceptability must be identified. For LRFD, the minimum acceptable value for the resistance (ϕR_n) equals $\sum \gamma_i Q_i$, (where γ_i are load factors and Q_i are load effects).

In the case of rating, the minimum acceptability is established in terms of rating factor. Rating factor (RF) is provided in the MBE by

$$RF = \frac{\phi R_n - 1.25DC - 1.5DW}{\gamma_{LL}(LL + IM)} \quad (4.5)$$

where the minimum acceptable value (i.e. no need to restrict traffic) can be established when $RF=1$. In equation 4.5, ϕ varies depending on the failure mode and girder type, R_n is the nominal resistance of the component, DC and DW are the dead loads of the structure and the wearing surface, respectively; IM is specified as 1.33, LL is the rating vehicle live load effect, and γ_{LL} is the rating vehicle load factor. In the MBE, the load factor was chosen such that all cases met the minimum target reliability index of 1.5 and the average target reliability index of all cases met

2.5. Setting the rating factor equals one in Equation 4.5, the required nominal resistance(R_n) can be determined as:

$$R_n = (1/\phi)(1.25DC + 1.5DW + \gamma_{LL}(LL + IM)) \quad (4.6)$$

Here it should be noted that the required nominal resistance determined from Equation 4.6 is a theoretical resistance of the component/girder used for the reliability based evaluation in the rating process.

By knowing the dead load (DC, DW) and live load (γ_{LL} , LL, IM) effects, the nominal resistance (R_n) in Equation 4.6 can be calculated. After calculating the R_n , the mean value (\bar{R}) of the girder resistance random variable R can be calculated using the bias factor shown in Table 3.9. Knowing mean value (\bar{R}) of the girder resistance, the reliability index of the limit state provided in Equation 4.4 can be computed. Recall that the reliability index of each bridge case should be greater than 1.5 and the average reliability index of all bridge cases should be above 2.5.

Here, the total live load effect produced by the rating model ($\gamma_{LL}(LL+IM)$) is unknown. The minimum needed value of ($\gamma_{LL}(LL+IM)$) to produce the mean value of girder resistance random variable (R) that satisfies the target limit index mentioned above can be determined. The quantity $\gamma_{LL}(LL+IM)$ is referred to as the required load effect (RLE) in this study. RLE is the total load effect required by the live load rating model such that for any girder, $\beta = 1.5$ when RF=1.0. The reliability analysis was conducted using the FOSM procedure as described in chapter 3. Based on the strong correlation between GVW and load effects, the exact approach (i.e. using all vehicle data) is compared with the results obtained after reducing the number of vehicle dataset based on GVW.

4.3 Implementation of the Proposed Approach

The main objective of the proposed approach is to reduce the computational effect by reducing the number of vehicles used in the analysis. Therefore, it is important to determine how much of the database can be removed such that the level of accuracy is not compromised. As described in chapter 3, the statistics of the live load random variable used in the reliability analysis depend on the data used to generate load effects. Therefore, reducing the dataset may change the statistics of the live load random variables such as the mean maximum live load effect (\bar{L}_{max}); the coefficient of variation with respect to location (V_{site}); and coefficient of variation of the mean maximum load ($V_{projection}$); see equation 4.3.

Considering MI-LEP and Simplified CFR datasets, the vehicle datasets were reduced to the top 50, 20, 10, 5, and 1 percent of single vehicle records by GVW. The load effects of the reduced single-vehicle data pools were calculated and then combined with the all load effects constituting multiple vehicles in the same lane (i.e. the “following” vehicle effects). Recall that the ratio of multiple vehicles in one lane over single vehicles is less than 2% (Eamon and Siavashi 2018; Eamon et al. 2014). Therefore, reducing the number of following vehicles is not a concern in this study.

After the single vehicles were reduced to smaller portions, the load effects were calculated and three affected live load random variable statistics (mean maximum live load effect (\bar{L}_{max}); the coefficient of variation with respect to location (V_{site}); and coefficient of variation of the mean maximum load ($V_{projection}$)) were recomputed for comparison. Typical values for V_{maxL} (Equation 4.3), which describes the total effective variation in live load, were also computed. Results for MI-LEP data are shown in Figures 4.10-4.11. Note that in Figure 4.10 and 4.11, the V_{DF} , V_{data} , and

V_{IM} are assumed to be 0.11, 0.02, and 0.09, respectively. V_{DF} of 0.11 can represent the 20 ft. steel girder and 20 ft. Prestressed concrete I-girder for moment and shear, respectively.

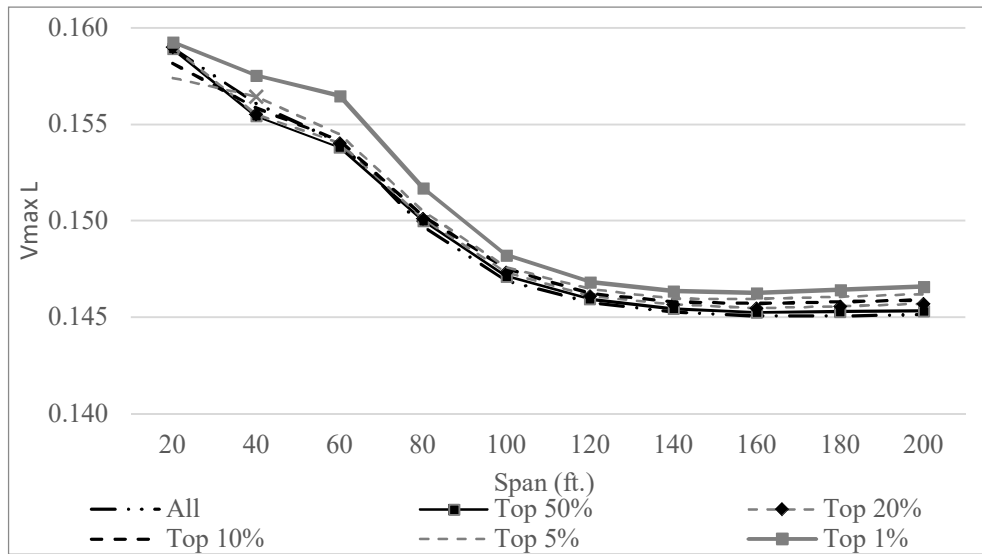


Figure 4. 10 Effect of Database Reduction on V_{maxL} for Moment, MI-LEP Vehicles.

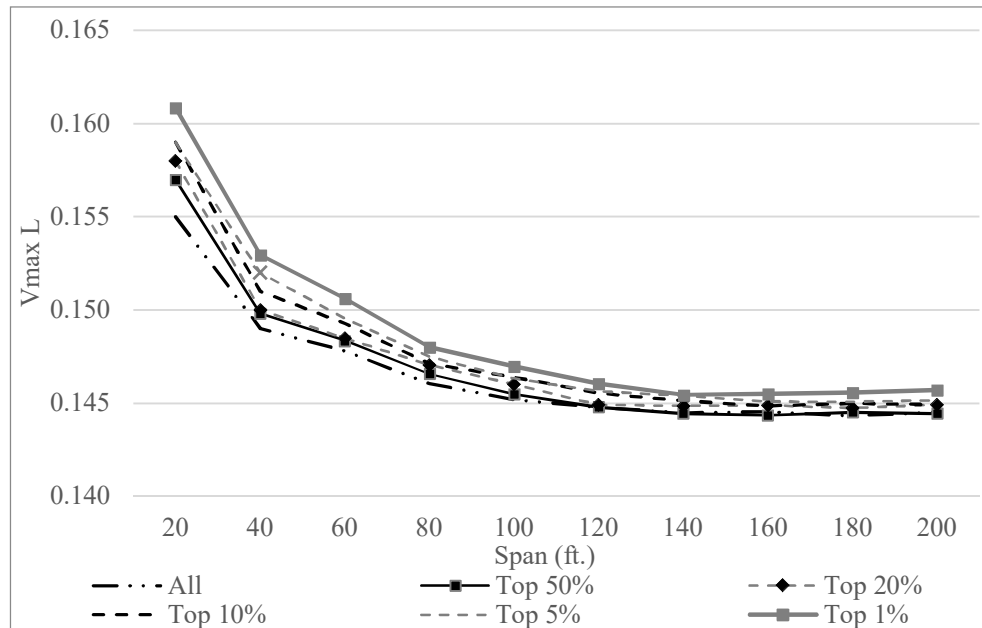


Figure 4. 11 Effect of Database Reduction on V_{maxL} for Shear, MI-LEP Vehicles.

In general, as the data reduces, the V_{maxL} increases. The similar trend was observed for the Simplified CFR dataset. V_{maxL} also reduces as the span length increases.

In general, as the data reduces, the V_{site} increases but $V_{projection}$ decreases. A higher V_{site} compared to $V_{projection}$ was observed. As a result, a small increase in $V_{max L}$ was observed as the data reduces. An example of data reduction on V_{site} and $V_{projection}$ for MI-LEP are presented in figures 4.12 and 4.13.

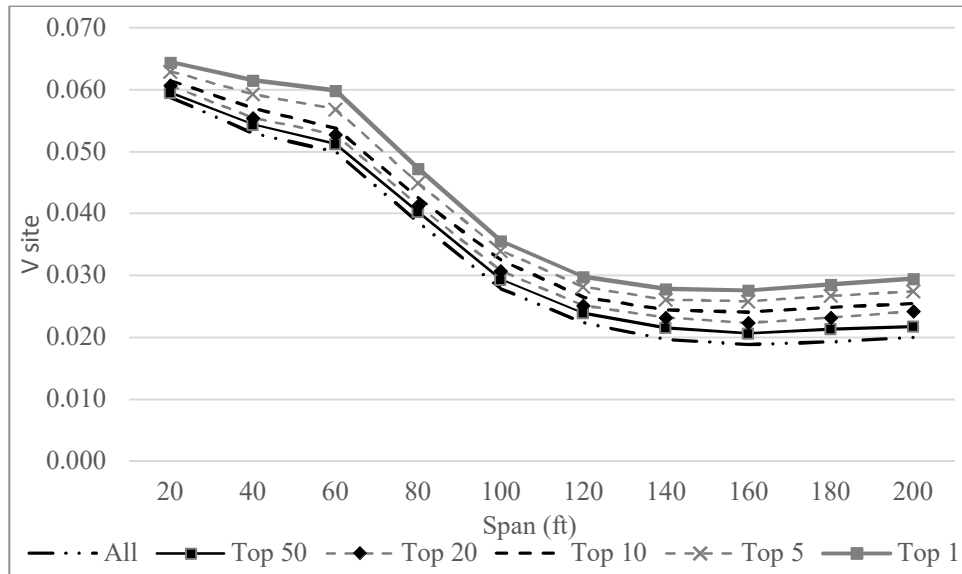


Figure 4. 12 Effect of Database Reduction on V_{site} for Moment, MI-LEP Vehicles.

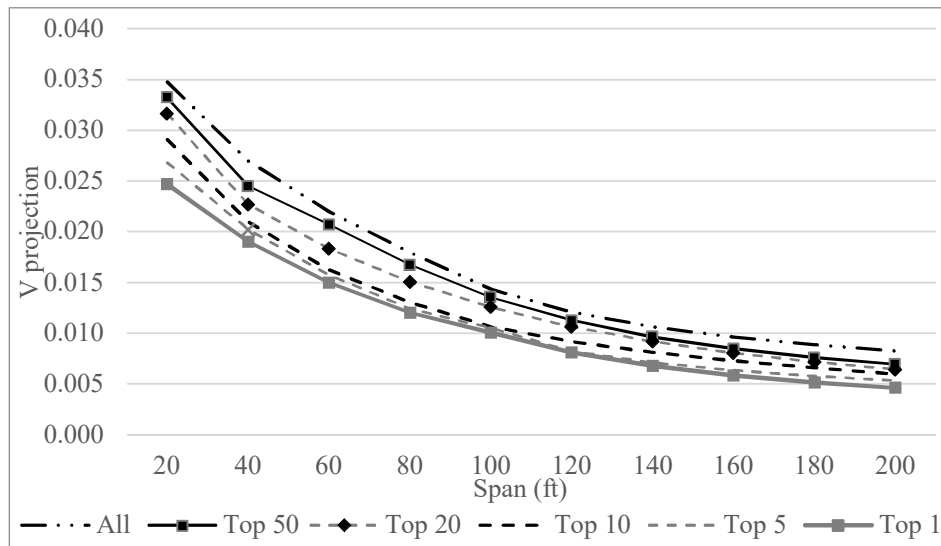


Figure 4. 13 Effect of Database Reduction on $V_{projection}$ for Moment, MI-LEP Vehicles.

After the single vehicles were reduced to smaller portions, the load effects from the smaller portions were calculated. From the computed load effects, the CDF of load effects is formed. From the CDF, the mean maximum load statistics for a five-year return period are developed and compared with the projected load effect using all data. The projected load effect of smaller portions over all-data projected load effect ratio for MI-LEP and Simplified CFR for both moment and shear are presented in Figures 4.14 to 4.17.

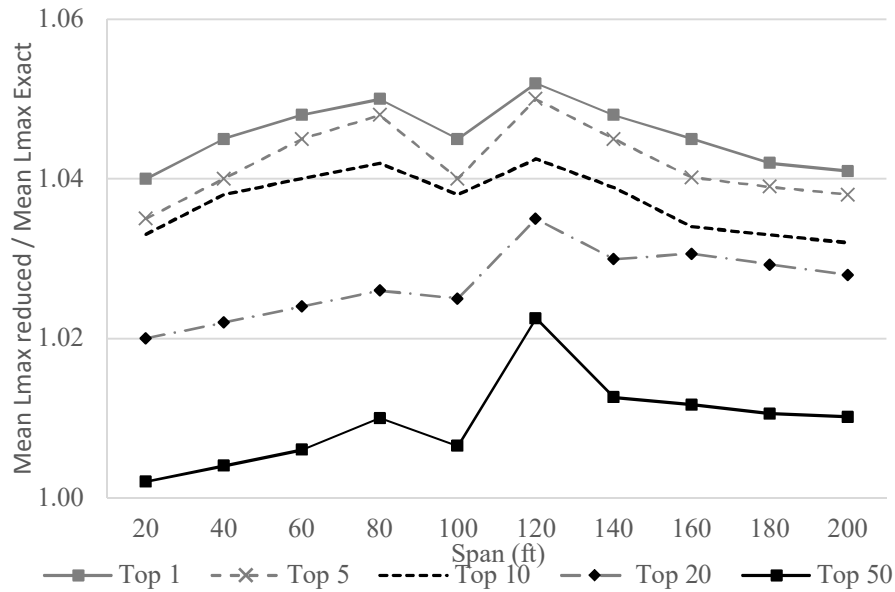


Figure 4. 14 Effect of Database Reduction on Mean Maximum Load Effect, MI-LEP Moment.

For the MI-LEP moment, \bar{L}_{max} for a reduced dataset to the exact case using of all data approximately varies from 1.00 to 1.02 for top 50%, 1.00 to 1.04 for top 20% and top 10%, 1.00 to 1.05 for top 5%, and top 1%.

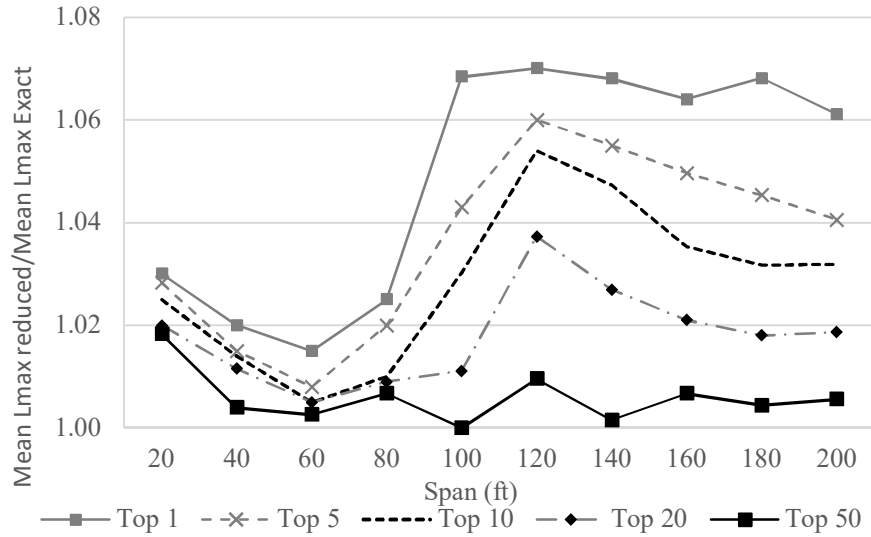


Figure 4. 15 Effect of Database Reduction on Mean Maximum Load Effect, MI-LEP Shear.

For the MI-LEP shear, the projected load effect ratio approximately varies from 1.00 to 1.02 for top 50%, 1.00 to 1.04 for top 20%, 1.00 to 1.05 for top 10%, 1.00 to 1.06 for top 5%, and 1.00 to 1.07 for top 1%.

For the simplified CFR moment, the projected load effect ratio approximately varies from 1.00 to 1.02 for top 50%, 1.00 to 1.04 for top 20%, 1.00 to 1.06 for top 10% and top 5%, and 1.00 to 1.07 for top 1%.

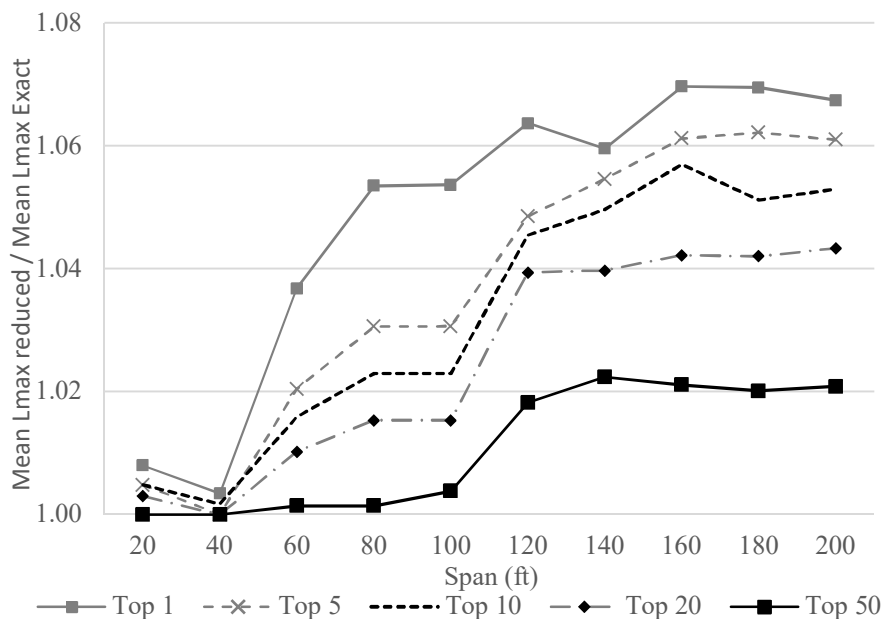


Figure 4. 16 Effect of Database Reduction on Mean Maximum Load Effect, Simplified CFR
Moment.

For the simplified CFR shear, the projected load effect ratio varies from 1.00 to 1.03 for top 50%, 1.00 to 1.05 for top 20%, 1.00 to 1.06 for top 10%, and 1.00 to 1.07 for top 5% and top 1%. In summary, the maximum projected load effect ratio for MI-LEP and simplified CFR, moment and shear found to be 1.03 for top 50%, 1.05 for top 20%, 1.06 for top 10%, and 1.07 for top 5% and top 1%.

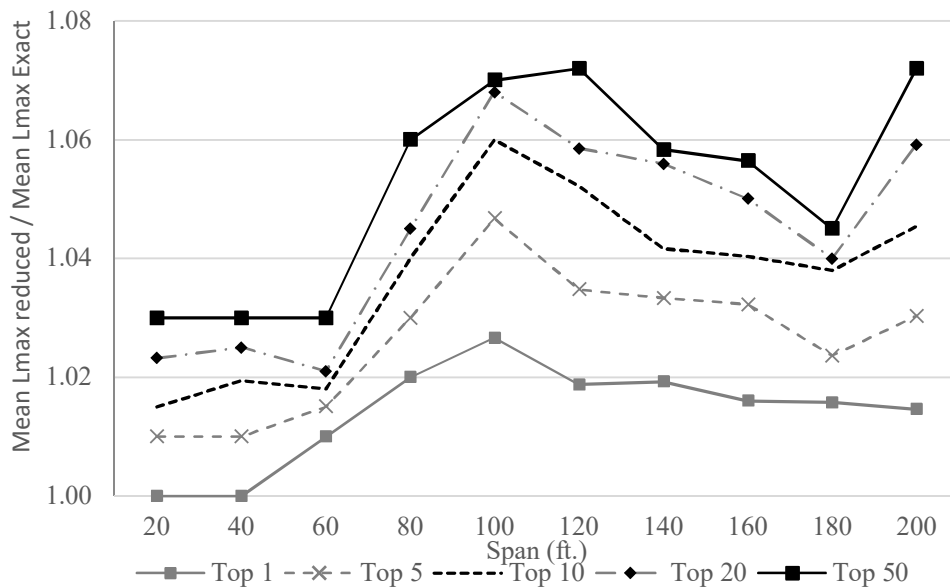


Figure 4. 17 Effect of Database Reduction on Mean Maximum Load Effect, Simplified CFR
Shear.

4.4 Effect of Data Reduction on Live Load Factors

After examining the effect of reducing data on the load random variable statistics, the main concern is by reducing the database by GVW, how the required load effect (RLE) and the corresponding reliability indices of the bridge girders change. After reducing the vehicles based on the GVW and by using the revised live load random variable statistical parameters mentioned earlier, RLE values were recomputed. The ratio of the RLE for the reduced dataset (RLE_r) to the

exact case (RLE_e) are given in Table 4.1. As it can be observed in Table 4.1, the (RLE_r / RLE_e) ratios are all greater than unity. This implies that reducing the dataset based on the GVW produce conservative results.

Table 4.1 provides values for the minimum, average, and maximum ratios from the 195 bridge girder cases described earlier. As it can be observed in Table 4.1, the average RLE_r / RLE_e ratio using top 20% of data is less than 1.06.

Table 4. 1 Required Load Effect Ratios.

Reduced Dataset	MI-LEP		Simplified CFR		
	RLE_r/RLE_e	Moment	Shear	Moment	Shear
Top 50%	maximum	1.09	1.03	1.07	1.08
	mean	1.01	1.01	1.02	1.02
	minimum	1.00	1.00	1.00	1.00
Top 20%	maximum	1.14	1.05	1.24	1.19
	mean	1.03	1.01	1.04	1.06
	minimum	1.01	1.00	1.01	1.00
Top 10%	maximum	1.19	1.08	1.24	1.20
	mean	1.05	1.03	1.06	1.07
	minimum	1.03	1.01	1.01	1.02
Top 5%	maximum	1.22	1.12	1.26	1.21
	mean	1.06	1.04	1.06	1.07
	minimum	1.04	1.01	1.02	1.04
Top 1%	maximum	1.25	1.19	1.32	1.24
	mean	1.06	1.07	1.09	1.08
	minimum	1.04	1.01	1.04	1.04

The maximum, minimum and average reliability indices for all cases are presented in Table 4.2. It is found that changing \bar{L}_{max} , $V_{projection}$, and V_{site} as a result of reducing the dataset, increases the reliability indices. It is found that the change in the average reliability indices as the data reduces is negligible. These are computed using the RLE_r values found from the GVW-reduced data pools, but then reassessing reliability using the exact live load statistics found from

all of the data (again, considering the single-lane load effects). In other words, if RLE_r is the same as RLE_e , the mean, maximum and minimum reliability indices in the Table 4.2 is 1.50. It is observed that the change in the average reliability indices is negligible if only the heaviest top 20% of data is considered. “AASHTO” load model in Table 4.2 is determined by considering AASHTO legal trucks for Simplified CFR and MDOT legal trucks for MI-LEP datasets and applying the load factor calculated from Equation 4.2. This analysis is recommended by MBE for a specific bridge with a load-load rating using generalized load factors. This further investigation of site-specific loading may result in load rating improvement (MBE 2018).

Table 4. 2 Reliability Results for Different Vehicle Database Sizes

Reduced Dataset	Reliability Index (β)	MI-LEP		Simplified CFR	
		Moment	Shear	Moment	Shear
Top 50%	maximum	1.56	1.59	1.64	1.67
	Mean	1.52	1.52	1.54	1.53
	minimum	1.51	1.50	1.51	1.50
Top 20%	maximum	1.61	1.63	1.73	1.75
	Mean	1.57	1.54	1.57	1.56
	minimum	1.52	1.51	1.51	1.51
Top 10%	maximum	1.67	1.69	1.81	1.84
	Mean	1.60	1.57	1.59	1.58
	minimum	1.53	1.51	1.51	1.52
Top 5%	maximum	1.84	1.71	1.91	1.91
	Mean	1.62	1.58	1.60	1.59
	minimum	1.53	1.52	1.52	1.53
Top 1%	maximum	1.95	1.74	2.03	1.97
	Mean	1.68	1.61	1.63	1.53
	minimum	1.54	1.54	1.52	1.61
AASHTO ¹	maximum	8.84	4.85	4.52	3.74
	Mean	4.95	3.65	3.25	2.78
	Minimum	6.89	2.78	2.70	1.63

1. Load factors of 2.98 and 1.36 are calculated for MI LEP moment and shear and Simplified CFR moment and shear, respectively.

To further compare the proposed simplified procedure with the AASHTO simplified procedure, the analysis was conducted on 14 individual sites. From the 14 sites considered, 2 sites with ADTT around 500, 2 sites with ADTT around 2000 and 10 sites with ADTT greater than

5000 were used. Sites with ADTT less than 5000 are located in US and M roads. It is important to note that the sites used in this study are not in a low-volume road carry unusually heavy trucks. In addition, the limit on the right side of Equation 4.2 (≥ 1.80) for the load factor is not considered. Not considering the limit is to compare the effectiveness of the AASHTO simplified procedure compare with the proposed simplified procedure. In the proposed simplified procedure, the load effects (i.e. moment and shear) of the heaviest 20 percent of the data are combined with the one-lane “following” load effects. The load effects are then projected to 5 years using the projection technique used by MBE (AASHTO 2018) as described earlier. The maximum load factor from the all 195 considered bridges is compared with the single-lane load factor calculated by AASHTO simplified procedure. The load factor calculating from AASHTO method and the Proposed Simplified Procedure (PSP) are then compared with the load factor determined from the load projection using all data (i.e., no simplification is used for the load factor calculation). This calculation is conducted on MI-LEP and simplified CFR datasets. From the total 195 considered bridge cases, load factor such that minimum and average reliability indices of respectively 1.5 and 2.5 are met is used and compared with the AASHTO simplified procedure. The comparison between AASHTO method and proposed simplified procedure (PSP) method are shown in Figures 4.18 and 4.19. It was observed that for both datasets considering moment and shear, the simplified procedure produce the load factor close to the actual result (i.e., no simplification).

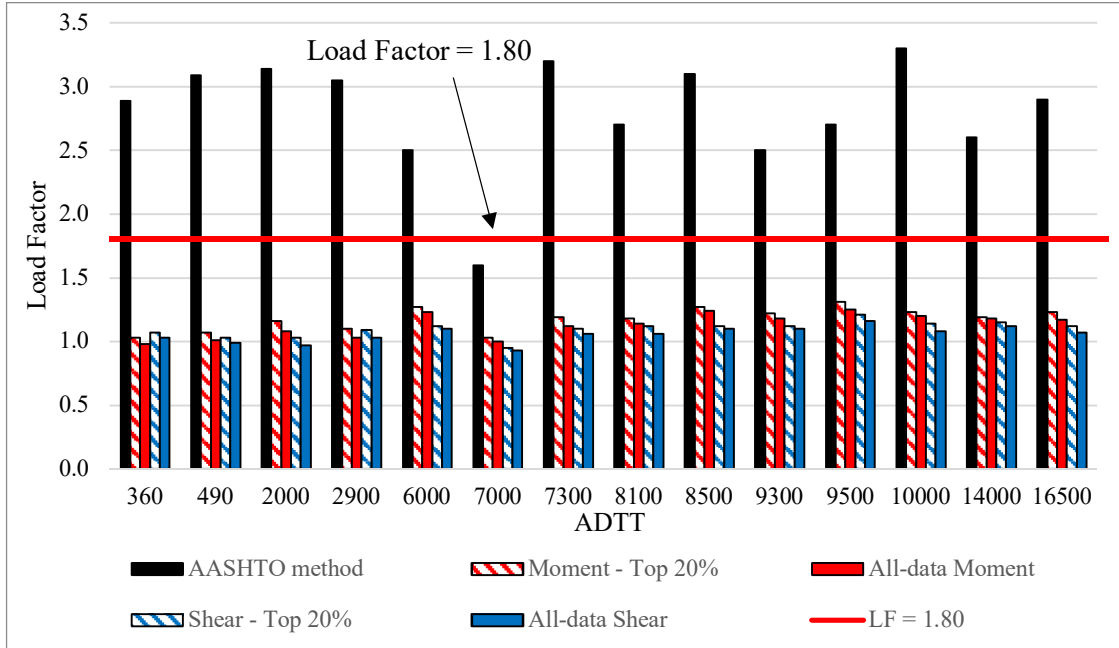


Figure 4. 18 Comparison between AASHTO and Proposed simplified procedure, MI-LEP data pool

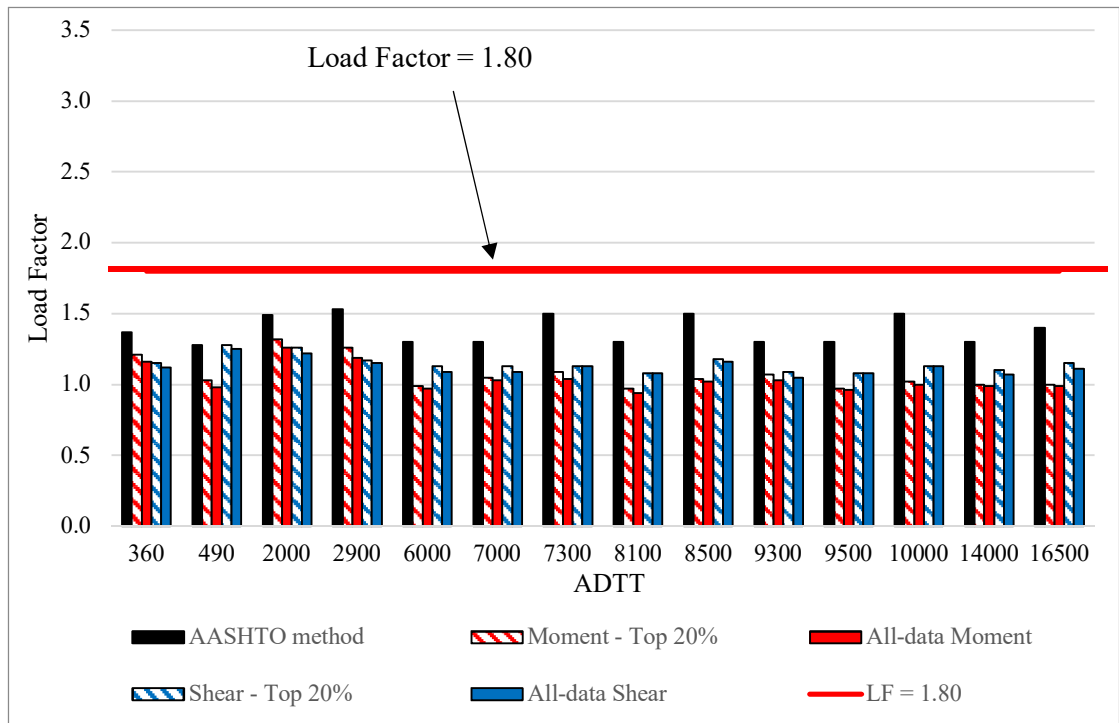
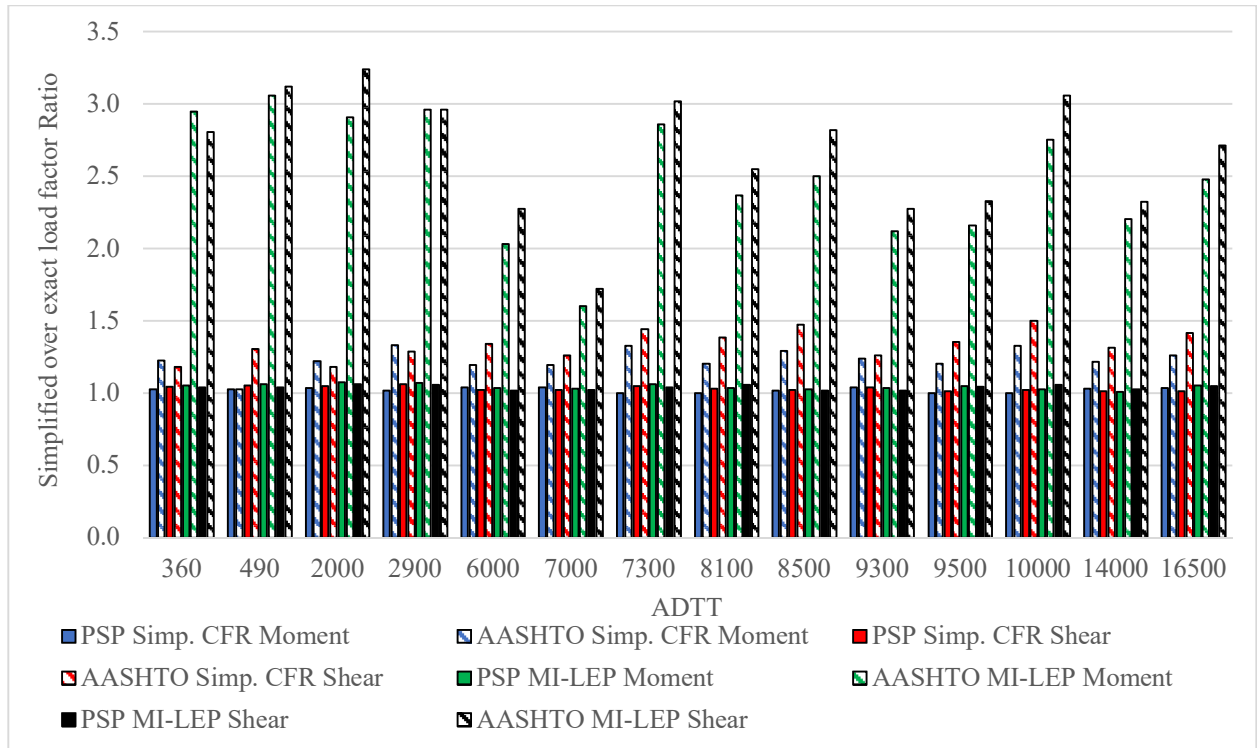


Figure 4. 19 Comparison between AASHTO and Proposed simplified procedure, Simplified CFR data pool

The AASHTO simplified procedure and proposed simplified procedure over exact (i.e. no simplification) load factor ratios in the considered 14 sites are compared in Figure 4.20. It is found that both AASHTO and proposed simplified procedure conservatively predicts the required load factor. However, the degree of conservatism is much higher in the AASHTO simplified procedure. The degree of conservatism is compared in Table 4.3.



* PSP mean proposed simplified procedure

Figure 4. 20 AASHTO and proposed simplified procedure over all-data load factor ratio

The AASHTO simplified procedure and proposed simplified procedure over exact (i.e. all-data) load factor ratios are compared in Table 4.3. The minimum ratio, average ratio, and maximum ratio of considered 14 sites are presented in Table 4.3. Considering proposed simplified procedure in the simplified CFR dataset, the maximum load factor ratio is 1.06 while the maximum load factor ratio for AASHTO simplified procedure is found to be 1.50. The maximum ratio for MI-LEP dataset is found to be 1.07 and 3.24 for the proposed and AASHTO simplified methods,

respectively. Therefore, the proposed procedure can predict the load factor within 7% discrepancy while the predicted load factor using AASHTO procedure is as high as more than three times than needed. Note that increasing the degree of conservatism (higher than needed load factor) in the rating causes posting, closing, or rehabilitation of bridges.

Table 4. 3 AASHTO and Proposed simplified procedure over exact method ratio

	Minimum Ratio	Average Ratio	Maximum Ratio
PSP Moment, Simplified CFR	1.00	1.02	1.04
AASHTO Moment, Simplified CFR	1.02	1.23	1.33
PSP Shear, Simplified CFR	1.01	1.03	1.06
AASHTO Shear, Simplified CFR	1.18	1.34	1.50
PSP Moment, MI-LEP	1.01	1.04	1.07
AASHTO Moment, MI-LEP	1.60	2.50	3.06
PSP Shear, MI-LEP	1.02	1.04	1.06
AASHTO Shear, MI-LEP	1.72	2.66	3.24

* PSP mean proposed simplified procedure

CHAPTER 5: RBDO AND MODIFIED BEST SELECTION APPROACH

The main target of calibration of load model/factor for the load and resistance factor is to achieve a uniform target reliability indices across all the span lengths and considered bridge types. The selection of the target reliability index is an economic issue where selecting a high value for the target reliability index increases the safety but can apply the limitation for the vehicles passing the bridge. If the considered bridge does not meet the target reliability index, bridge needs to be posted or closed. On the other hand, lowering the target reliability index may cause bridge component failures. It is important to note that the degree of conservatism in rating costs much more money comparing to the design. For example, in the design of a reinforced concrete bridge, increasing the degree of conservatism may result in increasing the area of reinforcement or member geometry. However, increasing the degree of conservatism in rating may result in the fact that the bridge cannot carry the legal loads and as a result posting, closing, rehabilitation or replacing the bridge.

There are several methods available to determine the live load model. One possibility is using Reliability Based Design Optimization (RBDO) to generate trucks (i.e., by generating truck axles and spacing) and calculate the corresponding load effect. The number of axles, axle spacing, and axle weights can be determined by the optimization. An optimization algorithm can be used such that the best option(s) for the axle weight and spacing can be determined (Kamjoo and Eamon 2018). However, this method may require a high computational cost and result in a load model that may bear little resemblance to any realistic vehicle configuration. The unrealistic vehicle especially if the vehicle does not meet the Legal limits applied by each State may cause confusion for the drivers as well as rating engineers. This concern is one of the reasons that AASHTO Legal trucks were used rather than HL-93 for the rating (NCHRP 454 2001).

The second method is simply considering the maximum load effects of AASHTO legal trucks and State legal trucks (described later) and increase the load factor such that the minimum reliability index is meet for all span lengths and considered bridge types. Obviously, this may result in unnecessarily high reliability indices for some bridge types.

The third method could be applying different load factor for different bridges. For example, in this study, one load factor for each 195 bridge cases can be considered. Although accurate, this option is not practical.

The fourth method could be using a reliability based design optimization to develop an expression for the load model (described later).

The fifth method which was initially developed by Siavashi and Eamon (2019) is choosing the best truck with the appropriate load factor from the WIM-data used in the analysis to calculate the required load effect such that the minimum reliability index can meet. This method is further modified. The last two methods (RBDO and Modified Best Selection) were examined in this study.

5.1 RBDO Model

Probability theory is most commonly used to model uncertainty in reliability-based design optimization. Correspondingly, an RBDO problem defines a set of NDV design variables $Y = \{Y_1, Y_2, \dots, Y_{NDV}\}^T$ to be determined that minimizes or maximizes given performance criteria, as well as a set of n random variables $X = \{X_1, X_2, \dots, X_n\}^T$ that describe load, resistance, and other uncertainties. Considering a probabilistic limit state function $g(X, Y)$, a failure may occur if $g(X, Y) \leq 0$. The structure (design) is safe if $g(X, Y) > 0$. Correspondingly, $g(X, Y) = 0$ implies the boundary between the failed and safe regions.

Various methods of formulating and solving RBDO problems have been proposed (Enevoldsen and Sorensen 1994; Tu et al. 1999; Rais-Rohani and Xie 2005; Kharmanda and

Olhoff 2007; Aoues and Chateauneuf 2010, etc), including numerous approximate methods for assessing probabilistic constraints to reduce computational effort (Enevoldsen and Sorensen 1994; Tu et al. 1999; Du and Chen 2004; Qu and Haftka 2004). In this study, an RBDO approach is used to develop a live load rating and design models that meet the minimum specified level of reliability for all of the considered bridge types across all the span lengths.

With this approach in mind, the optimization problem is described as:

$$\begin{aligned} & \min f(\mathbf{X}, \mathbf{Y}) \\ & \text{s. t. } \beta_i \geq \beta_{\min}; i = 1, N_p \\ & Y_k^l \leq Y_k \leq Y_k^u; k = 1, NDV \end{aligned} \quad (5.1)$$

where $f(\mathbf{X}, \mathbf{Y})$ is an objective function quantifying variability in structural reliability among the different bridge girders considered for rating, as described below; β_i is the reliability index constraint for girder i among N_p structures considered; β_{\min} is the minimum acceptable reliability index; and Y_k is the k^{th} design variable among NDV design variables, with lower and upper bounds given as Y_k^l and Y_k^u .

In this study, it is tried to minimize the variation in reliability indices among all considered bridge types. Therefore, $f(\mathbf{X}, \mathbf{Y})$ was formulated to quantify this variation. Here, an ideal solution can be defined as the desired reliability index is meet for all considered bridge types with a variation equals zero (i.e. ideally the reliability index is equal to target reliability index for all considered bridges). There are different metric to quantify the variation from a target reliability level such as mean absolute error, mean squared error, R-squared, root mean squared error, and many others. In this study, Mean square error is used which results in an objective function formulated as:

$$f(X, Y) = \sum_{i=1}^{N_p} \frac{(\beta_i - \beta_T)^2}{N_p} \quad (5.2)$$

5.2 Reliability Analysis

Random variables X used for reliability assessment are girder resistance (R) and load effects. The live load effects include vehicle live load (LL), dynamic load (IM), and dead load from prefabricated (D_p), deck wearing surface (D_w), and site-cast (D_s) components. Uncertainty in the distribution of vehicular live load to an individual girder is also considered (DF). For the consistency, the same random variable statistical parameters used by AASHTO LRFD (NCHRP 368 1999) and MBE calibration (AASHTO 2018) were used. The bias factor (ratio of mean to nominal value) and coefficient of variation (COV) for the random variables are presented in Table 5.1. The only exception is the live load random variables which were calculated from the Michigan-specific data. Furthermore, to be consistent with the previous calibrations, it is assumed that girder resistance is lognormally distributed and the sum of load effects is normally distributed (NCHRP 368 1999; Sivakumar et al. 2011).

Table 5. 1 Random Variables.

Random Variable		Bias Factor	COV
Resistance RVs	R	λ	
Prestressed Concrete, Moment		1.05	0.075
Prestressed Concrete, Shear		1.15	0.14
Reinforced Concrete, Moment		1.14	0.13
Reinforced Concrete, Shear ¹		1.20	0.155
Steel, Moment		1.12	0.10
Steel, Shear		1.14	0.105
Load RVs			
Vehicle Live Load, Moment	LL	1.07-2.08 ²	0.16-0.27 ³
Vehicle Live Load, Shear	LL	1.0-1.64 ²	0.16-0.30 ³
Live Load Impact Factor	IM	1.13;1.10 ⁴	0.09;0.055 ⁴
Vehicle Load Distribution Factor	DF	0.72-0.99	0.11-0.18

Dead Load, Prefabricated	D_p	1.03	0.08
Dead Load, Site-Cast	D_s	1.05	0.10
Dead Load, Wearing Surface	D_w	mean 89 mm	0.25

1. Assumes shear stirrups present.

2. Bias factor is given as the ratio of mean load effect to the nominal Michigan legal rating truck load effect; varies as a function of span.

3. Includes uncertainties from data projection, site, WIM data, impact factor, and load distribution; varies as a function of span.

4. Bias factor is given as a multiple of static LL, such that the total vehicular load effect is $LL \cdot \text{bias}_{IM}$. First values refer to single lane load effects; second values refer to two-lane load effects.

Having all the random variables, the general limit state function g for each bridge girder i can be written as:

$$g_i = R - (D_p + D_s + D_w) - DF(LL + IM) \quad (5.3)$$

with random variables R , D_p , D_s , D_w , DF , IM , and LL defined earlier. Recall that Limit states are formed for simple span load effects (moment and shear) for prestressed concrete I-shaped girders, composite steel girders, reinforced concrete girders, and spread and side-by-side prestressed concrete box beams. Bridges are assumed to support a reinforced concrete deck and have a wearing surface and additional items such as barriers and diaphragms relevant for dead load calculation. Bridges are taken as two lane, with span lengths from 20-200 feet in increments of 20 ft.. Girder spacing varied from 4 to 12 feet at 2 ft. increments, while for side-by-side box beams, two widths (36 and 48 inches) were considered. Therefore, considering all combinations of length (10) and girder spacing (5) increments results in 50 geometries each for prestressed concrete, steel, and spread box beam bridge types; 25 for reinforced concrete (limited to 100 ft.) ; and 20 side-by-side box beams, for 195 cases. Considering both one-lane and two-lane, 195 cases each, 390 cases were considered for the analysis.

The target reliability index associated with the MBE is $\beta_T = 2.5$, which represents the average required reliability level across all girders considered (AASHTO 2018). Although in the MBE calibration, the minimum reliability index of 1.50 and the average reliability index of 2.50

is considered, the upper limit for the reliability index may be more desirable to be used by DOTs. Therefore, in this study, the minimum reliability of 2.50 is used for the target reliability index.

In case of designing a structure based on LRFD, the structure is safe if the capacity of the bridge (ϕR_n) is equal or greater than the load applied to the bridge ($\sum \gamma_i Q_i$). If the load effect Q and the corresponding load factor γ_i is known, the minimum acceptable value for the capacity R_n can be determined. In the case of rating, the safety of the bridge is acceptable (no need for traffic restriction) is the rating factor is greater than 1.0. MBE (AASHTO 2018) defines the rating factor (RF) as follow:

$$RF = \frac{\phi R_n - 1.25DC - 1.5DW}{\gamma_{LL}(LL + IM)} \quad (5.4)$$

where the resistance factor ϕ varies depending on girder type and failure mode; R_n is the nominal resistance of the component; DC and DW are the dead loads of the structure and the wearing surface, respectively; IM is specified as 1.33, LL is the rating vehicle live load effect, and γ_{LL} is the rating vehicle load factor.

To meet the required reliability level, the rating vehicle must produce a live load effect (LL) that produces $\beta_T = 2.5$ when $RF = 1.0$. Thus, setting $RF = 1.0$ and solving for the required R_n results in:

$$R_n = (1/\phi)(1.25DC + 1.5DW + \gamma_{LL}(LL + IM)) \quad (5.5)$$

which is the minimum nominal resistance for consideration in reliability rating.

Knowing the dead load and live load effects, R_n can be established. With R_n , known, the mean value \bar{R} of the girder resistance random variable R can be determined using the bias factors λ shown in Table 5.1 ($\bar{R} = \lambda \times R_n$), and then the reliability index of the limit state in equation 5.3 computed. However, the goal of this study is to determine the live load model, therefore, the total

live load effect produced by the rating model ($\gamma_{LL}(LL+IM)$) is unknown. By knowing the target reliability index (here is 2.5), the minimum value of $\gamma_{LL}(LL+IM)$ needed to produce an R_n (and in particular, the mean value of R) that will satisfy the target reliability index can be determined. For convenience, the quantity $\gamma_{LL}(LL+IM)$ is referred to as the required load effect (RLE); i.e. the total load effect required by the live load rating model such that $\beta = 2.5$ when $RF=1.0$.

The step by step of reliability analysis is given below:

- 1- The nominal and mean (using the bias factors given in Table 5.1) values for dead load random variables (D_p, D_s, D_w) and live load distribution factor (DF) are calculated from a selection of typical bridge designs from the previous reliability-based calibration efforts as described above.
- 2- The mean value of R ($\bar{R} = \lambda \times R_n$) which is needed for the reliability analysis is calculated by using the equation 5.5 for R_n and Table 5.1 for λ (depending on the type of girder and considered failure mode). In this step, R_n remains a function of unknown required load effect ($\gamma_{LL}(LL+IM)$).
- 3- Considering the limit state function given in equation 5.3 and the target reliability index (here is 2.50), the limit state can be expressed as a function of the random variables ($R, D_p, D_s, D_w, DF, IM, \text{ and } LL$) discussed earlier. In this calculation, mean girder resistance \bar{R} remains a function of the unknown RLE.
- 4- In the calculation of β , since the reliability index is preset to a known value, the only unknown is the RLE, which is solved for. Thus, the live load effect needed to be produced by the rating live load model (RLE) in order to meet the minimum reliability target can be determined.

As mentioned earlier, in this study 195 bridge types were considered. Considering the load effects (moment and shear) and multiple lane (one-lane and two-lane), in total, 780 (4×195) reliability constraints must be evaluated. This results in the calculation 780 calculation of reliability index for each optimization iteration. There are several approaches available to calculate the reliability index. One approach is the First Order, Second Moment (FOSM) method, as a closed-form function of the means and standard deviations of random variables.

It is important to note that FOSM produces a conservative estimate if the limit state functions are nonlinear or composed of non-normal random variables. As mentioned earlier, in this study, the girder resistance is assumed to be lognormal to be consistent with the previous study (AASHTO 368 1999, Sivakumar et al. 2011).

Eamon et al. (2014) investigate the degree of conservatism using FOSM with the limit state functions and random variables considered here. It was found that the error in FOSM from the exact solution is consistent at a given level of reliability. That is, regardless of bridge geometry or girder type, the FOSM approach produced a reliability index with a consistent level of conservativeness from the exact value. For the target reliability index used in this study ($\beta_T=2.5$), the ratio of the exact value to the FOSM solution was found to be approximately 1.04.

Therefore, in this study, the FOSM method is used with the modification suggested by Eamon et al. (2014), where the solution is adjusted by the factor of 1.04 when the target reliability index constraint of 2.5 is imposed in the optimization. It should be emphasized that this adjustment is valid only for the specific limit state functions and random variable parameters used in this study. For verification, a sample of girder reliability indices was computed with Monte Carlo Simulation (MCS) with 1×10^6 simulations at the completion of the RBDO. It was found that the indices

estimated with the modified FOSM approach described above were within 1% of the “exact” MCS values.

5.3 Design Variables

As noted above, design variables within previous RBDO procedures applied to bridges were used to describe geometric and potentially material properties. In this study, however, rather than optimizing a structural configuration, it is tried to develop a rating load model.

Therefore, design variables must describe critical parameters that define the load model. The existing nominal vehicular load rating model given in the MBE(AASHTO 2018) is the governing load effects of three AASHTO trucks (Types 3, 3S2, and 3-3), with a load factor of 1.80 if the ADTT is unknown or equal or greater than 1.80. The AASHTO trucks configurations are presented in figure 5.1. The load factor is reduced to 1.65 and 1.40 for ADTT equals to 1000, and less than 100, respectively.

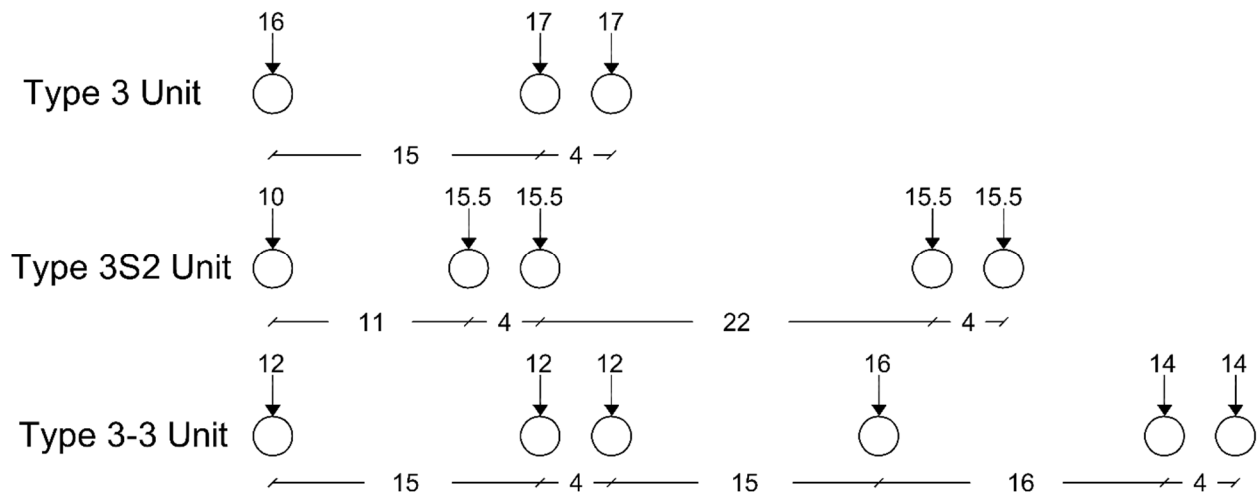


Figure 5. 1 AASHTO Rating Trucks (kips, ft.)

The critical load effects can be taken as the maximum of the AASHTO legal trucks or state legal loads. To consider the load vehicle load requirements, which can be much higher than the federal standard, some states such as Michigan have increased this rating load. In particular,

MDOT specifies 28 vehicles with different load factors for rating, which are meant to model possible legal configurations (MDOT 2005). From all 28 rating trucks, the trucks that provided the maximum load effects (moment or shear) for the spans considered in this study are given in figure 5.2.

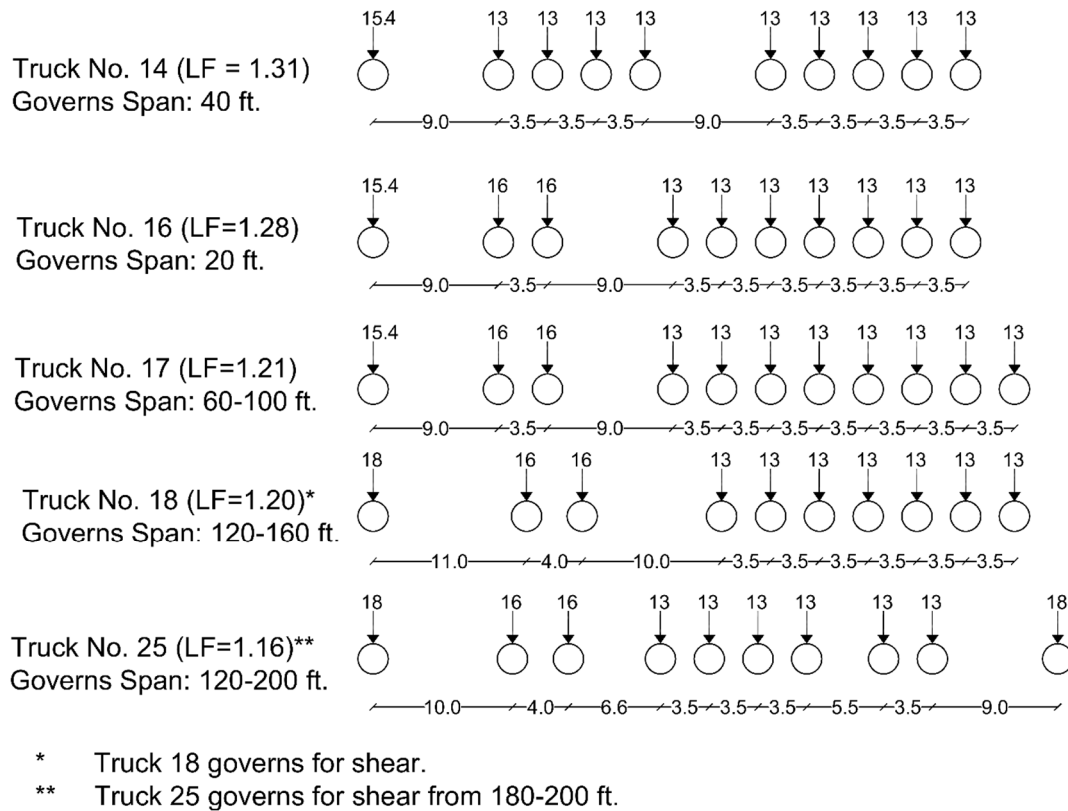


Figure 5. 2 MDOT Rating Trucks (kips, ft.)

Using the MDOT rating trucks as well as AASHTO legal trucks produced highly incontinent girder reliabilities in rating (Eamon and Siavashi 2018).

In this study, to allow the optimizer to reach the greatest possibility of an ideal rating model with minimal variation in reliability and thus minimizing the objective function in equation 5.2, it is tried to determine a function which can directly describe the required load effect (RLE) caused by a rating vehicle. First, a preliminary evaluation was done by fitting various expressions to a selection of RLE values corresponding to different span lengths. If the sample of RLEs can be well

described by a certain expression, by using RBDO, the variation in the reliability index can be well minimized. Various curves including logarithmic, power, compound, logistic, growth, polynomial, and sum of sines functions were considered. These are typical expressions used for fitting the data (Fan et al. 2013; Siavashi et al. 2017; Siavashi et al. 2019).

Using root mean square error as a metric, it was found that a sum of sines function, similar to a Fourier series, could best fit the required rating load effect, and is given as:

$$RLE = \sum_{i=1}^n a_i \sin(b_i x + c_i) \quad (5.6)$$

where for n terms, constants a_i , b_i , and c_i represent design variables to be determined in the optimization and x is bridge span length. It was observed that the RLE with respect to moment is different from that of shear, therefore, the analysis was conducted separately for shear and moment load effects to maximize the goodness of fit that could be obtained in each case. It was found that for both moment and shear, 3 terms are sufficient for describing required load effects, producing 9 design variables for load effects. It is important to note that Equation 6 is much for flexible than using a single vehicle for rating. In addition, it is less complex in the RBDO. To compare the complexity of this model, assume that an optimization problem is developed to generate a truck. Assuming a 6-axle truck require 11 design variables to describe axle weight (6 variables) and axle spacing (5 variables). After generating the truck, the load effects need to be calculated to convert the truck configuration to the load effects (i.e. moment and shear) on a given span.

Lower (Y_k^l) and upper (Y_k^u) bounds for the design variables (i.e. constants within equation 6) are specified to be from $-1000000 \leq Y_k \leq 1000000$. In the optimization, the RLE within Equation 5 (i.e. the quantity $\gamma_{LL}(LL+IM)$) is taken as a function given by equation 6, with design variables

a_i , b_i , and c_i ($i = 1-3$). Following the reliability procedure described above, equation 5 in turn determines R_n , which then affects the calculation of girder reliability.

Therefore, for each cycle of the RBDO, trial values for design variables a_i-c_i are found, then the RLE, R_n , and finally reliability index for all girders is computed. The objective function given in equation 5.2 is then evaluated. Based on the results of the objective function, which quantifies the inconsistency in reliability for different girders, new trial values of the design variables can be determined by the optimizer.

5.4 Solution of RBDO Problem

A simple RBDO approach required two iterations. In the first iteration, the ‘outer’ loop concerns optimizing the design variables and the ‘inner’ loop involves the reliability algorithm. In each cycle of the optimization, the objective function as described in equation 5.2 and the reliability constraints (the target reliability index of 2.50) are evaluated based on the current design variable values (here the constants in the equation 5.6). Design variable values are updated for use in the next iteration based on the results.

To update these values, each optimization iteration requires multiple evaluations of the objective function, while if an iterative reliability algorithm is used, multiple evaluations of the limit state function are also required. Thus, the double-loop procedure demands a high computational effort. As mentioned earlier, in this research, it is tried to increase the efficiency of the reliability method by using a non-iterative reliability algorithm.

One approach to optimization is represented by heuristic methods, which often use a form of probabilistic simulation in lieu of computing numerical derivatives. Some of these methods include Particle Swarm Optimization (Kennedy 2011; Baghi et al. 2019), Insect Colony Optimization (Karaboga and Georgiou 1994), Simulated Annealing (Kirkpatrick 1984), and

Genetic Algorithm (Koumoussis and Georgiou 1994; Roostaei 2018). In this study, a genetic algorithm (GA) is used.

The GA method does not require derivative information, but only direct evaluation of the objective function. At each iteration, new design variable values are determined with directed probabilistic simulation. In general, the process starts with a large set of randomly generated possible solutions (i.e. sets of design variable values), which are refined at each cycle by evaluating how effectively the objective function is satisfied. New potential solutions are generated from the most successful previous solutions until an optimal set is found. To generate new solutions, for each successive iteration, two primary procedures, crossover and mutation, are used. In the crossover procedure, subparts of two randomly selected previous solutions are combined to form a new solution, whereas the mutation procedure applies random changes to randomly selected individual solutions. The purpose of these operators is to retain potentially effective solutions while avoiding convergence to a local rather than global optimum (Man et al. 1996; Tang et al. 1996; Konak et al. 2006; Hao and Xia 2002).

In this study, a possible solution refers to a set of design variable values that represent the values of the constants (a_i, b_i, c_i) given in equation 5.6. The optimization starts by determining 1×10^6 possible solutions with Monte Carlo Simulation (MCS), using uniform distributions bound by the limits Y_k^l and Y_k^u given above. This solution set size remains constant for all iterations. Once this initial set of solutions is generated, the objective function (Equation 5.2) is evaluated using all of the potential solutions, and these results are recorded. The next iteration begins by generating a refined set of solutions from several different sources: 1) 80% are obtained by randomly choosing two solutions from the previous set and producing a new solution by taking a weighted average of these two solution values, such that the more effective solution (that with the

lowest objective function value) is given proportionally more weight (crossover); 2) the top 10% of most effective solutions are retained from the previous iteration; 3) 9.8% are obtained from MCS, as with the initial set; 4) 0.2% are obtained by randomly choosing a solution from the previous iteration, then randomly choosing one of its design variables and replacing that value with a new, randomly generated value using the MCS process (mutation).

The objective function is then evaluated with this new set of potential solutions, and the process repeats during subsequent iterations until the solution converges. Here, convergence implies that additional iterations cannot produce a more optimal solution than that found in previous iterations; i.e. that the objective function cannot be further minimized.

5.5 Modified Best Selection Method

According to MBE (AASHTO 2018), AASHTO legal trucks (Figure 5.1) are sufficiently representative average truck configurations in use today and used for load models for load rating. However, it was found that the current legal vehicles (both AASHTO vehicles and MDOT legal trucks) produced significant inconsistencies in reliability. Therefore, due to the complexity of RBDO, Siavashi and Eamon (2019) proposed a novel approach to select the “best” truck(s) with the appropriate load factor such that the consistent results across the considered bridge types can be determined. It is important to note that although using RBDO result may result in a theoretically ideal result, it has some drawbacks. The first drawback is the possibility of resulting in a load model (vehicles or expression) that does not resemble to a realistic or actual vehicle. In addition, depending on problem formulation and solution approach, its computational complexity and high computational cost may make RBDO undesirable to be implemented by DOTs. To determine a realistic using an RBDO, as described earlier, various trucks with different axle weights and axle spacings within the range of legal vehicles can be generated. The load effects of

each vehicle need to be calculated. This process can be optimized such that an ideal truck(s) can be generated. Due to this drawback, Siavashi and Eamon (2019) proposed an approach which does not require any optimizer, design variables, objective function, or iteration. The proposed model was found not only to be more simple but to have a substantial computational advantage over RBDO for load model development (Siavashi and Eamon 2019). The step by step procedure of “Best Selection Approach” is provided in figure 5.3.

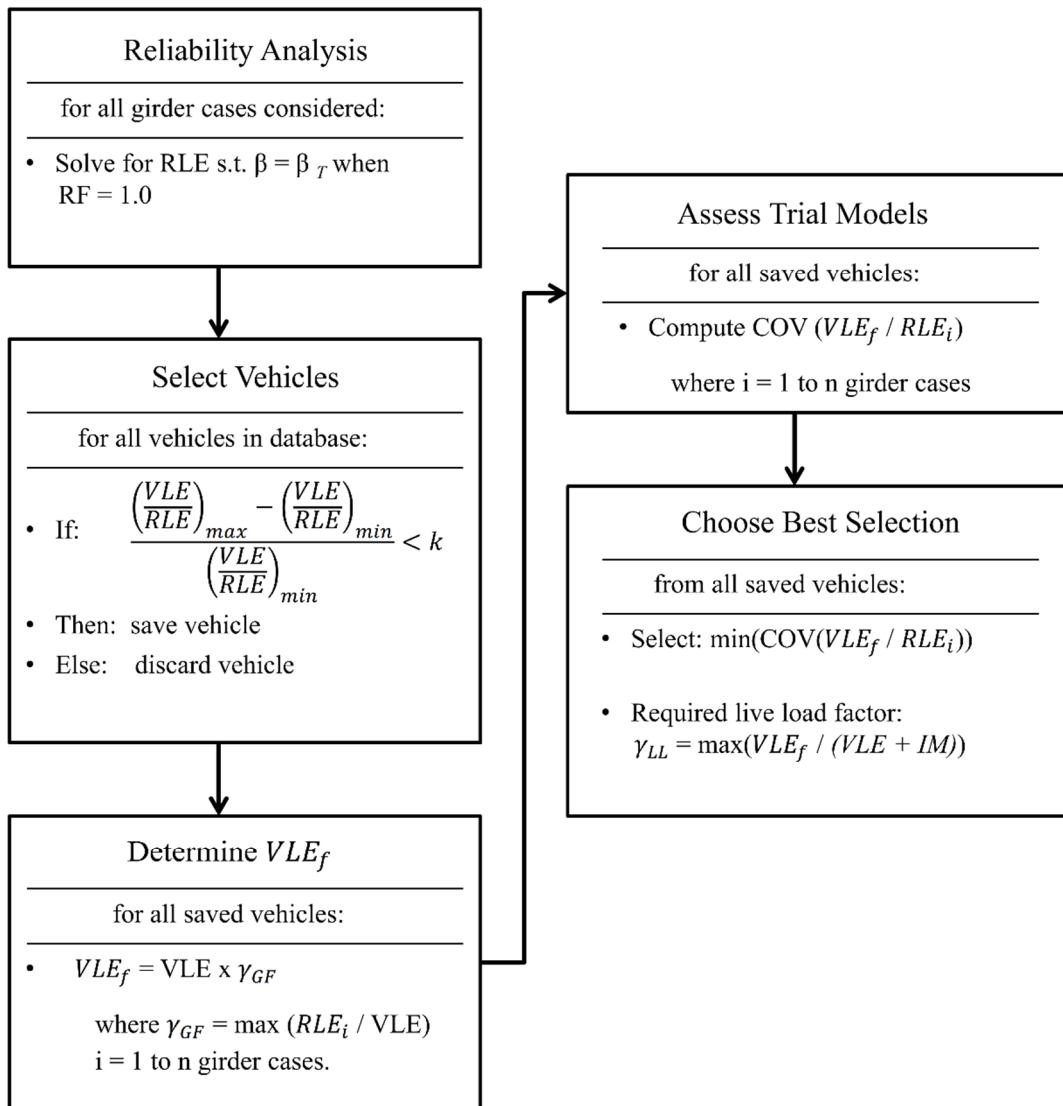


Figure 5. 3 Best Selection Method Flowchart.

In this study, a “Best Selection” approach is modified. In this approach, rather than generating an ideal load model by optimization, a set of truck records from the WIM data that produce the least variation from the RLE across all spans and bridge types is formed. Then, an appropriate load factor is chosen for each vehicle in the dataset such that the least variation from the RLE is provided while the imposed minimum required reliability requirement (here is 2.50) is met. The resulting vehicle after applying the load factor that has the least variation from the RLE across all span length can be selected.

Although it may appear intuitive to do so, the vehicle with the single lowest range of (VLE/RLE) cannot simply be selected as an ideal load model; i.e. simply selecting the vehicle producing the lowest discrepancy in reliability across the bridge spans considered. The reason for this is that after calculating the appropriate load factor(s) such that its total load effect at least meets the RLE across all bridge spans, the range of (VLE/RLE) ratios may substantially change. An example to demonstrate this issue is provided in figure 5.4 where before applying the load factors, Truck 2 has the lowest range of (VLE/RLE) from spans of 20-200 ft.. However, after applying the required load factors to meet the RLE (1.60 for Truck 1 and 15.01 for Truck 2), the (VLE/RLE) range of Truck 1 is lowest.

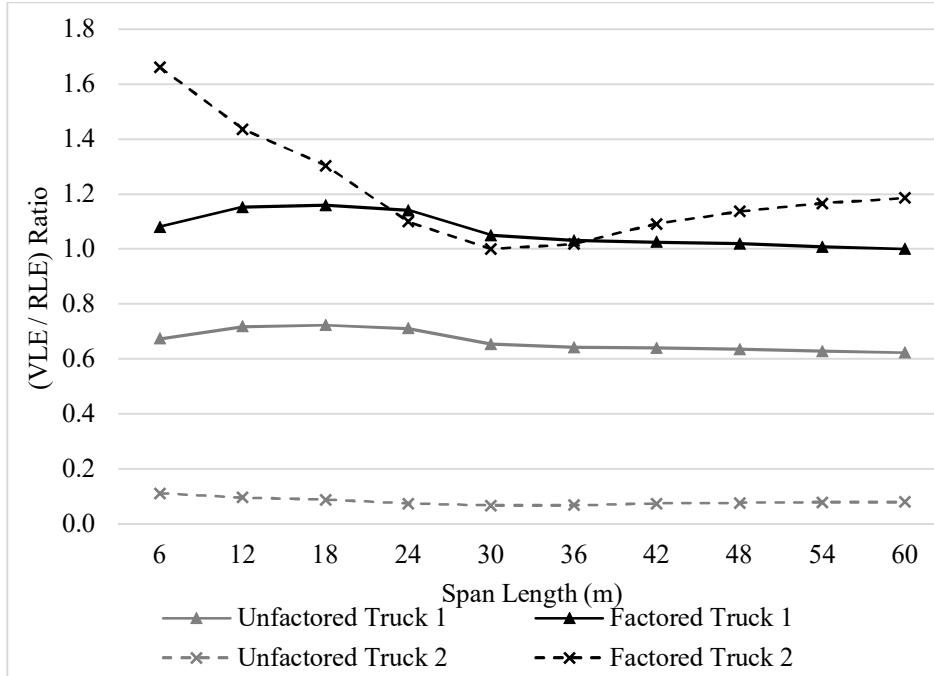


Figure 5. 4 Example Comparison of Load Effect Ratios Using Best Selection Method

The first step in this process is to determine the minimum load factor such that the minimum ratio of load effect multiplied by load factor over RLE of one is met for all span lengths and bridge types. The minimum load factor (LF) can be determined as follows:

$$\text{Load factor} = \frac{1}{\min\left(\frac{VLE}{RLE}\right)_i} \quad (5.7)$$

where i is the considered span lengths, VLE is the vehicle load effect, and RLE is the required load effect. Basically, in this step, the appropriate load factor (LF) is calculated such that after applying to vehicle load effects, all the $VLE \times LF / RLE$ across all span lengths shift above one.

The second step in this process is to select a set of initial trucks for further consideration. The amount of WIM data available for load model development is typically large. The database used for this study, for example, as noted above, contains 89 million legal and extended permit (MI-LEP) vehicle records and about 78 million simplified CFR vehicle records, and full consideration of all vehicles in this set is costly. A much smaller subset of these vehicles can be

considered for further consideration by comparing the range of ratios of load effect produced by the vehicle multiplied by calculated load effect to that required load effect across the bridge spans considered. Vehicles that produce a range of provided to required load effect ratios within a specified limit are taken for further consideration. This selection limit can be expressed as:

$$\left(\frac{VLE \times LF}{RLE}\right)_{max} < 1 + k \quad (5.8)$$

where LF is the load factor calculated such that $\left(\frac{VLE \times LF}{RLE}\right)_{min}$ of 1.0 can be met. k is the fractional range limit imposed. Depending on the load effect (i.e. moment and shear), the k can be determined. The higher k value increases the conservatism across the bridge span lengths. Recall that the applying load factor shifts the load effects over RLE ratio of each vehicle across all span lengths above 1.00. Therefore k shows the maximum acceptable range for load effects over RLE ratio across all span lengths. In this study, the k is limited to 20% which reduces the initial MI-LEP database of 89 million to about 2 million vehicles. Increasing k beyond 20% may result in analyzing too many unnecessary selections that are highly unlikely to be the optimal solution. On the other hand, lowering k below 10% may result in eliminating potentially optimal solutions. Note that due to the variation in the load effect over RLE ratio a k equals to 20% is suggested. However, k can be selected based on the total number of vehicles in the database.

So far, in the first step, $\left(\frac{VLE \times LF}{RLE}\right)$ ratio shifts above one and in the second step, the maximum $\left(\frac{VLE \times LF}{RLE}\right)$ ratio is limited to 1.20 (i.e $1 + k$). Again, it may appear intuitive to do so, choosing the lowest $\left(\frac{VLE \times LF}{RLE}\right)_{max}$ does not simply select the best vehicle across all span lengths. Although the $\left(\frac{VLE \times LF}{RLE}\right)_{max}$ produces the worst scenario for all considered span lengths, it is important to consider the range of variation of $\left(\frac{VLE \times LF}{RLE}\right)$ across all different span lengths as well.

This can be seen in Figure 5.5, which shows two trucks taken from the WIM data used in this study. After applying the required load factors to meet the RLE (1.50 for Truck 1 and 1.96 for Truck 2), the maximum ($VLE \times LF / RLE$) of both Trucks are the same (1.29 here). However, it is clear that truck 1 is a better selection.

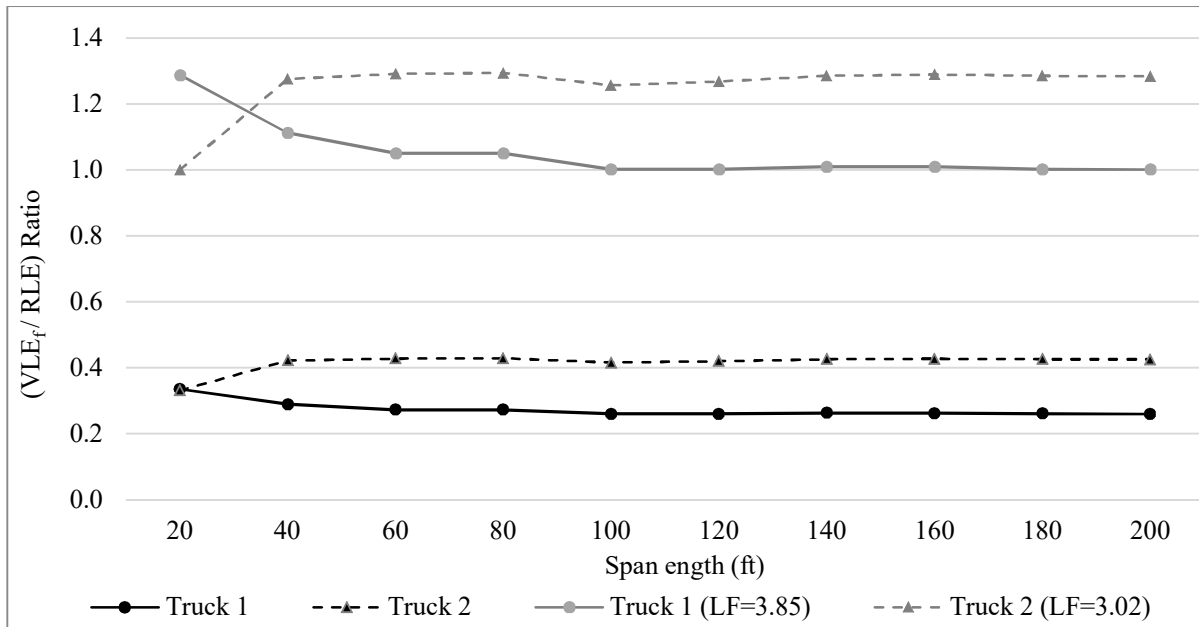


Figure 5. 5 Example Comparison of Load Effect Ratios Using Modified Best Selection Method.

After the desired vehicles are selected, the next step is to determine the metric used for the best selection. In this case, it may be more desirable to select a vehicle that minimizes the amount of discrepancy among all bridge spans. Various metrics of this nature are available. In this study, the metric suggested by Collins (2001) is modified and used for selecting the best vehicle(s). The Demerit Points Classification was initially suggested by Collins (2001) and used by many researchers (Oller Ibars et al. 2009, Neto et al. 2013, Kassem 2015, Baghi and Barros 2017; Baghi et al. 2019) to compare the analytical model to experimental model. The Demerit Points Classification proposed by Collins (2001) is presented in Table 5.2

Table 5. 2 Demerit Points Classification

Experimental over prediction ratio, λ	Classification	Penalty
< 0.50	Extremely dangerous	10
$0.50 - 0.65$	Dangerous	5
$0.65 - 0.85$	Low safety	2
$0.85 - 1.30$	Appropriate safety	0
$1.30 - 2.00$	Conservative	1
> 2.00	Extremely conservative	2

As mentioned earlier, the load factor is calculated such that $\left(\frac{VLE \times LF}{RLE}\right)$ for all spans is above 1.00. Therefore, the Demerit Points Classification needs to be modified. The suggested Demerit Points Classification is provided in Table 5.3.

Table 5. 3 Modified Demerit Points Classification Used in this study

$\lambda = \frac{VLE * LF}{RLE}$	Classification	Penalty (PEN)
$1.00 \leq \lambda \leq 1.025$	Best	0
$1.025 < \lambda \leq 1.05$	Very Good	1
$1.05 < \lambda \leq 1.10$	Good	2
$1.10 < \lambda \leq 1.15$	Appropriate	5
$1.15 < \lambda \leq 1.20$	Conservative	10
$1.20 < \lambda$	Extremely conservative	20

In this model, depending on the ratio between the $\left(\frac{VLE * LF}{RLE}\right)$ for each span, a penalty point is assigned. Total penalty points for each vehicle can be determined by adding the penalty point of all spans. Here, 10 spans are considered, therefore, the penalty point for each span is calculated separately and the total penalty points can be calculated. The vehicle with the lowest penalty point can be selected as an ideal vehicle. However, depending on the size of dataset, it is possible that multiple vehicles with the same penalty points can be determined. Recall that in this step, vehicle with the lowest penalty points is supposed to produce uniform results across all spans (which is the purpose of development of LRFD/LRFR).

If multiple vehicles with the same penalty points are determined, as the final step, the vehicle with the minimum average $\left(\frac{VLE \times LF}{RLE}\right)$ across all bridge span lengths can be selected. One example with two vehicles with the same penalty points (4) is presented in figure 5.6. It is clear that the vehicle number 1 ($\text{ave}\left(\frac{VLE \times LF}{RLE}\right) = 1.014$) with the lower average $\left(\frac{VLE \times LF}{RLE}\right)$ across all bridge span lengths is a better candidate compare to vehicle number 2 ($\text{ave}\left(\frac{VLE \times LF}{RLE}\right) = 1.023$).

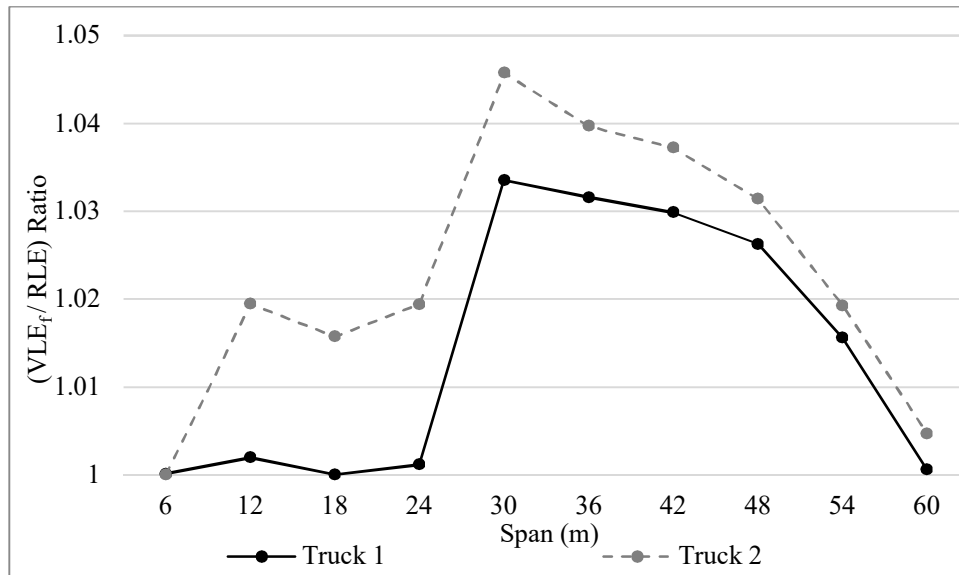


Figure 5. 6 Example Comparison of Load Effect Ratios With The Same Penalty Points.

As mentioned earlier, due to the high variation in girder reliability with respect to moment compare to shear, the analysis was conducted separately for moment and shear load effects. Therefore for rating, comparing simplified CFR and MI-LEP, moment and shear, 4 different analyses were conducted. In each scenario, 195 hypothetical girder bridge design including prestressed concrete I and box-shapes, composite steel, and reinforced concrete were considered. For each scenario, two rating vehicles are proposed using RBDO and Modified Best Selection approach. The results are then compared with the three AASHTO legal trucks and 28 Michigan

legal trucks for both moment and shear. The final set of values obtained for the parameters of equation 5.6 are presented in Table 5.4.

Table 5. 4 Coefficients for Sum of Sines Model.

Load Effect	Parameter								
	a_1	b_1	c_1	a_2	b_2	c_2	a_3	b_3	c_3
Simplified CFR Moment	18670	.010	0.403	18130	0.012	3.50	1422	0.022	5.61
Simplified CFR Shear	4.71	3632	-1649	-655	-508	2171	3.57	-7573	-2301
MI-LEP Moment	8556	0.015	-0.621	4879	0.022	2.07	295	0.053	1.91
MI-LEP Shear	244	0.002	.021	113	0.002	6.30	4.59	0.062	-1.67

The proposed trucks obtained from the Modified Best Selection approach are given in figure 5.7.

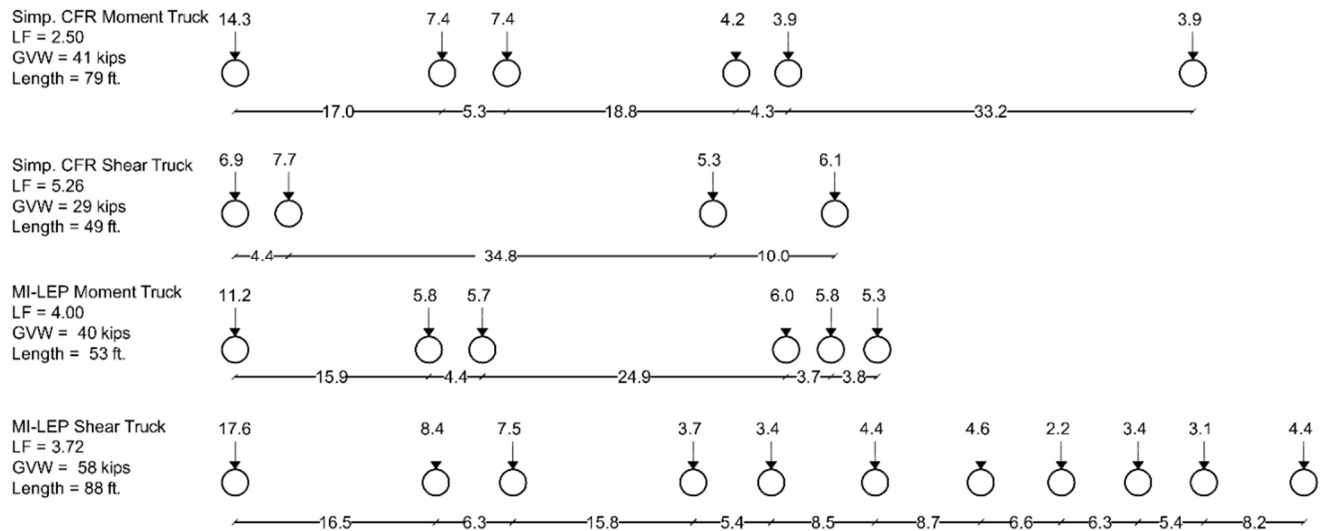


Figure 5. 7 Modified Best Selection Approach Trucks (kips, ft.).

The ratio of the factored vehicle load effect to the RLE (VLE_f/RLE) for the simplified CFR considering moment is given in figure 5.8. For all considered load models (RBDO solutions, the Modified Best Selection Truck, MDOT ,and AASHTO legal trucks), the appropriate load factor is applied such that all load models meet the minimum RLE (i.e. $VLE_f/RLE \geq 1.0$). Note that the

values given in the Figures represent the governing case of all bridge girder types considered (steel, prestressed concrete, steel, side by side and spaced box beams) for a particular span. As it can be observed in Figure 5.8, considering load factor equals 1.00, MDOT trucks producing higher load effect than RLE. In order to meet the minimum RLE (i.e. $VLE_f/RLE = 1.0$), the load factor of 0.94 is needed. This was expected since the MI legal vehicles are much heavier compare to other states legal vehicles (i.e. almost double). The load factor needed to meet the minimum RLE are found to be 1.28, and 2.50 for AASHTO legal trucks and Modified Best Selection Approach.

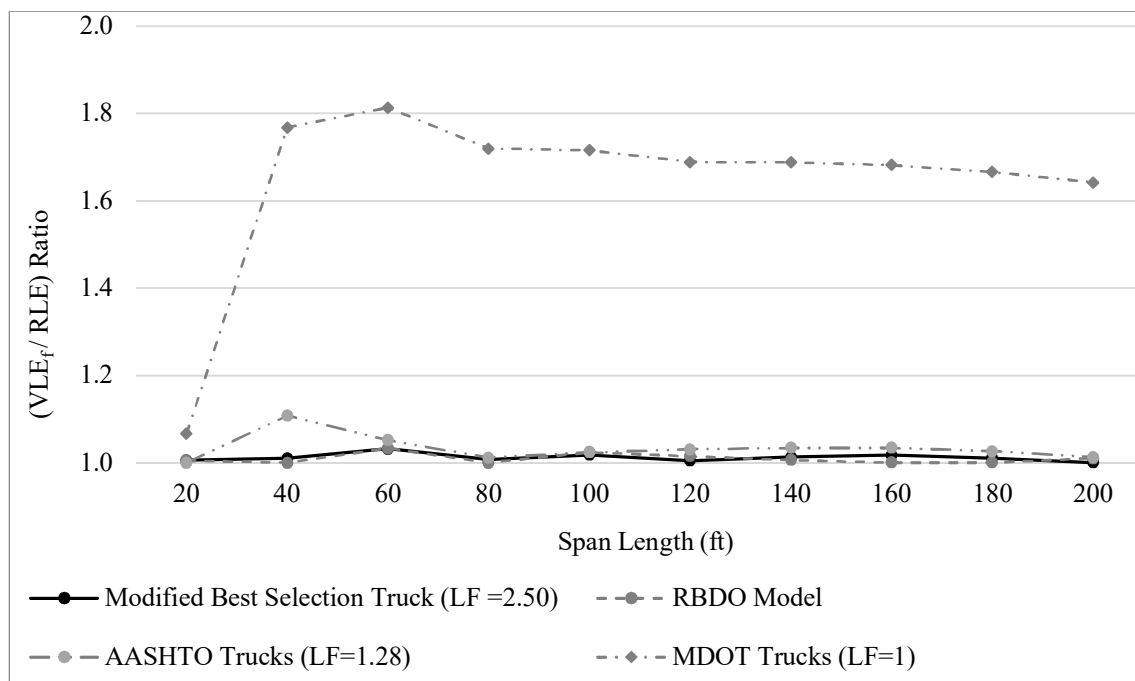


Figure 5. 8 Vehicle to Required Load Effect Ratios for Simplified CFR Moment

As shown, most consistency as well as closeness to RLE, and as a result, target reliability index can be obtained with the RBDOT and Modified Best Selection approach. Significant conservatism was found for MDOT rating trucks where the maximum (VLE_f/RLE) ratio reached approximately 1.81 at the 60 ft. span. Results from all rating models shown in Figure 5.8 are quantified in Table 5.5, where the minimum (β_{min}) and maximum (β_{max}) reliability indices corresponding to the largest discrepancies shown in Figure 5.8 are given, as well as the coefficient

of variation of reliability index (V_β) from all 195 girders considered across all bridge types and span is given. To fairly compare results, a best possible outcome is also given, provided that the same rating load model would be used for all bridge types, as is expected in rating practice. This is given as the “Exact (using RLE)” result. For this case, the results presented in the table correspond to a (VLE_f/RLE) ratio of 1.0 for all spans on Figure 5.8.

Table 5. 5 Comparison of Moment Design Load Models, Simplified CFR Moment

Design Load	Load Factor	β_{\min}	β_{\max}	β_{average}	COV
Exact (using RLE)	-	2.50	4.30	2.89	0.12
RBDO Load Model	-	2.50	4.32	2.92	0.12
Modified Best Selection Truck	2.50	2.50	4.32	2.92	0.12
MDOT Trucks (current LF)	varies ¹	3.30	6.99	4.73	0.18
MDOT Trucks (required LF)	0.94	2.50	5.61	3.96	0.15
AASHTO Legal Trucks (current LF)	1.80	2.93	6.01	3.89	0.17
AASHTO Legal Trucks (required LF)	1.28	2.50	4.29	2.98	0.12

1. See Figure 5.2 for load factors.

As shown in Table 5.5, the RBDO model and Modified Best Selection approach produce results nearly identical to the Exact model, with only a slightly higher average reliability index among all cases (β_{ave} , Exact = 2.89; β_{ave} , RBDO and Modified Best Selection = 2.92). Both Modified Best Selection and RBDO model produce the same average and maximum reliability index (β_{max} ; 4.32 and β_{ave} ; 2.92). The COV of reliability indices for all bridge cases using Exact, RBDO and Modified Best Selection is identical (to 2 decimal places) of 0.12.

Shear results are given in Figure 5.9 and Table 5.6. The same bridge that governs for moment did so for shear as well (60 ft., side by side box beam), with the minimum required load factors of 5.26, 1.46, and 2.05 for the Modified Best Selection, MDOT, and AASHTO Trucks, respectively. Moreover, discrepancies with the MDOT model decreased, where the maximum load ratio (VLE_f/RLE) increase from about 1.81 for moment to 2.05 for shear. The same increase for

the AASHTO model was observed, where maximum load ratios increased from 1.11 for moment to 1.42 for shear.

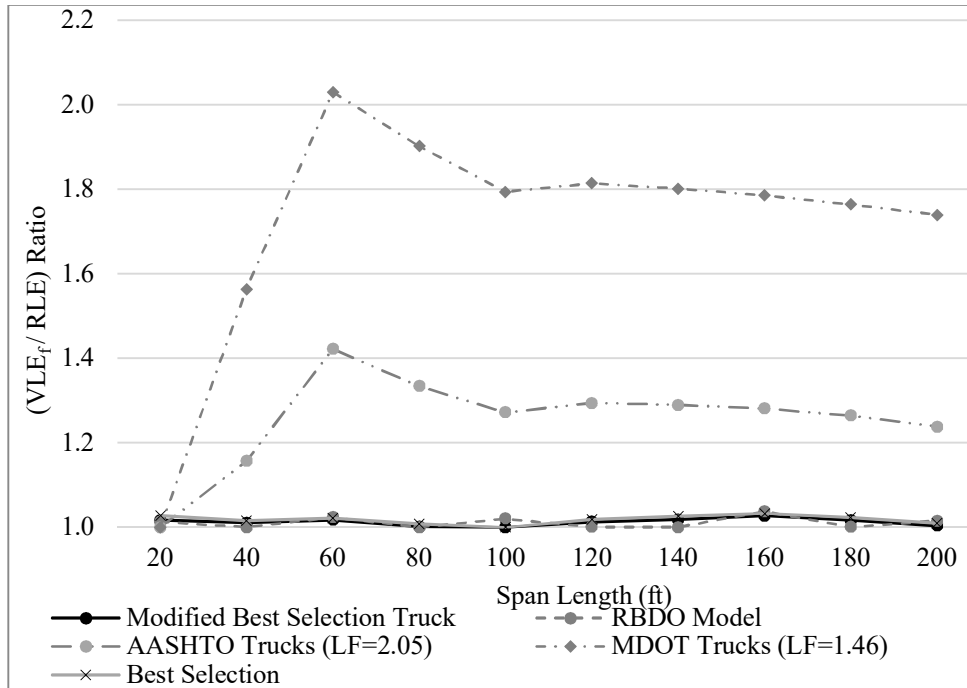


Figure 5. 9 Vehicle to Required Load Effect Ratios for Simplified CFR Shear

A maximum discrepancy of 3% and 4% from the exact results (i.e. $VLE_f/RLE = 1$) were observed for RBDO and Modified Best Selection approach, respectively.

Table 5. 6 Comparison of Moment Design Load Models, Simplified CFR Shear

Design Load	Load Factor	β_{min}	β_{max}	$\beta_{average}$	COV
Exact (using RLE)	-	2.50	4.66	3.04	0.13
RBDO Load Model	-	2.50	4.70	3.06	0.13
Modified Best Selection Truck	5.26	2.50	4.72	3.06	0.13
MDOT Trucks (current LF)	varies ¹	1.36	5.46	3.70	0.16
MDOT Trucks (required LF)	1.46	2.50	5.99	4.07	0.16
AASHTO Legal Trucks (current LF)	1.80	1.98	4.55	3.19	0.12
AASHTO Legal Trucks (required LF)	2.05	2.50	4.95	3.47	0.13

1. See Figure 5.2 for load factors.

As shown in Table 5.6, the range of shear reliability index for the exact solution has increased somewhat from that of moment, with β_{max} and β_{ave} increasing from 4.30 to 4.66 and 2.89

to 3.04, respectively. The variance of all results has increased as well from 0.12 to 0.13. It was observed that both the RBDO and Modified Best Selection models producing nearly identical solutions, with the same β_{ave} (3.06), COV (0.13) and a slightly higher β_{max} for Modified Best Selection (4.72) compare to RBDO (4.70).

A very similar trend was observed considering MI-LEP for both moment and shear. The results for moment are provided in Table 5.7 and Figure 5.10. The results for shear are provided in Table 5.7 and Figure 5.11. The minimum required load factors of respectively 4.00, 1.38, and 1.92 for the Modified Best Selection, MDOT, and AASHTO Trucks are needed for MI-LEP moment to meet the minimum reliability index of 2.50 for all considered bridge cases. The maximum VLE_f/RLE ratio of 1.89, and 1.19 were observed for MDOT and AASHTO legal trucks. This maximum ratio was found to be 1.03 and 1.01 for Modified Best Selection and RBDO, respectively.

As shown in Table 5.7, the RBDO model and Modified Best Selection approach produce results nearly identical to the Exact model, with only a slightly higher average reliability index among all cases (β_{ave} , Exact = 2.83; β_{ave} , RBDO = 2.84, and Modified Best Selection = 2.87). Both Exact, Modified Best Selection and RBDO model produce the same β_{max} of 3.95. The COV of reliability indices for all bridge cases using Exact, RBDO and Modified Best Selection is identical (to 2 decimal places) of 0.13.

Table 5. 7 Comparison of Moment Design Load Models, MI-LEP Moment

Design Load	Load Factor	β_{min}	β_{max}	$\beta_{average}$	COV
Exact (using RLE)	-	2.50	3.95	2.83	0.13
RBDO Load Model	-	2.50	3.95	2.84	0.13
Modified Best Selection Truck	4.00	2.50	3.95	2.87	0.13
MDOT Trucks (current LF)	varies ¹	2.13	5.52	3.74	0.20
MDOT Trucks (required LF)	1.35	2.50	5.74	4.09	0.18
AASHTO Trucks (current LF)	1.80	2.25	3.85	2.84	0.15

AASHTO Trucks (required LF)	1.93	2.50	4.14	3.05	0.15
-----------------------------	------	------	------	------	------

1. See Figure 5.2 for load factors.

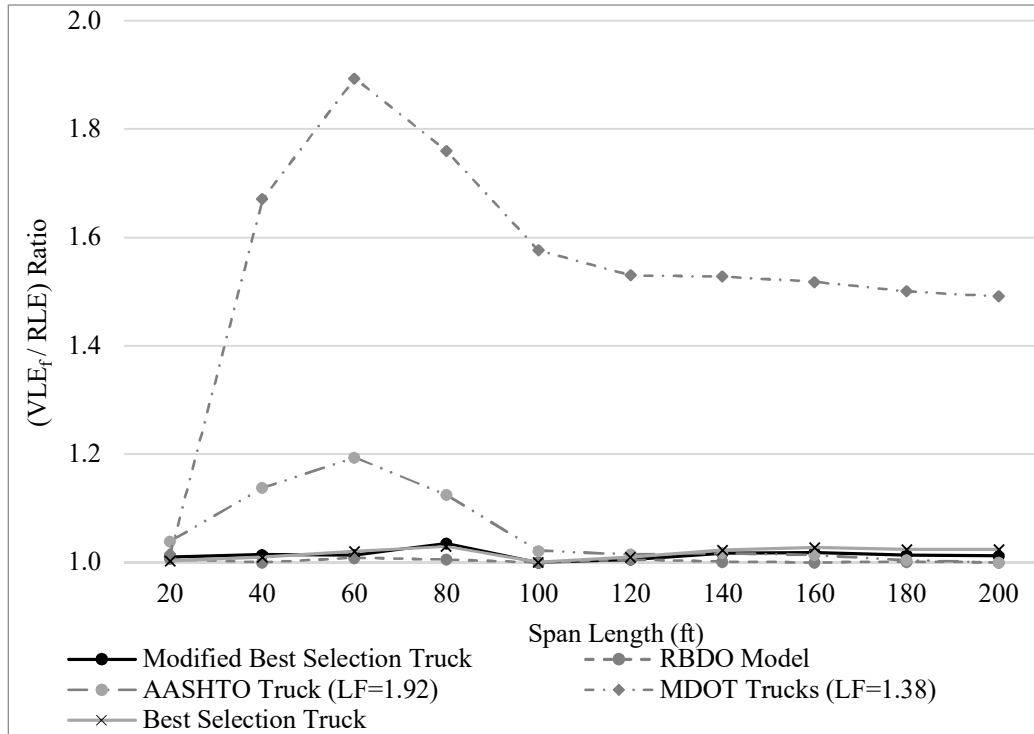


Figure 5. 10 Vehicle to Required Load Effect Ratios for MI-LEP Moment

Shear results are given in Figure 5.10 and Table 5.8. The minimum required load factors of respectively 3.72, 1.4, and 2.4 for the Modified Best Selection, MDOT, and AASHTO Trucks are needed to meet the minimum reliability index of 2.50 for all considered bridge cases.

As shown in Table 5.8, the range of shear reliability index for the exact solution has increased somewhat from that of moment, with β_{max} and β_{ave} increasing from 3.95 to 4.20 and 2.83 to 2.90, respectively. The variance of all results has decreased from 0.13 to 0.10. It was observed that both the RBDO and Modified Best Selection models producing close solutions, with the β_{ave} and β_{max} of 2.91 and 4.25 for RBDO and 2.93 and 4.26 for Modified Best Selection, respectively.

Table 5. 8 Comparison of Shear Design Load Models, MI-LEP Shear

Design Load	Load Factor	β_{min}	β_{max}	$\beta_{average}$	COV
-------------	-------------	---------------	---------------	-------------------	-----

Exact (using RLE)	-	2.50	4.20	2.90	0.10
RBDO Load Model	-	2.50	4.25	2.91	0.10
Modified Best Selection Truck	3.72	2.50	4.26	2.93	0.11
MDOT Trucks (current LF)	varies ¹	2.10	4.67	3.22	0.14
MDOT Trucks (required LF)	1.40	2.50	5.05	3.55	0.14
AASHTO Legal Trucks (current LF)	1.80	1.70	3.85	2.67	0.13
AASHTO Legal Trucks (required LF)	2.40	2.50	4.97	3.33	0.14

1. See Figure for load factors.

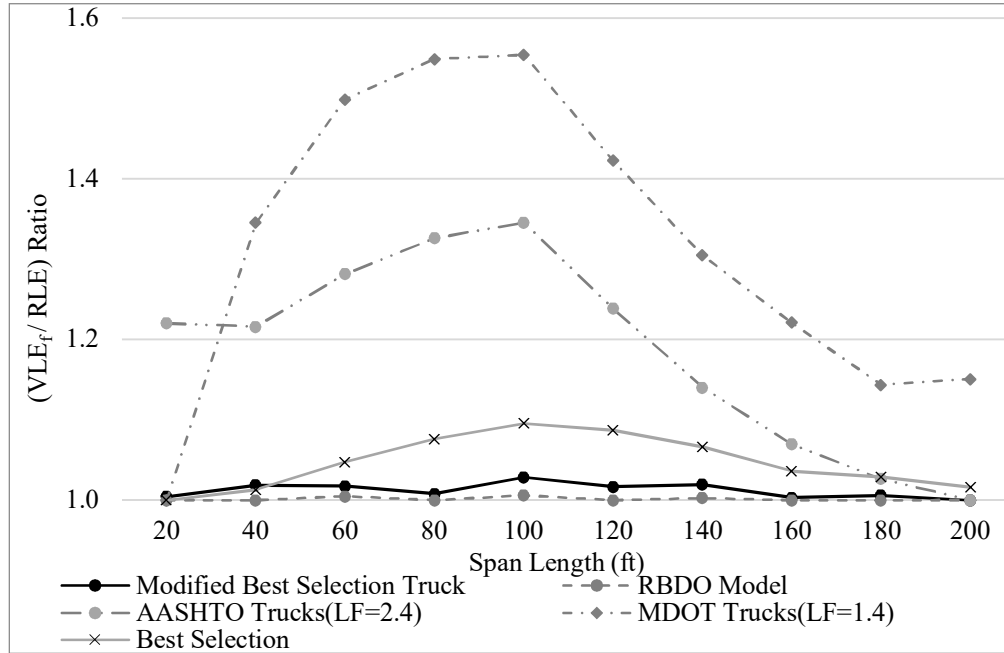


Figure 5. 11 Vehicle to Required Load Effect Ratios for MI-LEP Shear

The comparison of total penalty points (PEN) and average (VLE_f/RLE) across all span lengths (20 ft. to 200 ft.) are presented in Table 5.9. It observed that both RBDO and Modified Best Selection produce the lowest penalty points as well as lowest average (VLE_f/RLE) . MDOT is the most conservative load model.

Table 5. 9 Comparison of Total Penalty Points and average $VLE*LF/RLE$

Database		RBDO	Mod. Best Selection	Best Selection	AASHTO ²	MDOT ³
Simp. CFR Moment	PEN ¹	1	1	1	10	180
	Mean ²	1.01	1.01	1.02	1.03	1.55
Simp. CFR Shear	PEN	0	1	1	170	180
	Mean	1.01	1.01	1.02	1.26	1.72

MI-LEP Moment	PEN	1	0	1	21	180
	Mean	1.01	1.01	1.02	1.06	1.55
MI-LEP Shear	PEN	0	0	10	127	155
	Mean	1.00	1.01	1.05	1.19	1.32

1- Total Penalty Points

2- Mean $VLE*LF/RLE$ of all 10 span lengths

To compare the effectiveness of Best Selection method and Modified Best Selection approaches, a very small dataset of a site with the ADTT of approximately 350 is used. The dataset contains about 350,000 vehicles from which it is tried to find the optimal vehicle with the appropriate load factor. Considering the MI-LEP moment and shear, it is found that both “Best Selection” approach and “Modified Best Selection” approach can catch the best possible option. In MI-LEP moment, the average $\left(\frac{VLE*LF}{RLE}\right)$ ratio of 1.01 and 1.02 was observed using “Modified Best Selection” and “Best Selection” approaches, respectively with the total penalty points of 1.0 for both approaches. The comparison of $\left(\frac{VLE*LF}{RLE}\right)$ ratio for MI-LEP dataset is presented in figure 5.12.

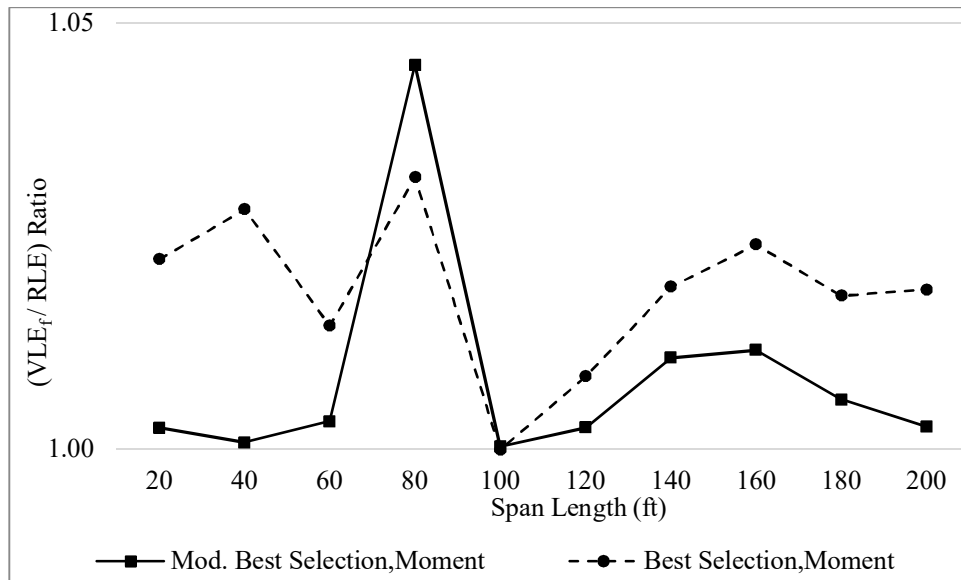


Figure 5. 12 Comparing Best Selection and Modified Best Selection, MI-LEP Moment (ADTT

350)

Considering the MI-LEP shear, the average $\left(\frac{VLE*LF}{RLE}\right)$ ratio of 1.04 and 1.05 across the span lengths was observed using “Modified Best Selection” and “Best Selection” approaches, respectively with the total penalty point of 11 for “Modified Best Selection” and 16 for “Best Selection” approaches. The comparison of both approaches is presented in Figure 5.13.

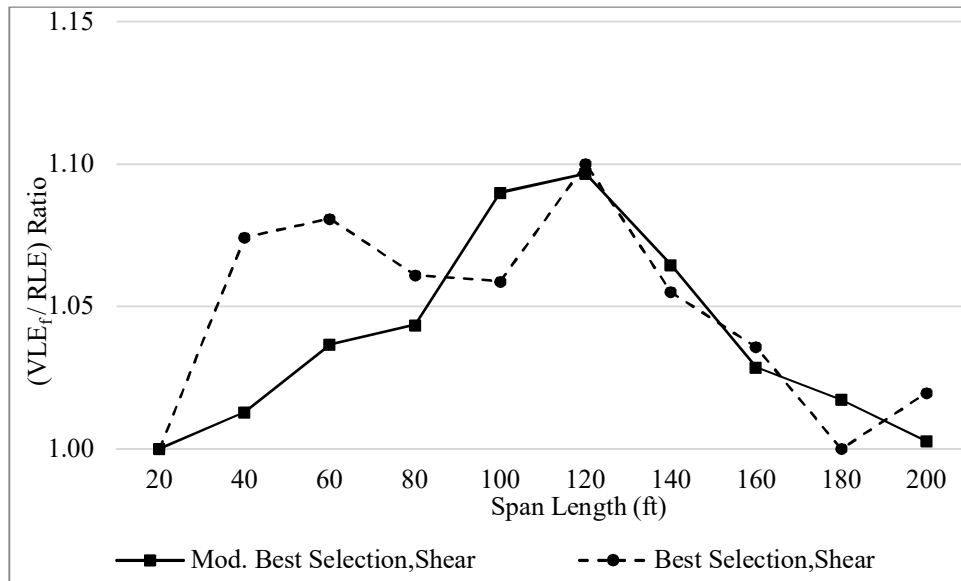


Figure 5. 13 Comparing Best Selection and Modified Best Selection, MI-LEP Shear (ADTT 350)
The process of Modified Best Selection approach is summarized in figure 5.14.

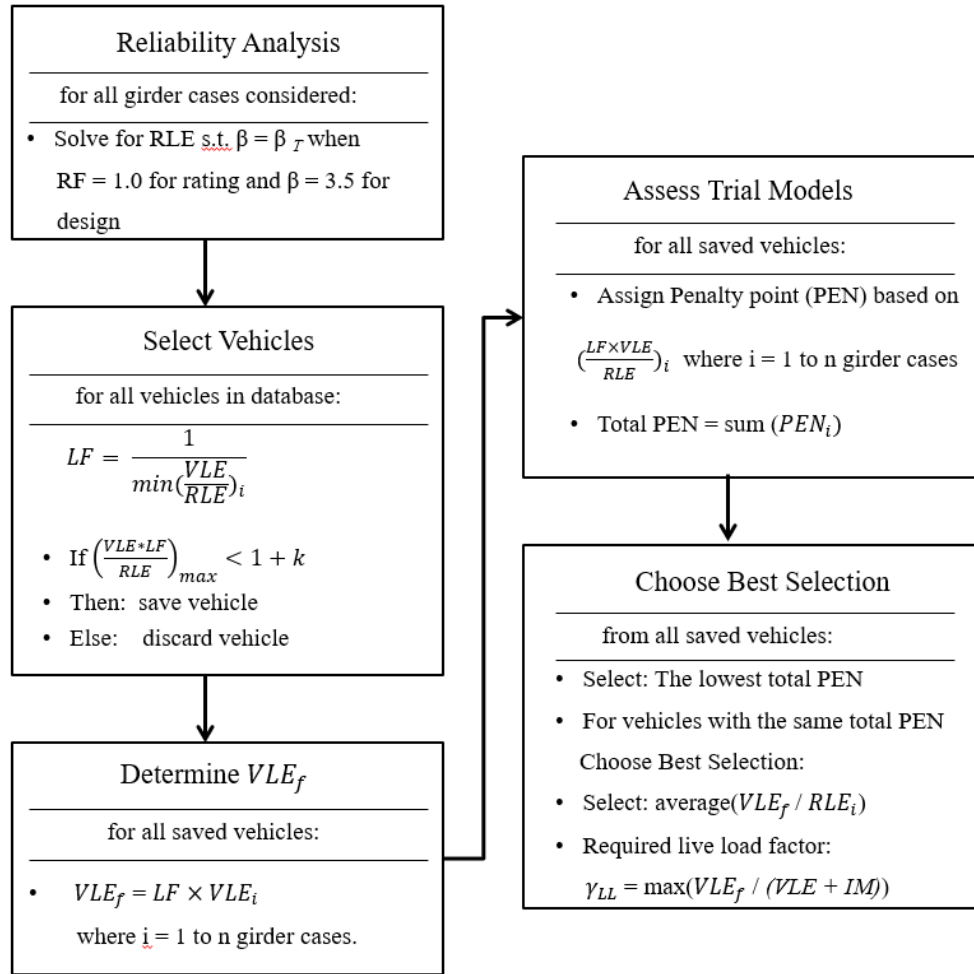


Figure 5. 14 Modified Best Selection Method Flowchart

It is found that the proposed RBDO model as well as Modified Best Selection Method produce consistent results in rating factor and corresponding reliability level among the considered bridge types compare to the current used load models (i.e. AASHTO Legal trucks and MI-Legal trucks).

CHAPTER 6 SUMMARY, CONCLUSION AND RECOMMENDATIONS

The first objective of this research is to propose a simplified procedure to reduce the vehicle dataset need to be considered for load rating of bridge superstructures. The second objective is to explore the effectiveness of Reliability Based Design Optimization (RBDO) to develop a State-specific rating load model for a set of bridge superstructures. Finally, an alternative novel approach to develop rating models as reasonably accurate as compare to RBDO solution is proposed. The proposed solutions can substantially reduce the computational effort resulting in a minimal loss of accuracy while not compromising the level of accuracy.

The objectives of this study were achieved by collecting and analyzing weigh-in-motion (WIM) data over a two year period across the 20 selected WIM sites across Michigan. The collected data was further filtered to remove any fictitious vehicles that considered axle weight and spacing; length; number of axles and speed. The filtered WIM data were further divided into two categories: MI-LEP and Simplified CFR. These categories consider vehicle pool used in the rating and representative of Michigan as well as most other states that follow the Federal limit. The load effects for simple moments and shears for hypothetical bridge spans from 20 to 200 ft. with 20 ft. increment were generated. Both single lane and two lane load effects were considered. Load effects were then statistically projected to 5 years using an extreme type I projection to obtain estimates for the maximum load effect statistics. Limit states were formed for two-lane bridges with span length from 20-200 feet in increments of 20 ft. Bridge beam types considered for the analysis were steel, prestressed concrete, reinforced concrete, spread box, and side-by-side box. Girder spacing varied from 4 to 12 feet at 2 ft. increments, while for side-by-side box beams, two widths (36 and 48 inches) were considered. Therefore, considering all combinations of length (10) and girder spacing (5) increments results in 50 geometries each for prestressed concrete, steel, and

spread box beam bridge types; 25 for reinforced concrete (limited to 100 ft.) ; and 20 side-by-side box beams, for 195 cases. Considering both one-lane and two-lane, 195 cases each, 390 cases were considered for the analysis.

Due to the significant inconsistencies observed in bridge reliability under the current rating process, the potential effectiveness of using RBDO to develop a reliability-based load rating model considering both databases was studied. The objective function was set to minimizing the variation of reliability index from the target reliability index of 2.50 across the mentioned girder type and bridge geometries. The Genetic algorithm is used as an optimizer. It was found that the sum of sines expression can be used for load model. The proposed procedure is less complex and more effective than the current load models used by AASHTO and MDOT models. Although the proposed solution is effective, it is new for engineers in practice and the adaptability of this model is questionable.

A novel Modified Best Selection Approach was proposed to select a vehicle directly from the WIM data that minimizes discrepancies in load effects. The proposed method is not an RBDO-base approach (i.e. there is no optimizer, design variables, objective function, nor iteration). The proposed method is more effective than the current load models used by AASHTO and MDOT. The two vehicles developed from the Modified Best Selection approach (one for moment and one for shear) for each database produced significantly more consistent results overall comparing to the multiple vehicles (3 for AASHTO and 28 for MDOT) used by alternative models. Providing an actual truck as well as the significant reduction in the computational cost and problem complexity comparing to RBDO solution make this model a suitable solution for state-specific load rating model development.

Finally, a simplified approach which significantly reduces the computational time was proposed. The majority of computational time in the reliability-base rating analysis is spent for load effect calculation of single vehicles. The ratio of multiple vehicles (i.e. following or side-by-side) over single vehicles is found to be less than two percent. This ratio is typical and observed in other studies as well. Therefore, the focus is to reduce the vehicle dataset of single vehicles. The correlation between truck parameters (i.e. GVW, length, number of axles, etc.) and load effects (i.e. moments and shears) were studied. It was found that there is a strong correlation between GVW and load effects (i.e. moments and shears). The data is further reduced based on the GVW and reliability indices are calculated and compared with the true results (i.e. no simplification). The proposed method was compared with the simplified approach used in the MBE. The load factor of 14 different sites is calculated and compared with the load factor calculating from all-data (i.e., no simplification). It is found that the proposed simplified procedure produces much better results (within 7% discrepancy from the true results) compared to the AASHTO simplified procedure (as high as more than three times the true results). The proposed method can be used for both site-specific and all-data rating analysis.

For future research, it is recommended to study the effect of reducing the dataset based on the GVW on the fatigue effect. Although it is found that the single-vehicle database can be reduced based on the GVW for reliability-based rating analysis, it is essential to further study the fatigue effects.

It is further recommended to study the application of machine learning on the prediction of maximum live load. In the last two decades, various techniques were proposed to project the expected maximum live load during the service life of bridges. Different assumptions and different data pools were used for each method. However, these are generally ad-hoc procedures that vary

in effectiveness and may produce significantly different results. Failing to predict the maximum expected load effects on the bridge during its lifetime may increase the risk of distress, damage, and even failure when the actual truck load effects are higher than the assumed load effects. On the other hand, conservative prediction of maximum live load effects may result in the unnecessarily posting of the bridge.

It is finally recommended to study the application of RBDO, Modified Best Selection Approach, and Proposed Simplified Procedure on other bridge types not considered in this study such as truss structures.

REFERENCES

- AASHTO LRFD Bridge Design Specifications, 8st ed. (2017) American Association of State Highway and Transportation Officials, Washington, D.C.
- AASHTO Manual for Bridge Evaluation, 3nd ed. (2011) American Association of State Highway and Transportation Officials, Washington, D.C.
- AASHTO Manual for Condition Evaluation and Load and Resistance Factor Rating (LRFR) of Highway Bridges (2003), American Association of State Highway and Transportation Officials, Washington, D.C.
- AASHTO Manual for Condition Evaluation of Bridges (1998), American Association of State Highway and Transportation Officials, Washington, D.C.
- AASHTO Standard Specifications for Highway Bridges (2002), American Association of State Highway and Transportation Officials, Washington, D.C.
- Anitori, G., Casas, J.R., and Ghosn, M. (2017) “WIM-Based Live-Load Model for Advanced Analysis of Simply Supported Short-and Medium-Span Highway Bridges.” *Journal of Bridge Engineering*, 10.1061/(ASCE)BE.1943-5592.0001081.
- Aoues, Y., and Chateauneuf, A. (2010) “Benchmark study of numerical methods for reliability-based design optimization.” *Structural and Multidisciplinary Optimization* 41: 277–294.
- Baghi, H. and Barros, J.A., 2017. Design approach to determine shear capacity of reinforced concrete beams shear strengthened with NSM systems. *Journal of Structural Engineering*, 143(8), p.04017061.
- Baghi, H., Baghi, H., and Siavashi, S., 2019. “Novel Empirical Expression to Predict the Shear Strength of Reinforced Concrete Walls Based on Particle Swarm Optimization”, *ACI Structural Journal*, in press.

- Bailey, S. and Bez, R. (1999) "Site specific probability distribution of extreme traffic action effects." Probabilistic engineering mechanics, Vol 14, No. 1, 1999.
- Barros, J. A., & Foster, S. J. (2018) An integrated approach for predicting the shear capacity of fibre reinforced concrete beams. Engineering Structures, 174, 346-357.
- Bruls A, Croce P, Sanpaolesi L, Sedlacek O. ENV1991 - Part 3: traffic loads on bridges; calibration of load models for road bridges. (1996) In: Proceedings of IABSE colloquium, Delft, The Netherlands: IABSE-AIPC-IVBH; pp. 439-53.
- Chang, B., Bourland, M., Couch, T., Zou, H., and Jung, T. (2015) "Evaluation of Texas Superheavy- Load Criteria for Bridges." ASCE Journal of Performance of Constructed Facilities, Vol. 29, No. 4.
- Collins, M. P. "Evaluation of shear design procedures for concrete structures." (2001) Rep. Prepared for the CSA Technical Committee on Reinforced Concrete Design, Canada.
- Croce, P. and Salvatore, W. (2001) "Stochastic model for multilane traffic effects on bridges." ASCE Journal of Bridge Engineering, Vol. 6, No.2, pp. 136-143.
- Curtis, R. and Till, R. (2008) "Recommendations for Michigan Specific Load and Resistance Factor Design Loads and Load and Resistance Factor Rating Procedures." MOOT Research Report R-1511.
- Du, X., and Chen, W. (2004) "Sequential optimization and reliability assessment method for efficient probabilistic design." ASME Journal of Mechanical Design 126(2): 225-233, 2004.
- Eamon, C., Kamjoo, V., and Shinki, K. (2015) "Design Live Load Factor Calibration for Michigan Highway Bridges." ASCE Journal of Bridge Engineering.
- Eamon, C., Kamjoo, V., and Shinki, K. (2014) "Side-by-side Probability for Bridge Design and

- Analysis.” MDOT Research Report RC-1601.
- Eamon, C.D. and Siavashi, S., 2018. “Developing Representative Michigan Truck Configurations for Bridge Load Rating” (No. SPR-1640). Michigan. Dept. of Transportation. Research Administration.
- Eamon, C.D., Wu, H.C., Makkawy, A.A. and Siavashi, S., 2014. “Design and construction guidelines for strengthening bridges using fiber reinforced polymers (FRP)” (No. RC-1614). Michigan. Dept. of Transportation. Office of Research Administration.
- Enevoldsen, I., and Sorensen, J. (1994) “Reliability-based optimization in structural engineering.” *Structural Safety* 15: 169-196.
- Enright B. and O’Brien, E. (2010) “Management Strategies for Special Permit Vehicles for Bridge Loading.” Transport Research Arena Europe, Brussels.
- Enright, B. and O’Brien, E. (2013) “Monte Carlo simulation of extreme traffic loading on short and medium span bridges”. *Structure and Infrastructure Engineering*, Vol 9, No. 12.
- Enright, B., Obrien, E., and Leahy, C. (2015) “Identifying and Modelling Permit Trucks for Bridge Loading.” *Proceedings of the ICE – Bridge Engineering*.
- Fan, S. K. S., Y. J. Chang, and N. Aidara. 2013. “Nonlinear profile monitoring of reflow process data based on the sum of sine functions.” *Qual. Reliab. Eng. Int.* 29 (5): 743–758.
- Federal Highway Administration. (2015) Code of Federal Regulations, Title 23 (Highways), Chapter I (FHWA, DOT), Subchapter G (Engineering and Traffic Operations), Part 658: Truck Size and Weight, Routine Designations – Length, Width, and Weight Limitations, 2015.
- Federal Highway Administration. (2004) Federal Size Regulations for Commercial Motor Vehicles.

- Fu, G., and Fu, C. (2006) "Bridge Rating Practices and Policies for Overweight Vehicles." NCHRP Report 359. Washington, D.C., Transportation Research Board.
- Fu, G. and Hag-Elsafi, O. (2000) "Vehicular Overloads: Load Model, Bridge Safety, and Permit Checking." ASCE Journal of Bridge Engineering, Vol. 5, No.1, pp. 49-57.
- Fu, G., Feng, J., Dekelbab, W., Moses, F., Cohen, H., Meliz, D., and Thompson, P. (2003) "Effect of Truck Weight on Bridge Network Costs." NCHRP Report 495. Washington, D.C., Transportation Research Board.
- Fu, G. and Moses, F. (1991) "Overload Permit Checking Based on Structural Reliability." Transportation Research Record 1290.
- Fu, O. and Van de Lindt. (2006) "LRFD Load Calibration for State of Michigan Trunkline Bridges." MDOT Research Report RC-1466, August, 2006.
- Fu, O. and You, J. (2009) "Truck Loads and Bridge Capacity Evaluation in China." ASCE Journal of Bridge Engineering, Vol. 14, No.5, pp. 327-335,.
- Ghosn, M. (2008) "Development of Truck Weight Regulations Using Bridge Reliability Model." ASCE Journal of Bridge Engineering, Vol. 5, No.4, pp. 293-303.
- Ghosn, M. and Moses, F. (1986) "Reliability Calibration of Bridge Design Code." Journal of Structural Engineering, Vol. 112, no. 4.
- Ghosn, M., Sivakumar, B., and Miao, F. (2011) "Load and Resistance Factor Rating (LRFR) in NYS, Volume II, Final Report." NYSDOT Report C-06-13., 2011.
- Ghosn, M., Sivakumar, B., and Moses, F. (2008) "Modeling maximum live load effects on highway bridges." Proceedings from the First International Symposium on Live-Cycle Civil Engineering, Varenna, Italy, June, pp. 335-341.

- Ghosn, M., Sivakumar, B., and Moses, F. (2010) "Using weigh-in-motion data for modeling maximum live load effects on highway bridges." Proceedings of the Fifth International IABMAS Conference, Philadelphia, USA.
- Hao, H., & Xia, Y. (2002). "Vibration-based damage detection of structures by genetic algorithm." *Journal of Computing in Civil Engineering*, 16, no. 3: 222-229.
- Humphrey, T.F. (1988) "Uniformity Efforts in Oversize/Overweight Permits." NCHRP Report 143. Washington, D.C., Transportation Research Board.
- Imbsen, R.A. (1984) "Bridge Weight-Limit Posting Practice." NCHRP Report 108. Washington, D.C., Transportation Research Board, 1984.
- Kamjoo, V. and Eamon, C.. (2018) "Reliability-Based Design Optimization of a Vehicular Live Load Model." *Engineering Structures*, no. 168: 799-808, 2018.
- Kamyab, M., Remias, S., Najmi, E., Hood, K., Al-Akshar, M. and Ustun, I., (2019). "Evaluation of Interstate Work Zone Mobility using Probe Vehicle Data and Machine Learning Techniques." *Transportation Research Record*, p.0361198119827936.
- Kassem, W. (2015) Non-linear analysis of shear-critical reinforced concrete beams using the softened membrane model. *Structural Concrete*, 16(4), 524-536.
- Karaboga, D., and Basturk, B. (2007) "A powerful and efficient algorithm for numerical function optimization: artificial bee colony (ABC) algorithm." *Journal of global optimization* 39(3): 459-471.
- Kennedy, J. (2011) "Particle swarm optimization. *Encyclopedia of machine learning*" Springer.
- Kharmanda, G., Mohamed, A., and Lemaire, M. (2002) "Efficient reliability-based design optimization using a hybrid space with application to finite element analysis." *Structural and Multidisciplinary Optimization* 24 (3): 233-245.

- Kharmanda, G., and Olhoff, N. (2007) "Extension of optimum safety factor method to nonlinear reliability-based design optimization." *Structural and Multidisciplinary Optimization* 34 (5): 367-380.
- Kirkpatrick, S. (1984) "Optimization by simulated annealing: Quantitative studies." *Journal of statistical physics* 34 (5-6): 975-986.
- Konak, A., Coit, D. W., and Smith, A. E.. (2006) "Multi-objective optimization using genetic algorithms: A tutorial." *Reliability Engineering & System Safety*, 91, no. 9: 992-1007.
- Koumoussis, V. K., and Georgiou, P. G. (1994) "Genetic algorithms in discrete optimization of steel truss roofs." *Journal of Computing in Civil Engineering* 8, no. 3: 309-325.
- Kwon, O-S, Kim, E., Orton, S, Salim, H., and Hazlett, T. (2010) "Calibration of the Live Load Factor in LRFD Design Guidelines", MODOT Report ORI1-003, Sept.
- Lee, C.E. and Garnet, J.E. (1996) "Collection and Analysis of Augmented Weight-in-Motion Data." Center for Transportation Research Bureau of Engineering Research, the University of Texas at Austin, Report no. 987-8.
- Lee, C.E. and Souny-Slitine, N. (1998) "Final Research Findings on Traffic-Load Forecasting Using Weight-in-Motion Data." Center for Transportation Research Bureau of Engineering Research, the University of Texas at Austin, Report no. 987-7.
- Lu, Q., Harvey, J., Le, J., Quinley, R., Redo, D., and Avis, J. (2002) "Truck Traffic Analysis using Weigh-In-Motion (WIM) Data in California." University of California, Berkeley Institute of Transportation Studies, Pavement Research Center.
- MDOT Bridge Analysis Guide, 2005 Ed, with 2009 Interim Update (2009), Parts 1 and 2. MDOT Construction and Technology Support Area.

- Miao, T.J. and Chan. T.H.T. (2002) "Bridge live load models from WIM data." *Engineering Structures*, Vol. 24, No. 8, pp. 1071-1084.
- Mehrara Molan, Amirarsalan, "Evaluation Of Milwaukee B And Synchronized As New Service Interchange Designs" (2017). Wayne State University Dissertations. 1845.
- Molan, A.M., Hummer, J.E. and Ksaibati, K., 2019. Introducing the Super DDI as a Promising Alternative Service Interchange. *Transportation Research Record*, p.0361198119833682.
- Mehrara Molan, A. and Hummer, J.E., 2017. Travel Time Evaluation of Synchronized and Milwaukee B as New Interchange Designs. *Journal of Transportation Engineering, Part A: Systems*, 144(2), p.04017074.
- Monsere, L., Higgins, Ch. and Nichols, A. (2011) "Application of WIM Data for Improved Modeling, Design, and Rating." Oregon Transportation Research and Education Consortium, Oregon Department of Transportation.
- Moses, F. (2001) "Calibration of load factors for LRFR bridge evaluation." NCHRP Report no. 454, Washington, D.C., Transportation Research Board.
- Moses, F. and Ghosn, M. (1983) "Instrumentation for Weighing Trucks-In-Motion for Highway Bridge Loads." Final Report, FHWA/OH-83-001 to Ohio DOT, Case Western Reserve University, August.
- Neto, B. N. M., Barros, J. A., & Melo, G. S. A (2013) "model for the prediction of the punching resistance of steel fibre reinforced concrete slabs centrally loaded." *Construction and Building Materials*, 46, 211-223.
- Nowak, A.S. (1999) "Calibration of LRFD Bridge Design Code." NCHRP 368, Washington, D.C., Transportation Research Board.

- Nowak, A.S. (1995) "Calibration of LRFD Bridge Code." *Journal of Structural Engineering*, Vol. 121, No. 8, pp. 1245-1251.
- Nowak, A.S. (1993) "Live load model for highway bridges." *Structural Safety*, Vol. 13, pp. 53-66.
- Nowak, A.S., Lutomirska, M., and Sheikh Ibrahim, F.I. (2010) "The development of live load factors for long span bridges." *Bridge Structures*, Vol. 6, No. 1, pp. 73-79.
- O'Brien, E.J. and Caprani, C. (2005) "Headway modeling for traffic load assessment of short to medium span bridges." *The Structural Engineer*, Vol. 83, No. 16, pp. 33-36.
- O'Brien, E.J. and Enright, B. (2011) "Modeling same-direction two-lane traffic for bridge loading." *Structural Safety*, No. 33, pp. 296-304.
- O'Brien, E.J. Enright, B., and Getacollew, A. (2010) "Importance of the Tail in Truck Weight Modeling for Bridge Assessment." *ASCE Journal of Bridge Engineering*, Vol. 15, No.2, pp. 210-213.
- O'Connor A, Jacob B, O'Brien EJ, Prat M. (2001) Report of current studies performed on normal load model of ECI Part 2. Traffic loads on bridges. *Rev Francaise de Genie Civ*. Vol. 5, No.4, pp. 411-33.
- Oller Ibars, E., Cobo del Arco, D., & Marí Bernat, A. R.. (2009) Design proposal to avoid peeling failure in FRP-strengthened reinforced concrete beams. *Journal of composites for construction*, 13(5), 384-393.
- Pelphery, J., Higgins, CH., Sivakumar, B., Groff, R.L., Hartman, B.H., Charbonneau, J.P., Rooper, J.W., and Johnson, B.V. (2008) "State-Specific LRFR Live Load Factors Using Weigh-in-Motion Data." *ASCE Journal of Bridge Engineering*, Vol. 13, no. 4, pp. 339-350.

- Pelphrey, J. and Higgins, C. (2006) "Calibration of LRFR Live Load Factors Using Weigh-In-Motion Data, Interim Report SPR 635, June.
- Qu, X., and Haftka, R. T. (2004) "Reliability-based design optimization using probabilistic sufficiency factor." *Structural and Multidisciplinary Optimization* 27, no. 5: 314-325.
- Raz, O., Buchheit, R., Shaw, M., Koopman, P., and Faloutsos, Ch. (2004) "Detecting Semantic Anomalies in Truck Weigh-In-Motion Traffic Data Using Data Mining." *American Society of Civil Engineers, Journal of Computing in Civil Engineering*, ISSN : 0887-3801.
- Rais-Rohani, M., Eamon, C., and Keesecker, A. (2005) "Structural analysis and sizing optimization of a composite advanced sail design concept." *Marine Technology*, Vol. 42.
- Rais-Rohani, M., Solanki, K., Acar, E., and Eamon, C. (2010) "Shape and sizing optimization of automotive structures with deterministic and probabilistic design constraints." *International Journal of Vehicle Design*, Vol. 54, No. 4.
- Roostaei, Javad, "Integrated Strategies For Sustainable Wastewater-Based Algal Biofuel Production And Environmental Mitigation In The Us" (2018). Wayne State University Dissertations. 2062.
- Siavashi, S., Makkawy, A., Eamon, C. and Wu, H.C., 2017, May. Long term degradation of FRP bond in harsh climate. In SAMPE Conference Proceedings. Seattle, WA.
- Siavashi, S., and Eamon, C., 2018, Reliability-based assessment of bond strength in FRP strengthened RC bridges. In SAMPE Conference Proceedings. Long Beach, CA.
- Siavashi, S., Eamon, C.D., Makkawy, A.A. and Wu, H.C., 2019. Long-Term Durability of FRP Bond in the Midwest United States for Externally Strengthened Bridge Components. *Journal of Composites for Construction*, 23(2), p.05019001.

- Siavashi, S. and Eamon, C. D., 2019 "Development of Traffic Live Load Models for Bridge Superstructure Rating with RBDO and Best Selection Approach." *Journal of Bridge Engineering*, 24(8) 10.1061/(ASCE)BE.1943-5592.0001457.
- Sivakumar, B. (2008) "LRFR Limit States, Reliability Indices & Load Factors." *Load & Resistance Factor Rating of Highway Bridge, Session 4, FHWA LRFR Seminar, HNTB Corp.*
- Sivakuman, B. and Ghosn, M. (2011) "Recalibration of LRFR Live Load Factors in the AASHTO Manual for Bridge Evaluation." NCHRP Project 20-07, Task 285.
- Sivakumar, B., Moses, F., Fu, G., and Ghosn, M. (2007) "Legal truck loads and AASHTO legal loads or posting." NCHRP Report 575.
- Sivakumar, B., Ghosn, M., and Moses, F. (2011) "Protocols for collecting and using traffic data in bridge design." NCHRP Report 683, Washington, D.C., Transportation Research Board.
- Tabatabai, H., Zhao, J., and Lee, C-W. (2009) "Statistical Analysis of Heavy Truck Loads Using Wisconsin Weigh-In-Motion Data." WDOT Project CFIRE 01-02.
- Thompson, M., Eamon, C. and Rais-Rohani, M. (2006) "Reliability-based optimization of fiber-reinforced polymer composite bridge deck panels." *Journal of Structural Engineering*, Vol. 132, No. 12.
- Van de Lindt, J. and Fu, G. (2002) "Investigation of the Adequacy of Current Bridge Design Loads in the State of Michigan." MDOT Research Report RC-1413.
- Zhao, J. and Tabatabai, H. (2012) "Evaluation of a Permit Vehicle Model Using Weigh-in-Motion Trucks Records." *ASCE Journal of Bridge Engineering*, Vol. 17, No. 2.

ABSTRACT**OPTIMAL ASSESSMENT OF WEIGH-IN-MOTION DATA FOR STRUCTURAL
RELIABILITY BASED RATING OF BRIDGE SUPERSTRUCTURES**

by

SASAN SIAVASHI**August 2019****Advisor:** Dr. Christopher D. Eamon**Major:** Civil Engineering (Structural)**Degree:** Doctor of Philosophy

The objectives of this research are to: propose a simplified procedure to reduce the vehicle dataset need to be considered for load rating of bridge superstructures; examine the effectiveness of a Reliability Based Design Optimization (RBDO) procedure to develop State-specific rating load models for a set of bridge superstructures; and to develop an alternative approach to develop rating models more efficiently than the ideal RBDO procedure. The proposed solutions can substantially reduce the computational effort while maintaining reasonable levels of accuracy.

AUTOBIOGRAPHICAL STATEMENT

Sasan Siavashi joined Wayne State University (WSU) in 2013. He received his M.Sc. in Civil Engineering (Structural) in 2015. He continued studying towards his doctoral degree since that time. During his education at WSU, he has worked as a Graduate Teaching Assistant and Graduate Research Assistant. His research interests are reliability-based design and rating of bridges, repair and rehabilitation of structures, and code calibration.